Interaction effects in spin-valve structures

Interaction effects in spin-valve structures

Proefschrift

ter verkrijging van de graad van doctor
aan de Technische Universiteit Delft,
op gezag van de Rector Magnificus prof. dr. ir. J. T. Fokkema,
voorzitter van het College voor Promoties,
in het openbaar te verdedigen op dinsdag 10 april 2007 om 15.00 uur

door

Wouter Wetzels

doctorandus in de natuurkunde
geboren te Tilburg.

Dit proefschrift is goedgekeurd door de promotoren:
 Prof. dr. ir. G. E. W. Bauer
 Prof. dr. M. Grifoni

Samenstelling promotiecommissie:

Rector Magnificus,	Voorzitter
Prof. dr. ir. G. E. W. Bauer,	Technische Universiteit Delft
Prof. dr. M. Grifoni,	Universität Regensburg
Prof. dr. J. König,	Ruhr-Universität Bochum
Prof. dr. Y. V. Nazarov,	Technische Universiteit Delft
Prof. dr. ir. H. S. J. van der Zant,	Technische Universiteit Delft
Dr. A. F. Morpurgo,	Technische Universiteit Delft
Dr. O. N. Zhuravlev,	Schlumberger Research and Development, Moskou

TUDelft   N*W*O
Nederlandse Organisatie voor Wetenschappelijk Onderzoek

Printed in the Netherlands

CONTENTS

1. INTRODUCTION

A magnetic compass needle aligns itself with the earth's magnetic field. This is one of the many applications of the familiar property of ferromagnets that they can exert an attractive or repulsive force on each other. Magnetism also plays an interesting and important role in electronics and currently a lot of research is aimed at understanding the fundamental science and at finding applications of magnetic components in electronic circuits.

1.1 Ferromagnetism

What makes a material ferromagnetic? A magnetic moment is associated with the spin (intrinsic angular momentum) and orbital motion of electrons. Ordinary metals do not have a net magnetic moment, but the spins in a ferromagnetic material (like iron) align. The regions in which this alignment is frozen in are called domains. When a magnetic field is applied, the magnetic dipoles experience a torque that tries to line them up with the magnetic field. At the domain boundaries there is a competition between domains with different magnetization directions, and domains with magnetization more parallel to the magnetic field can grow. This results in a
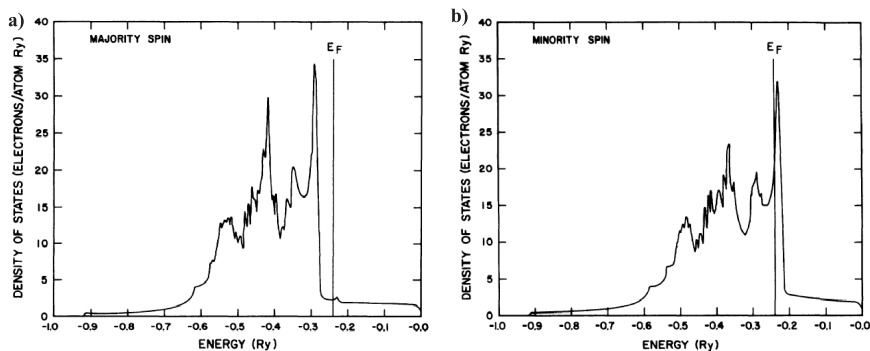
Fig. 1.1: a) Density of states for majority and minority spin in ferromagnetic nickel. This figure shows results from Ref. [1] (1 Ry=13.6 eV).

ferromagnet with a large total magnetic moment.

The eigenstates of electrons are characterized by the electron spin. In a ferromagnet, electrons with majority and minority spin have a different density of states. As an example, the result of an electronic structure calculation for ferromagnetic nickel is shown in Fig. 1.1. Because of the spin-dependence of the electronic structure and the scattering cross section of impurities, the electron mobility in a ferromagnet is spin dependent. The larger part of the current is carried by the high-mobility carriers, and therefore the current is spin polarized.

When the scattering processes that change the spin of the electrons (so-called spin-flip processes) are sufficiently weak, the electron transport can be described by a two-channel resistance model, in which the currents of spin-up and spin-down electrons flow in two separate channels with unequal resistances (See Fig. 1.2).
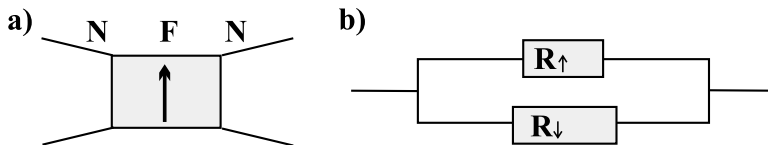
Fig. 1.2: a,b) Schematic picture of a ferromagnetic (F) layer between two normal-metal (N) leads and the corresponding effective circuit model. The resistance for spin-up electrons is $R_\uparrow$ and the resistance for spin-down electrons is $R_\downarrow$.

1.2 Magnetoelectronics

Magnetoelectronics [2] studies hybrid systems consisting of ferromagnetic metals, paramagnetic metals and insulators. It is a subfield of spintronics, which is more generally concerned with the manipulation of spin degrees of freedom in solid-state systems.

A current that is passed through a ferromagnet-normal metal (FN) contact can inject spins into the normal-metal region [3]. A non-equilibrium magnetization (also called spin accumulation) then builds up. As a result,

there is a difference in chemical potential for the spin-up and spin-down subbands. Spin-flip relaxation, which can be parametrized by a spin-flip time τ_{sf}, causes the spin accumulation to decay. For a disordered system, the length scale over which the spin accumulation decays is characterized by the spin-flip diffusion length $l_{sd} = \sqrt{D\tau_{sf}}$ (see Ref. [4]), where D is the diffusion constant. For copper at 4.2K, l_{sd} is about 1 μm [5].

We now give a short overview of some important developments in magnetoelectronics. An essential concept in magnetoelectronics is the magnetoresistance, which is the property that a resistance can be changed by application of a magnetic field. The anisotropic magnetoresistance effect (AMR), by which the resistivity of a bulk ferromagnet depends on the relative orientations of the magnetization and the direction of flow of the charge current, has been known for well over a century [6]. In 1975, the tunneling magnetoresistance effect (TMR) was discovered [7], i.e. the resistance of systems with ferromagnets separated by an insulator was found to depend on the relative orientations of the magnetizations of the ferromagnets. Since the TMR persists at room temperature [8], the effect can be applied in non-volatile, so-called magnetoresistive random access, memories (MRAM) [9].

An important discovery was the non-local exchange coupling in multilayers with alternating ferromagnetic and non-magnetic layers [10]. By this effect, the energy of these magnetic multilayers depends on the relative directions of the magnetizations. Another prominent advance in the field was the discovery of the giant magnetoresistance (GMR) in magnetic multilayers in 1988 [11, 12]. This effect (see Sec. 1.3) was much larger than the AMR, and soon after its discovery the GMR effect was applied as magnetic field sensor, e.g. in read heads for hard-disk drives [9].

It is now well-established that a spin-polarized current passing through a thin ferromagnetic film can induce switching or precession of the magnetization [13, 14, 15]. The mechanism responsible for this, the spin-transfer torque, was predicted by Berger [16] and Slonczewski [17] and will be discussed in Sec. 1.5.

Besides metal-based magnetoelectronics, there is also a lot of activity in semiconductor spintronics [18]. It is now possible to manipulate single

spins in quantum dots [19] and there are investigations into the possibility to perform quantum computations based on the electron spin [20].

1.3 Spin valves

An example of a system that shows magnetoresistance is the perpendicular spin valve, which is schematically shown in Fig. 1.3. A spin valve consists of two ferromagnetic elements connected by a layer of normal-metal material. When a bias voltage V is applied over this system, the current flowing through the FN contacts generates a spin accumulation $\mathbf{V_s}$ in the normal metal. The size and direction of this spin accumulation vector depend on the directions of the two magnetizations ($\mathbf{m}_1$ and $\mathbf{m}_2$), and affect the electron transport. When the two ferromagnets have a different coercive field (for example because they have a different shape), the magnetizations can be controlled independently by an external magnetic field. In this way the current can be modulated. The transport is governed by the spin-dependent contact resistances when these are much larger than the resistance of the layers, e.g. in the case of tunneling barriers or thin layers. The measure
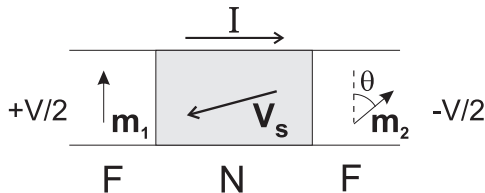
Fig. 1.3: A schematic picture of a spin valve. The magnetizations of the two ferromagnets, $\mathbf{m}_1$ and $\mathbf{m}_2$, make an angle θ. $\mathbf{V}_s$ is the spin accumulation in the normal metal.

for the magnetoresistance is $MR \equiv (R_{AP} - R_P)/R_P$. This is the change of the resistance when the magnetizations are switched from parallel (P) to antiparallel (AP) normalized by the resistance in the parallel configuration. More information is contained in the dependence of transport on an arbitrary angle θ between the magnetization directions (angular magnetoresistance). This angular dependence of the giant magnetoresistance of

CPP multilayers was measured by Urazhdin *et al.* [21]. In this experiment one of the two ferromagnetic layers could be rotated with a magnetic field in the plane of the films, while the other remained pinned.

1.4   Magnetoelectronic circuit theory

Electronic circuit theory provides a powerful method to analyze conducting circuits. Focusing on the stationary state, the voltage distribution in a circuit can be found from Ohm's law and the conservation of charge (the Kirchhoff laws). Circuit theory cannot straightaway be applied to hybrid systems with ferromagnetic and normal metal elements, but there is a generalization in the form of magnetoelectronic circuit theory [22, 23]. This theory allows to study spin and charge transport in disordered or chaotic systems with arbitrary noncollinear magnetizations. For a detailed explanation we refer to a recent review [2].

A magnetoelectronic circuit may be analyzed by the following steps. First, the system has to be divided into large reservoirs and "nodes" that are connected by resistive junctions. In the stationary state, each of the nodes is characterized by a charge potential and a spin accumulation, which have to be determined from the equations for the conservation of charge and spin.

Every FN contact is completely specified by a set of four conductance parameters: the conductance for spin-up electrons $G^{\uparrow\uparrow}$, the conductance for spin-down electrons $G^{\downarrow\downarrow}$ and a complex "mixing conductance" $G^{\uparrow\downarrow} = \mathrm{Re}G^{\uparrow\downarrow} + i\mathrm{Im}G^{\uparrow\downarrow}$. These conductance parameters are defined as

$$G^{ss'} \equiv \frac{e^2}{h} \sum_{nm} \left(\delta_{nm} - r_s^{nm} \left(r_{s'}^{nm} \right)^* \right), \tag{1.1}$$

in terms of spin-dependent reflection coefficients $r_\uparrow^{nm}$ and $r_\downarrow^{nm}$ ($s, s' \in \{\uparrow, \downarrow\}$). Here n and m denote the transport channels in the normal metal. The contact parameters can in principle be calculated from a microscopic description of the contacts [24]. It is convenient to introduce a total conductance $G = G^{\uparrow\uparrow} + G^{\downarrow\downarrow}$ and a contact polarization $P = (G^{\uparrow\uparrow} - G^{\downarrow\downarrow})/(G^{\uparrow\uparrow} +$

$G^{\downarrow\downarrow}$). To give an idea of the order of magnitude, a value of $P \sim 0.7$ was found for Co/Cu interfaces [25].

The charge current through an FN contact depends on the charge bias voltage $V = V_F - V_N$, as well as on the projection of the spin accumulation vector $\mathbf{V}_s$ in the normal metal on the magnetization $\mathbf{m}$. It reads:

$$I = GV - PG\mathbf{m} \cdot \mathbf{V}_s. \tag{1.2}$$

The spin current flowing into the normal metal is given by

$$\begin{aligned}\mathbf{I}_s = {} & (PGV - G\mathbf{V}_s \cdot \mathbf{m})\,\mathbf{m} \\ & + 2\mathrm{Re}G^{\uparrow\downarrow}\mathbf{m} \times (\mathbf{V}_s \times \mathbf{m}) + 2\mathrm{Im}G^{\uparrow\downarrow}\,(\mathbf{V}_s \times \mathbf{m})\,. \end{aligned} \tag{1.3}$$

When the spin accumulation and the magnetization are collinear, only the first term of this expression remains. This describes the spin injected by the spin-polarized current through the contact. The second term, depending on $\mathrm{Re}\,G^{\uparrow\downarrow}$, relaxes the component of the spin accumulation perpendicular to $\mathbf{m}$. The last contribution, which depends on $\mathrm{Im}\,G^{\uparrow\downarrow}$, is a non-dissipative term that causes a precession of the spin accumulation around the magnetization vector. The action is identical to that of an external magnetic field parallel to $\mathbf{m}$ and is sometimes considered to be due to an "effective exchange field".

Using the above expressions for the charge and spin currents, a set of linear equations can be found that incorporates the conservation of charge and spin in a given node. Spin-flip can be taken into account as well in terms of a leakage current of spin angular momentum out of the electronic system. By solving this set of equations, the voltage and spin accumulation for each node can be determined. From these the quasi-equilibrium transport characteristics of the entire circuit can be found.

When magnetoelectronic circuit theory is applied to a symmetric spin valve, the following expression for the conductance is obtained [23]:

$$G_{sv}\left(\theta\right) = \frac{G}{2}\left(1 - P^2\frac{\tan^2\theta/2}{\kappa + \tan^2\theta/2}\right), \tag{1.4}$$

where

$$\kappa = \frac{2(\mathrm{Re}G^{\uparrow\downarrow})^2 + 2(\mathrm{Im}G^{\uparrow\downarrow})^2}{\mathrm{Re}G^{\uparrow\downarrow}G}. \tag{1.5}$$

This result is valid for spin valves that are symmetric in the sense that the two contacts are described by equal conductance parameters $G^{ss'}$. In Fig. 1.4 we show the spin-valve conductance as a function of the angle between the magnetizations. The conductance curves for $\kappa = 1$ show cosine behaviour with a minimum determined by the polarization P. The spin accumulation that builds up for non-aligned magnetizations impedes the transport of electrons, and this effect is maximal in the antiparallel configuration (at $\theta = \pi$). For larger values of κ, the suppression of the conductance near the antiparallel configuration is sharper, since the relaxation and precession described by the larger mixing conductance can reduce the spin accumulation for non-collinear magnetizations.
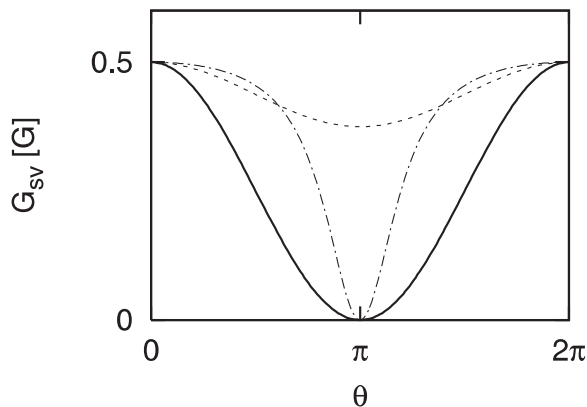

Fig. 1.4: Angular dependence of the conductance of a spin valve with equal contacts. Curves are shown for $P = 1$, $\kappa = 1$ (solid line), $P = 1$, $\kappa = 10$ (dash-dotted), and $P = 0.5$, $\kappa = 1$ (dashed).

1.5   Magnetization dynamics

To describe magnetization dynamics, we can often use the Landau-Lifschitz-Gilbert (LLG) equation [26, 27, 28]. A very small (single-domain) ferromagnetic particle has a uniform vector magnetization. The total energy of the system depends on the size and direction of the magnetization vector. The dependence of the energy on the direction of the magnetization is, among others, determined by the shape of the ferromagnet and the magnetocrystalline anisotropy. The shape anisotropy follows from the shape dependence of the magnetostatic self-energy. The magnetocrystalline anisotropy specifies how, due to the spin-orbit interaction, it is easier to magnetize the crystal in some direction compared to others. These effects and an additional external magnetic field can be lumped together into an effective magnetic field $\mathbf{H}_{\text{eff}}$, the functional derivative of the energy density with respect to the magnetization direction. The LLG equation is:

$$\dot{\mathbf{m}} = -\gamma \mathbf{m} \times \mathbf{H}_{\text{eff}} + \alpha \mathbf{m} \times \dot{\mathbf{m}} \qquad (1.6)$$

The parameter α is the Gilbert damping constant which takes into account energy dissipation mechanisms such as coupling of the magnetization to spin waves, lattice vibrations, magnetic disorder, spin-orbit interaction etc. (for a discussion, see Ref. [29]). When no energy is supplied to the system, the precession will be damped continuously and the magnetization will relax to an energy minimum.

The transverse component of a spin current cannot penetrate a ferromagnet. Instead, this component is absorbed within a few atomic layers from the interface. The absorption takes place because spins noncollinear to the magnetization are a coherent superposition of spin-up and spin-down states which have different Fermi wavevectors $k_F^{\uparrow}$ and $k_F^{\downarrow}$. As the electron moves, the up- and down-component obtain different phases and a rapid precession of the spin around the magnetic exchange field occurs. For a contact with a large number of modes, there is destructive interference from electrons following different paths and the transverse component of the spin current disappears on a length scale $\lambda_{sc} = \pi / \mid k_F^{\uparrow} - k_F^{\downarrow} \mid$, which

is called the transverse spin-coherence length [2]. The spin angular momentum that is absorbed in this way is transferred to the ferromagnet. The total angular momentum is conserved. This generates a torque on the magnetization vector called the spin-transfer torque [16, 17]. When a spin current $\mathbf{I_s}$ flows into the ferromagnet, the effect of the spin-transfer torque on the magnetization $\mathbf{m}$ can be written as (see e.g. Ref. [30]):

$$\dot{\mathbf{m}}_{\mathrm{torque}} = -(\gamma/\mathcal{M}_S)\mathbf{m} \times \mathbf{I_s} \times \mathbf{m}, \tag{1.7}$$

where $\mathcal{M}_S$ is the total magnetic moment of the ferromagnet and γ is the gyromagnetic ratio. The spin-transfer torque can switch the direction of a magnetization, provided that it is strong enough to overcome the anisotropy energy barrier and the damping torque.

The thermal fluctuations of a single-domain ferromagnet were discussed by Brown [31]. A random torque on the magnetization can be added to the LLG-equation to describe stochastic agitations of the magnetization at finite temperatures.

$$\dot{\mathbf{m}}_{\mathrm{fluct}} = \mathbf{m} \times \mathbf{h}, \tag{1.8}$$

where $\mathbf{h}$ is a stochastically fluctuating field with correlation function

$$\langle \mathbf{h}_i(t)\mathbf{h}_j(t') \rangle = \frac{2\gamma\alpha k_B T}{\mathcal{M}_S}\delta_{ij}\delta(t-t'), \tag{1.9}$$

in which α appears as a consequence of the fluctuation-dissipation theorem [31].

1.6 Single-electron transistors

As magnetoelectronic devices are becoming smaller and smaller, electron-electron interaction effects become increasingly important. The energy needed to charge a system with a single electron can to a good approximation be expressed in terms of an effective capacitance C. When the characteristic energy scale $e^2/2C$ is larger or comparable to the thermal
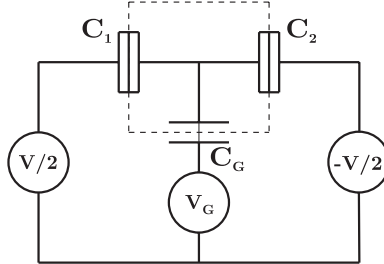
Fig. 1.5: Effective circuit model of the single-electron transistor.

energy $k_B T$, electric transport becomes strongly modified [32, 33]. For a discussion of single-electron effects see the review in Ref. [34].

A standard system to study charging effects is the single-electron transistor (See Fig. 1.5). It consists of a normal metal island contacted to two leads by tunnel junctions with a resistance larger than the resistance quantum $R_Q = h/e^2$. The island is only weakly connected to the leads, and when the charging energy is the dominant energy scale ($e^2/2C \gg k_B T, eV$) the number of electrons on the island n_N is quantized. The charge on the island changes by e when an electron tunnels into or out of the leads. When the island is small enough that the energy level splitting is larger than the thermal energy, it is possible to observe individual levels in transport measurements. Such islands are often called "quantum dots" [35].

A gate voltage V_G can be used to shift the potential of the island relative to that of the leads. We will assume that the gate capacitance C_G is much smaller than the contact capacitances C_1 and C_2. The effective capacitance of the island is then $C \sim C_1 + C_2$. The Coulomb interaction can often be described very well within the "orthodox model" as

$$H_{ch} = \frac{e^2 \left(n_N - C_G V_G/e\right)^2}{2C}. \tag{1.10}$$

Whether an electron can tunnel through the contacts is determined by the change of electrostatic energy associated with the tunneling process. In the "Coulomb blockade" electrons are not transmitted because the amount of

energy needed for the transitions is not available. This Coulomb block-ade can be lifted by a shift of the gate voltage. The low-bias conductance shows periodically repeating conductance peaks as a function of gate volt-age called "Coulomb oscillations". Measurements of the differential con-ductance versus gate- and bias voltage typically show "Coulomb diamond" patterns. The diamonds, regions in which electron transport is blocked, are bounded by lines indicating the threshold bias voltage at which current starts to flow. Fig. 1.6 (reproduced from Ref. [36]), shows an example of such a measurement for a carbon-nanotube quantum dot attached to leads. Besides Coulomb diamonds, several additional lines can be seen that indi-cate where higher excited states of the quantum dot start to participate in transport.
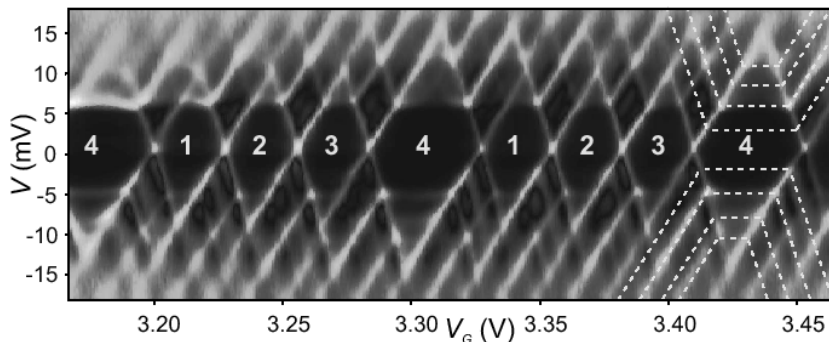
Fig. 1.6: Differential conductance of a carbon-nanotube quantum dot between leads from Ref. [36]. Carbon nanotubes are long cylindrical molecules made of carbon. The black color indicates $dI/dV \sim 0$.

Many experiments have been carried out on all-normal metal single-electron transistors. In chapter 2 we discuss transport through so-called spin-valve single-electron transistors (SV-SET's), which have ferromagnetic instead of normal-metal leads. In an SV-SET the effects of Coulomb block-ade and magnetoresistance effects occur simultaneously, which allows to study the interplay of spin- and charging effects.

1.7 Noise

Often it is satisfactory to simply characterize a current by its average value. But the random fluctuations around this mean value ("noise") are a field of study in itself and noise measurements can give interesting additional information about nanostructures [37].

We consider a current $I(t)$ with a time average given by

$$\langle I \rangle \equiv \lim_{T \to \infty} \frac{1}{T} \int_{-T/2}^{T/2} dt\, I(t) \qquad (1.11)$$

We can quantify the noise in terms of the squared deviation from this average $\Delta I(t) \equiv I(t) - \langle I \rangle$ or its Fourier transform

$$S(\omega) = \int dt\, e^{i\omega t} \langle \Delta I(t)\, \Delta I(0) \rangle, \qquad (1.12)$$

$S(\omega)$ is the so-called power spectrum of the noise.

Several types of noise play a role in mesoscopic conductors. Firstly, there is thermal noise (also called Johnson-Nyquist noise) [38]. It originates from thermal fluctuations around the average distribution functions, which are always present at nonzero temperature. For low frequencies ($\hbar\omega \ll k_B T$), this thermal noise is "white": the noise power is frequency independent. The noise power depends only on temperature and electrical resistance R, and for the case of two terminals it is given by $S = 4k_B T/R$. Shot noise [39, 37, 40] arises in the presence of a finite (average) current bias from the discreteness of the electron charge.

Due to the intrinsic spin angular momentum of the electron, a fluctuating current is always associated with a fluctuating spin current. In Sec. 1.5 we introduced the spin-transfer torque on a ferromagnetic particle, which depends on the spin current. A fluctuating spin current will then result in a randomly fluctuating torque. The effect of this fluctuating torque on the magnetization can be examined by solving a stochastic equation for the dynamics. In particular, a Fokker-Planck partial differential equation can describe the evolution of the probability density for the magnetization

directions [31]. In chapter 3 we discuss how the use of a noisy current for current-induced magnetization switching can be used as a strategy to reduce the switching times.

1.8 Spin-orbit interaction in a two-dimensional electron gas

Spin-orbit interaction is a relativistic effect that describes how the spin of an electron is affected by an effective magnetic field when it moves through an electric field. This effect gives a spin-orbit splitting of the electron energy states. Two-dimensional electron gas structures are influenced the spin-orbit interaction, and there are two dominating contributions to the spin-orbit Hamiltonian to leading (linear) order in k close to the Brillouin zone center or conduction band minimum. The Dresselhaus term [41] results from a the absence of inversion symmetry (bulk inversion asymmetry), and the Rashba term [42] is related to structure inversion asymmetry, which occurs for asymmetric quantum wells or in deformed bulk systems. Both give a spin splitting of the conduction band that is to leading order linear in k. The Hamiltonian for a two-dimensional electron gas with spin-orbit interaction reads:

$$H = \frac{\hbar^2 \mathbf{k^2}}{2m} \hat{I} + H_R + H_D \tag{1.13}$$

with

$$H_R = \frac{\alpha}{\hbar} \left(\hat{\sigma}_x k_y - \hat{\sigma}_y k_x \right) \tag{1.14}$$

$$H_D = \frac{\beta}{\hbar} \left(\hat{\sigma}_x k_x - \hat{\sigma}_y k_y \right). \tag{1.15}$$

In these expressions the σ_i ($i \in x, y, z$), are the Pauli matrices and α and β are the Rashba and Dresselhaus spin-orbit coupling strengths.

For convenience we introduce $\xi(\mathbf{k}) \equiv (\beta + i\alpha) k_x/\hbar + (\alpha + i\beta) k_y/\hbar$. The eigenstates of the Hamiltonian, denoted by wavevector $\mathbf{k}$ and $s \in \{+, -\}$, are then given by (cf. Ref. [43]):

$$\phi_{\mathbf{k,s}} = \frac{1}{\sqrt{2L^2}} e^{i\mathbf{k}\cdot\mathbf{r}} \left(s \frac{\xi(\mathbf{k})}{|\xi(\mathbf{k})|}, 1 \right)^T, \tag{1.16}$$

and the corresponding eigenenergies are $E_{\mathbf{k},s} = \frac{\hbar^2 \mathbf{k^2}}{2m} + s|\xi(\mathbf{k})|$. The spin of the eigenstates $\mathbf{s_{k,s}}$ is given by

$$\mathbf{s_{k,s}} = \left(s\frac{\mathrm{Re}\xi(\mathbf{k})}{\xi(\mathbf{k})}, -s\frac{\mathrm{Im}\xi(\mathbf{k})}{\xi(\mathbf{k})} \right)^T . \tag{1.17}$$

For $s = +$ the spins of the eigenstates point in the direction of the effective magnetic field. In Fig. 1.7 we schematically show the spin direction of the eigenstates at the Fermi energy, for different values of the two spin-orbit coupling parameters. We see that when the Rashba and Dresselhaus coupling strengths are exactly equal (Fig. 1.7c), the effective magnetic field is always in the same direction for any $\mathbf{k}$. A lot of research was stimulated by

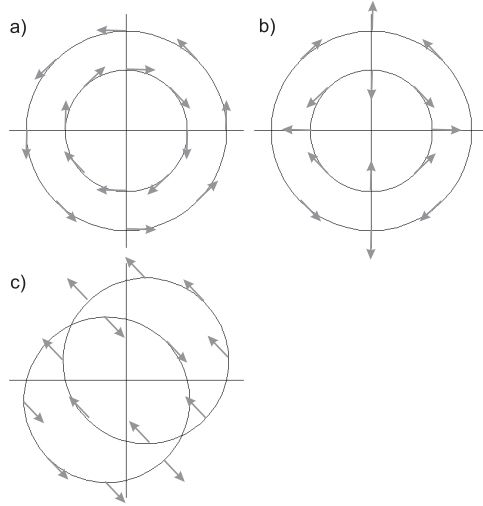Fig. 1.7: The spin direction of the eigenstates at the Fermi level for a two-dimensional electron gas. The values of the Rashba and Dresselhaus spin-orbit coupling parameters are a) $\alpha > 0, \beta = 0$, b) $\alpha = 0, \beta > 0$, and c) $\alpha = \beta > 0$.

the proposal of a spin field effect transistor by Datta and Das in 1990 [44]. It is based on coherent spin rotation in media with spin-orbit coupling. The

transistor has a drain and a source with a narrow one-dimensional channel in between through which electrons move ballistically. The source and the drain are ferromagnets that inject and detect the electron spin. In the transport channel there is an effective magnetic field that arises from the spin-orbit coupling in the substrate material, the confinement geometry and the potential of a nearby gate. This effective magnetic field, and thereby the precession of the electron spins, can be modulated by the gate voltage. Because the transmission of electrons is spin dependent, the conductance of this device depends on the total precession phase during the transport and can therefore be controlled by the gate voltage. This scheme has not been implemented yet. The main difficulty is that the injection of spin into a normal metal 2DEG is limited by the conductance mismatch [45, 46].

In chapter 4 we study a spin-valve system with a two-dimensional electron gas between ferromagnetic leads. The special characteristics of the effective magnetic field when the spin-orbit coupling strengths α and β are equal result in an anisotropy of the spin relaxation [47]. We discuss how this can be observed in the transport through this system.

1.9   Luttinger liquids

According to the Fermi-liquid paradigm [48] the elementary excitations in three-dimensional metals are weakly-interacting quasiparticles with spin and charge of the bare electron. In spite of the very high electron density and consequently strong Coulomb repulsive forces, conventional metals are therefore very well described by a gas of noninteracting quasiparticles.

For one-dimensional metals, however, Fermi-liquid theory is known to break down. Instead of a gas of non-interacting quasiparticles, the physics of interacting fermions in one dimension is closer to that of pearls on a string. Sufficiently weak excitations can be described with Luttinger-liquid theory [49, 50, 51, 52]. This theory applies to systems in which electrons are quantum confined in two directions with only one remaining translational degree of freedom. Examples are single wall metallic carbon nanotubes [53], spin chains [54], and quantum wires [55]. The collective many-body excitations that govern the low-energy physics of Luttinger liquids are plas-

mons that obey boson statistics. One-dimensional plasmons of charge or spin character propagate independently and with different velocities. This is often referred to as spin-charge separation, which has been observed in tunneling experiments [55]. The progress in spin injection from ferromagnetic leads into carbon nanotubes [56, 57, 58] might provide another route to measure this phenomenon.

It is often helpful to use bosonization techniques to study fermionic Luttinger liquids [59], *i.e.* to transform the interacting fermionic hamiltonian into an equivalent one of which the excitations are noninteracting bosons.

Interaction effects in Luttinger liquids can have a strong and distinctive influence on electronic transport. For example, the density of states for tunneling into a Luttinger liquid is suppressed by a power law with an exponent depending on the strength of the Coulomb interaction [60]. Non-Fermi liquid effects can also influence spin transport and spin injection from ferromagnets into a Luttinger liquid [61, 62]. The angular magnetoresistance of a Luttinger liquid attached to ferromagnetic contacts is affected by the interaction in a characteristic way [63, 64].

1.10   Outline

In this thesis we discuss the influence of interaction effects on electronic transport for a number of different physical systems. A common feature of these systems is that they show magnetoresistance based on the spin-valve concept.

In chapter 2 we study the interplay of spin and Coulomb-interaction effects for single-electron transistors with ferromagnetic leads, so-called single-electron spin-valve transistors. We examine how exchange through the F|N tunnel contacts acts on the spin accumulation in the island. The linear conductance depends on the angle between the two lead magnetization directions. It can also be controlled with a nearby gate and externally applied magnetic fields.

In chapter 3 we present a proposal to improve the efficiency of current-induced magnetization switching in F|N|F spin-valve systems. Switching occurs because an electric current that is polarized by a "fixed" ferromag-

netic layer exerts a spin-transfer torque on the second ferromagnet. Externally generated current fluctuations result in a fluctuating spin-transfer torque on the free magnetization. By solving a stochastic equation for the magnetization dynamics, we find how the switching time and power dissipation depend on the noise level.

Chapter 4 discusses the effect of spin-orbit coupling on electronic transport in a spin valve consisting of a two-dimensional quantum dot contacted to two ferromagnetic leads. When the Rashba and Dresselhaus spin-orbit coupling strengths are tuned properly, a giant anisotropy in the spin-relaxation times can affect the angular magnetoresistance and the spin-transfer torque.

For one-dimensional systems the Fermi-liquid picture breaks down. A Luttinger-liquid description is then appropriate. In chapter 5 we discuss a single-electron spin-valve transistor with a Luttinger-liquid island. Interaction effects and spin-charge separation can have a large influence on transport. We restrict the discussion to a regime in which the charging energy is the dominant energy scale and find the dependence of transport on the magnetic configuration. We then compare the results for Luttinger-liquid and Fermi-liquid islands.

BIBLIOGRAPHY

[1] C. S. Wang and J. Callaway, Phys. Rev. B **9**, 4897 (1974).

[2] A. Brataas, G. E. W. Bauer, and P. J. Kelly, Phys. Rep. **427**, 157 (2006).

[3] M. Johnson and R. H. Silsbee, Phys. Rev. Lett. **55**, 1790 (1985).

[4] T. Valet and A. Fert, Phys. Rev. B **48**, 7099 (1993).

[5] F. J. Jedema, A. T. Filip and B. J. van Wees, Nature **410**, 345 (2001).

[6] W. Thomson, Proc. R. Soc. London **8**, 546 (1857).

[7] M. Julliere, Phys. Lett. **54A**, 225 (1975).

[8] J. S. Moodera, L. S. Kinder, T. M. Wong, and R. Meservey, Phys. Rev. Lett. **74**, 3273 (1995).

[9] J. M. Daughton, J. Magn. Magn. Mat. **192**, 334 (1999).

[10] P. Grünberg, R. Schreiber, Y. Pang, M. B. Brodsky, and H. Sowers, Phys. Rev. Lett. **57**, 2442 (1986).

[11] M. N. Baibich, J. M. Broto, A. Fert, F. Nguyen Van Dau, F. Petroff, P. Eitenne, G. Creuzet, A. Friederich, and J. Chazelas, Phys. Rev. Lett. **61**, 2472 (1988).

[12] G. Binasch, P. Grünberg, F. Saurenbach, and W. Zinn, Phys. Rev. B **39**, 4828 (1989).

[13] F. J. Albert, J. A. Katine, R. A. Buhrman, and D. C. Ralph, Appl. Phys. Lett. **77**, 3809 (2000).

[14] J. A. Katine, F. J. Albert, R. A. Buhrman, E. B. Myers, and D. C. Ralph, Phys. Rev. Lett. **84**, 3149 (2000).

[15] J. Grollier, V. Cros, A. Hamzić, J. M. George, H. Jaffrès, A. Fert, G. Faini, J. Ben Youssef, and H. Legall, Appl. Phys. Lett. **78**, 3663 (2001).

[16] L. Berger, Phys. Rev. B **54**, 9353 (1996).

[17] J. C. Slonczewski, J. Magn. Magn. Mater. **159** L1-L7 (1996).

[18] I. Žutić, J. Fabian, and S. Das Sarma, Rev. Mod. Phys. **76**, 323 (2004).

[19] J. M. Elzerman, R. Hanson, L. H. Willems van Beveren, B. Witkamp, J. S. Greidanus, R. N. Schouten, S. De Franceschi, S. Tarucha, L. M. K. Vandersypen, and L.P. Kouwenhoven, Quantum Dots: a Doorway to Nanoscale Physics, Series: Lecture Notes in Physics, Vol. **667**, edited by W. D. Heiss, (2005).

[20] D. P. DiVincenzo, Science **270**, 255 (1995).

[21] S. Urazhdin, R. Loloee, and W. P. Pratt, jr., Phys. Rev. B **71**, 100401(R) (2005).

[22] A. Brataas, Y. V. Nazarov, and G. E. W. Bauer, Phys. Rev. Lett. **84**, 2481 (2000).

[23] A. Brataas, Y. V. Nazarov, and G. E. W. Bauer, Eur. Phys. J. B **22**, 99 (2001).

[24] K. Xia, P. J. Kelly, G. E. W. Bauer, A. Brataas, and I. Turek, Phys. Rev. B **65**, 220401(R) (2002).

[25] J. Bass and W. P. Pratt Jr., J. Magn. Magn. Mater, **200** 274 (1999)).

[26] B. Hillebrands and K. Ounadjela (Eds.), Spin Dynamics in Confined Magnetic Structures, (Springer, Berlin, 2003).

[27] S. Maekawa and T. Shinjo (Eds.), Applications of Magnetic Nanostructures, (Taylor and Francis, New York, 2002).

[28] Y. Tserkovnyak, A. Brataas, G. E. W. Bauer, and B. I. Halperin, Rev. Mod. Phys. **77**, 1375 (2005).

[29] T. L. Gilbert, IEEE Trans. Magn. **40**, 3443 (2004).

[30] D. M. Apalkov and P. B. Visscher, J. Magn. Magn. Mater. **286**, 370 (2005).

[31] W. F. Brown, Phys. Rev. **130**, 1677 (1963).

[32] I. O. Kulik and R. I. Shekhter, Zh. Eksp. Teor. Fiz. **68**, 623 (1975)[Sov. Phys. JETP **41**, 308 (1975)].

[33] H. Grabert, G.-L. Ingold, M. H. Devoret, D. Estève, H. Pothier, and C. Urbina, Z. Phys. B **84**, 143 (1991).

[34] H. Grabert and M. H. Devoret (Eds.), *Single charge tunneling*, (Plenum Press, New York, 1992).

[35] L. P. Kouwenhoven, D. G. Austing, and S. Tarucha, Rep. Prog. Phys. **64**, 701 (2001).

[36] S. Sapmaz, P. Jarillo Herrero, J. Kong, C. Dekker, L. P. Kouwenhoven, and H. S. J. van der Zant, Phys. Rev. B **71**, 153402 (2005).

[37] Ya. M. Blanter and M. Büttiker, Phys. Rep. **336**, 1 (2000).

[38] J. B. Johnson, Nature **119**, 50 (1927).

[39] W. Schottky, Ann. Phys. (Leipzig) **362**, 541 (1918).

[40] C. Beenakker and C. Schönenberger, Physics Today, May 2003, p.37.

[41] G. Dresselhaus, Phys. Rev. **100**, 580 (1955).

[42] Y. A. Bychkov and E. I. Rashba, J. Phys. C **17**, 6038 (1984).

[43] S. D. Ganichev, V. V. Bel'kov, L. E. Golub, E. L. Ivchenko, P. Schnei-
der, S. Giglberger, J. Eroms, J. DeBoeck, G. Borghs, W. Wegschneider,
D. Weiss, and W. Prettl, Phys. Rev. Lett. **92**, 256601 (2004).

[44] S. Datta and B. Das, Appl. Phys. Lett. **56**, 665 (1990).

[45] G. Schmidt, D. Ferrand, L. W. Molenkamp, A. T. Filip, and B. J. van
Wees, Phys. Rev. B **62**, 4790(R) (2000).

[46] G. Schmidt, J. Phys. D **38**, R107 (2005).

[47] N. S. Averkiev, L. E. Golub, and M. Willander, J. Phys. C **14**, R271
(2002).

[48] D. Landau, Sov. Phys. JETP 3, 920 (1957); 5, 101 (1957), 8, 70 (1959).

[49] S. Tomonaga, Prog. Theor. Phys. (Kyoto) **5**, 544 (1950).

[50] J. M. Luttinger, J. Math. Phys. **4**, 1154 (1963).

[51] J. Voit, Rep. Prog. Phys. **58**, 977 (1995).

[52] T. Giamarchi, *Quantum physics in one dimension*, (Clarendon Press,
Oxford, 2004).

[53] R. Egger and A. O. Gogolin, Eur. Phys. J. B **3**, 281 (1998).

[54] B. Lake, D. A. Tennant, C. D. Frost, and S. E. Nagler, Nat. Mat. **4**,
329 (2005).

[55] O. M. Auslaender, H. Steinberg, A. Yacoby, Y. Tserkovnyak, B. I.
Halperin, K. W. Baldwin, L. N. Pfeiffer, and K. W. West, Science
308, 88 (2005).

[56] K. Tsukagoshi, B. W. Alphenaar, and H. Ago, Nature **401**, 572 (1999).

[57] S. Sahoo, T. Kontos, J. Furer, C. Hoffmann, M. Gräber, A. Cottet, and C. Schönenberger, Nat. Phys. **1**, 99 (2005).

[58] H. T. Man, I. J. W. Wever, and A. F. Morpurgo, Phys. Rev. B **73**, 241401(R) (2006).

[59] J. von Delft and H. Schoeller, Ann. Phys. (Leipzig) **7**, 225 (1998).

[60] F. Anfuso and S. Eggert, Phys. Rev. B **68**, 241301(R) (2003).

[61] Q. Si, Phys. Rev. Lett. **81**, 3191 (1998).

[62] C. Bena and L. Balents, Phys. Rev. B **70**, 245318 (2004)

[63] L. Balents and R. Egger, Phys. Rev. Lett. **85**, 3464 (2000).

[64] L. Balents and R. Egger, Phys. Rev. B **64**, 035310 (2001).

2. EXCHANGE EFFECTS ON ELECTRON TRANSPORT THROUGH SINGLE-ELECTRON SPIN-VALVE TRANSISTORS

Wouter Wetzels, Gerrit E.W. Bauer, and Milena Grifoni

We study electron transport through single-electron spin-valve transistors in the presence of non-local exchange between the ferromagnetic leads and the central normal-metal island. The Coulomb interaction is described with the "orthodox model" for Coulomb blockade and we allow for noncollinear lead magnetization directions. Two distinct exchange mechanisms that have been discussed in the literature are shown to be of comparable strength and are taken into account on equal footing. We present results for the linear conductance as a function of gate voltage and magnetic configuration, and discuss the response of the system to applied magnetic fields.[1]

2.1   Introduction

Downscaling magnetoelectronic devices to the nanometer regime implies that electron-electron interaction effects become prominent, as has been amply demonstrated by many experimental studies on the Coulomb blockade in double tunnel junctions with ferromagnetic elements. Measurements were done on systems with nonmagnetic islands contacted to ferromagnetic leads [1, 2, 3, 4, 5, 6] as well as for all-ferromagnetic systems.[7, 8, 9] Much of the theoretical work focuses on F|N|F spin valves, in which the island is a normal metal (N) and the contacts are ferromagnets (F) with variable magnetization directions. Initially, the interest was mainly focused on the giant magnetoresistance, i.e. the difference in the transport properties for parallel or antiparallel magnetizations.[10, 11, 12, 13, 14] More recently, the interplay between spin and interaction effects for noncollinear magnetization configurations has attracted quite some interest. Besides spin-valve systems with quantum-dot islands [15, 16, 17, 18, 19, 20, 21], also islands consisting of metallic clusters[22], Luttinger liquids[23, 24], and nanomagnets[25] were studied.

A single-electron spin-valve transistor (SV-SET) is an F|N|F spin valve with a sufficiently small normal-metal (N) island that is coupled to the ferromagnetic leads by tunnel barriers. When the electrostatic charging energy of the island is larger than the thermal energy, charge transport can be controlled at the level of single electron charges by varying bias and gate voltage, as is well known for nonmagnetic SET's.[26] With spin-dependent electron tunneling rates and sufficiently long spin-decay lifetimes, a spin accumulation (or nonequilibrium magnetization) that strongly affects electron transport may build up in the nonmagnetic island.

In this paper, we discuss the transport characteristics of metallic SV-SETs in the Coulomb blockade regime, allowing for arbitrary, noncollinear magnetization directions. We obtain results to leading order in the transmission matrix elements, and therefore higher-order cotunneling processes are not taken into account. In particular, we examine the influence of exchange effects through F|N tunnel contacts on the spin accumulation in the center island, presenting a more complete discussion compared to that in

Ref. [22]. We argue that two separate exchange effects have to be taken into account. On one hand, there is the nonlocal interface exchange, let us call it "X1" in the following. In scattering theory for noninteracting systems it is described by the imaginary part of the spin-mixing conductance,[27] while in the context of current-induced magnetization dynamics X1 acts as an "effective field."[28] Such an effective field has been found experimentally to strongly affect the transport dynamics in spin valves with MgO tunnel junctions.[29] This effect has recently also been involved to explain magnetoresistance effects in carbon nanotube spin valves[5] and called spin-dependent interface phase shifts.[30] The second exchange term ("X2") is an interaction-dependent exchange effect due to virtual tunneling processes that is absent in noninteracting systems. It has been considered for islands in the electric quantum limit, in which transport is carried by a single quantized level only.[15] The X2 effect is potentially attractive for quantum information processing, since it allows to switch on and off effective magnetic fields in arbitrary directions just by a gate electric potential. We compute here X2 for a metallic island in which size quantization is not important. We find that both exchange effects are of comparable magnitude and affect the transport properties in a characteristic way, but can be separated in principle by employing the gate dependence of X2.

The paper is organized as follows. In Sec. 2.2 we introduce the model system for the SV-SET. In Sec. 2.3 the two relevant types of exchange processes are discussed. Charge and spin transfer rates are determined in Sec. 2.4. Finally, we present results for the transport characteristics as a function of magnetic configuration, gate voltage and applied magnetic field in Sec. 2.5.

2.2   Model system

An SV-SET [see Fig. 2.1(a)] is composed of a small metallic cluster in contact with two large ferromagnetic electron reservoirs in thermal equilibrium characterized by magnetization directions $\vec{m}_1$ and $\vec{m}_2$ with $\vec{m}_\alpha = (\sin\theta_\alpha, 0, \cos\theta_\alpha)$ (for $\alpha = 1, 2$), where $\theta_1 = \theta/2$ and $\theta_2 = -\theta/2$.

The $F_\alpha|N$ contacts are tunneling barriers with conductances that de-
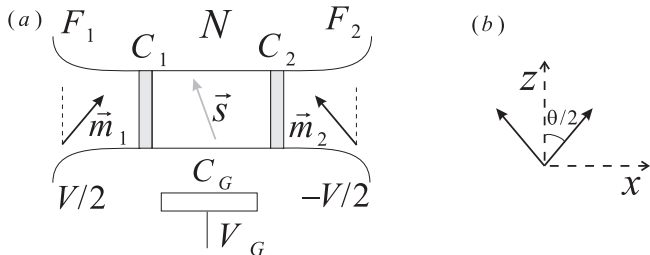
Fig. 2.1: (a) The spin-valve single-electron transistor: A small normal-metal island tunnel-coupled to two large ferromagnetic leads. The unpaired spin angular momentum on the island is denoted by $\vec{s}$. (b) The magnetization directions in the leads define an angle θ.

pend on the electron spin, $G_\alpha^{\uparrow\uparrow}$ for the majority and $G_\alpha^{\downarrow\downarrow}$ for the minority spin in the ferromagnet. The total conductance for contact α is then given by $G_\alpha \equiv \left(G_\alpha^{\uparrow\uparrow} + G_\alpha^{\downarrow\downarrow} \right)$ and the contact polarization is defined as $P_\alpha \equiv \left(G_\alpha^{\uparrow\uparrow} - G_\alpha^{\downarrow\downarrow} \right) / \left(G_\alpha^{\uparrow\uparrow} + G_\alpha^{\downarrow\downarrow} \right)$. The resistances $R_\alpha = 1/G_\alpha$ are taken to be much larger than the resistance quantum $R_Q = h/e^2$, which, at low enough temperatures and bias voltages, allows us to study the blockade of transport by the Coulomb interaction. The electron tunneling rates are governed by the change of electrostatic energy of the whole circuit upon transfer of an electron. The capacitances of the junctions C_α determine the charging energy of the island.

We limit our considerations to islands formed by metallic clusters for which the thermal energy $(k_B T)$ is much larger than the average single-particle energy separation (reciprocal density of states) $\delta = 1/\rho_N$, but much smaller than the single-electron charging energy. Therefore, many levels on the island participate in the transport and we may treat the electronic spectrum as continuous. For a gold cluster with a diameter of 10 nm, δ approximately corresponds to a temperature of 2 K. The Kondo physics of quantum dots connected to ferromagnetic leads[31, 32, 33, 2] is suppressed in this regime.

Since the currents flowing into and out of the cluster are spin polarized, the island may become magnetized. The number of unpaired spins on the island is limited by spin-flip scattering, which we parametrize by a spin-flip relaxation time τ_{sf}. There is evidence from several experiments that the spin-flip times in metallic nanoparticles can be much longer than in bulk systems, which implies that the effects of a spin accumulation on the island should be taken into account.[9, 6, 4] For later convenience we introduce the spin-flip conductance parameter $G_{sf} \equiv \rho_N e^2 / (2\tau_{\mathrm{sf}})$. We assume that the energy relaxation on the island is fast compared to the electron dwell time.

The total Hamiltonian for the SV-SET is

$$H = H_N + \sum_{\alpha=1,2} \left(H_{F\alpha} + H_{T\alpha} + H_{\mathrm{ex}\alpha} \right), \qquad (2.1)$$

where H_N is the Hamiltonian for the normal metal cluster in the "orthodox model" [26] for the Coulomb blockade,

$$H_N = \sum_{ks} \varepsilon_k c_{ks}^\dagger c_{ks} + \frac{e^2 \left(n_N - C_G V_G/e \right)^2}{2C}. \qquad (2.2)$$

Here $c_{ks}^\dagger$ is a creation operator for an electron state with orbital index k and spin $s \in \{\uparrow, \downarrow\}$, where the z axis is chosen as spin quantization axis. The Hamiltonian includes an electrostatic interaction energy which depends on the junction capacitances C_α, the gate voltage V_G, and the excess number of electrons on the island n_N. The gate voltage shifts the potential and induces a charge $C_G V_G$. We assume that the gate capacitance $C_G \ll C_1, C_2$, and in the following we use $C_1 = C_2 = C/2$. The energy levels in the two ferromagnetic leads (denoted by $\alpha = 1, 2$) are spin dependent:

$$H_{F\alpha} = \sum_{ks} \varepsilon_{\alpha ks} a_{\alpha ks}^\dagger a_{\alpha ks}. \qquad (2.3)$$

The operators $a_{\alpha ks}^\dagger$ create electrons with spin s in the spin-quantization axis along $\overrightarrow{m}_\alpha$.

It is convenient to introduce annihilation operators $c_{\alpha ks}$ for electrons in the normal metal defined for a quantization axis in the direction of $\overrightarrow{m}_\alpha$. The relation between operators in the two bases is then $c_{\alpha ks} = \hat{U}_{ss'}(\theta_\alpha) c_{ks'}$, expressed in terms of the spin $\frac{1}{2}$ rotation matrix

$$\hat{U}(\theta_\alpha) = e^{i\sigma_y \theta_\alpha/2} = \begin{pmatrix} \cos\theta_\alpha/2 & \sin\theta_\alpha/2 \\ -\sin\theta_\alpha/2 & \cos\theta_\alpha/2 \end{pmatrix}. \qquad (2.4)$$

Then, for each contact, a tunneling Hamiltonian

$$H_{T\alpha} = \sum_{kqs} T_{kqs}^\alpha a_{\alpha ks}^\dagger c_{\alpha qs} + H.c. \qquad (2.5)$$

describes the coupling to the island. The tunneling coefficients are assumed to not significantly depend on energy on the scale of the charging energy. We discuss the exchange contribution, represented by the Hamiltonian $H_{\text{ex}\alpha}$, in the next section.

2.3   Exchange effects

Here we discuss two different exchange effects that affect the electrons in the normal metal island attached to magnetic contacts. These two flavors arise when the transport properties for an SV-SET are determined to lowest order in the tunneling probabilities.

2.3.1   Nonlocal interface exchange (X1)

The nonlocal exchange coupling between ferromagnetic films through a normal-metal spacer is an important effect that determines the ground state of magnetic multilayers (see Ref. [34] for a recent review). Electrons in a normal metal that are reflected at a contact to a ferromagnet pick up a phase depending on the electron spin relative to the magnetization direction. In sufficiently clean and narrow F|N|F structures, quantum well states are formed in N whose energy depends on the magnetic configuration through the spin-dependent phase. By a rotation of the magnetization directions the energy spectrum and Fermi energy varies, causing the

ground-state energy to depend on the relative angle θ. In metallic multilayers with a suitable spacer thickness, this can lead to an antiparallel ground state, which displays the celebrated giant magnetoresistance when the magnetizations are forced into a parallel direction by a magnetic field. Even when the ground state energies are not significantly affected by the exchange coupling, configuration-dependent quantized states can still be observed in transport. This has been shown for high-quality planar tunnel junctions[35] as well as spin valves in which the node is formed by single carbon nanotubes with a quantized energy spectrum.[5, 36] In Ref. [30] the effect of interfacial phase shifts on the magnetoresistance of ballistic quantum wires between ferromagnetic leads was calculated. The spin-dependent phase shifts give rise to a slightly different quantization condition, which can spin-split the energy levels. Since we are here interested in classical islands with a continuous electron spectrum, we calculate energy shifts for a semiclassical island using the Bohr-Sommerfeld quantization rule in Appendix 2.8.

Here we consider the limit of tunnel junctions between a normal-metallic island and ferromagnetic electrodes. The torques on the ferromagnets are then very small. The exchange coupling does not significantly disturb the ferromagnets in this limit, but persists to affect transport. The present study focuses on the charge transport properties in the limit of small tunneling matrix elements, thus from the outset excluding resonant tunneling, co-tunneling or Kondo-type physics. The states on the island may be size quantized, i.e. the energy level spacing exceeds the thermal energy ("quantum dot"), or, in the opposite limit, better described by a semicontinuous density of states ("classical dot"). Here we concentrate on the latter, i.e. semiclassical, diffuse, or chaotic islands, for which it can be shown quite generally that equilibrium spin currents are suppressed.[37] The state of the island is then characterized by a semiclassical charge and spin distribution function that has to be determined self-consistently as a function of the junction parameters and the applied voltages. For noninteracting systems, the spin and charge currents through an F|N interface are determined not only by the conventional conductances $G_\alpha^{\uparrow\uparrow}$ and $G_\alpha^{\downarrow\downarrow}$ introduced above, but

also by the complex spin-mixing conductances $G_\alpha^{\uparrow\downarrow}$,[27] which are discussed in Sec. 2.4. The real part $\operatorname{Re} G_\alpha^{\uparrow\downarrow}$ is the material parameter that is proportional to the spin-transfer torque.[39, 38] The imaginary part $\operatorname{Im} G_\alpha^{\uparrow\downarrow}$ reflects the spin-dependent interface phase shifts and affects the magnetization and spin accumulation dynamics as an effective exchange magnetic field parallel to the magnetization direction.[40, 28, 38] $\operatorname{Im} G_\alpha^{\uparrow\downarrow}$ is relatively small for intermetallic interfaces,[41] but is in general comparable in magnitude to the other conductance parameters.[40, 45] The nonlocal interface exchange has been discussed in similar terms for spin valves consisting of Luttinger liquids with ferromagnetic contacts.[23]

The blocking of transport by the Coulomb charging is usually described by Fermi's Golden Rule (see below), which employs a probability (squared matrix elements) and energy conservation. As long as the charging energy is much smaller than atomic energy scales (like the Fermi energy), the junction parameters such as the interface transparency and spin-mixing conductance are unaffected and the Coulomb blockade is governed by the energy conservation criterion only. This implies that the exchange effect can be described by the $\operatorname{Im} G_\alpha^{\uparrow\downarrow}$ of the bare junction.

It remains to parametrize the exchange in the limit of the tunneling Hamiltonian, i.e. to lowest order in the interface transmission. We show below that this is achieved by adding the following exchange term $H_{\mathrm{ex}\alpha}$ to the Hamiltonian for the two leads:

$$H_{\mathrm{ex}\alpha} = \sum_{ks} \Delta\epsilon_{\alpha ks} c_{\alpha ks}^\dagger c_{\alpha ks}. \tag{2.6}$$

The energy shifts $\Delta\epsilon_{\alpha ks}$, see Eq. (2.42), are proportional to the inverse density of states, but they remain relevant for small level splitting because the dwell time is inversely proportional to the average energy-level separation or inverse density of states $\delta = \rho_N^{-1}$. This Hamiltonian is an effective Zeeman splitting caused by an exchange magnetic field in the direction of the magnetization, see Sec. 2.4.2.

2.3.2 Virtual tunneling processes (X2)

The interface exchange term X1 is a property of the separate interfaces and they contribute independently. The second type of exchange (X2) felt by the spins on the island is a property of the entire device. It originates from virtual tunneling processes, corresponding to single-electron transfer from and to the cluster. In the tunneling regime, this process can be treated and understood in terms of perturbation theory. In the absence of tunneling, the number of electrons on the island is a good quantum number. The perturbation by the contact to the electrodes allows mixing in of states in which the number of electrons on the island is changed by unity, at the cost of the charging energy. In second-order perturbation theory this results in an energy gain represented by a sum over (virtually) excited states in which the Coulomb energy appears in the denominator and the tunneling probability in the numerator. When the leads are nonmagnetic, these virtual processes correspond to a quantum correction to the average charge on the central electrode.[42, 43] This effect depends strongly on the applied gate voltage. When the unperturbed $N + 1$ ($N - 1$) particle ground state is tuned in energy just above the N particle state, the quantum correction will be large and positive (negative). At the degeneracy point, perturbation theory breaks down, but the ensuing divergence can be controlled by taking into account finite temperatures.

When the tunneling probabilities to the ferromagnetic contacts are spin dependent, the deviations from the exact quantized charge on the island become spin dependent, and therefore lead to a net excess of spins in the ground state that depends on the configuration of the contact magnetizations. For a symmetric spin valve it is easy to see that the island ground state magnetization due to these virtual processes X2 is maximal for parallel magnetizations and vanishes for antiparallel ones.

The additional exchange affects nonequilibrium electron transport, in contrast to higher-order so-called co-tunneling processes, to the same order as the in- and out-tunneling processes. For a quantum-dot island with a single quantized level, König and Martinek[15] showed that in the case of *noncollinear* magnetizations the nonequilibrium spins on an island injected

by a finite source-drain voltage are dephased by precessing around the effective exchange field. This effect was also discussed for few-level quantum dots.[20] Since X1 discussed in Sec. 2.3.1 is a material constant, the gate voltage dependence of X2 provides a handle for an experimental discrimination of the two effects. We derive an expression for the effective X2 exchange field for a classical SV-SET in Sec. 2.4.2.

2.4 Charge and spin transport

We compute the transport characteristics of the SV-SET in lowest-order perturbation theory[44] for a diffusive or chaotic island in the sequential tunneling regime. The rate equations lead to a probability distribution for the excess number of charges n_N. The excess spin accumulation $\vec{s}$ contains a large number of spins and we are interested in its average value in the steady state that is found from the condition $\langle d\vec{s}/dt \rangle = 0$.

2.4.1 Charge transfer

The operators for the excess number of electrons on the island and on the two leads are $n_N = \sum_{ks} c_{ks}^\dagger c_{ks}$ and $n_{F\alpha} = \sum_{ks} a_{\alpha ks}^\dagger a_{\alpha ks}$, respectively. The unpaired spin angular momentum on the cluster is written as $\vec{s} = (\hbar/2) \sum_{kss'} c_{ks}^\dagger \vec{\sigma}_{ss'} c_{ks'}$, where $\vec{\sigma} = (\sigma_x, \sigma_y, \sigma_z)$ is the vector of Pauli spin matrices. It is convenient to introduce a vector chemical potential $\overrightarrow{\Delta\mu}$ in the island, with size $\left|\overrightarrow{\Delta\mu}\right| = 2 \left|\langle \vec{s} \rangle\right| / (\rho_N \hbar)$ (see also Ref. [13]), where ρ_N is the density of states at the Fermi energy. We can take into account Stoner enhancement intra-island exchange effects in terms of the static susceptibility χ_s, and we may also write $\Delta\mu = 2\mu_B^2 \left|\langle \vec{s} \rangle\right| / (\chi_s \hbar)$. We denote the unit vector in the direction of the spin accumulation by $\hat{s}$.

The charge current is equal to the expectation values for the rate of change of n_N. In terms of the tunneling Hamiltonian $H_T = H_{T1} + H_{T2}$ the

time evolution is given by

$$\frac{dn_N}{dt} = \frac{i}{\hbar} [H_T, n_N]$$

$$= \frac{i}{\hbar} \sum_{\alpha kqs'} T^{\alpha}_{kqs'} a^{\dagger}_{\alpha ks'} c_{\alpha qs'} + H.c.. \tag{2.7}$$

We use the interaction representation, and write the total Hamiltonian as $H = H' + H_T$. To second order in H_T we have

$$\left\langle \frac{dn_N(t)}{dt} \right\rangle = \frac{i}{\hbar} \int\limits_{-\infty}^{t} dt' \left\langle \left[\frac{dn_N(t)}{dt}, H_T(t') \right] \right\rangle_{\circ}, \tag{2.8}$$

where $\langle .. \rangle_{\circ}$ denotes an expectation value with respect to Hamiltonian H'. The electrochemical potentials of the two reservoirs are $\mu_{cF1} = eV/2$ and $\mu_{cF2} = -eV/2$. It is convenient to introduce grand canonical Hamiltonians including the chemical potentials as[23, 44]

$$K_N = H_N - \hbar^{-1}\overrightarrow{\Delta\mu} \cdot \vec{s}, \tag{2.9}$$

$$K_{F_\alpha} = H_{F_\alpha} - \mu_{cF_\alpha} n_{F_\alpha}. \tag{2.10}$$

The time dependence $c_{ks}(t) = e^{(i/\hbar)K_N t} c_{ks} e^{-(i/\hbar)K_N t}$ can be formulated in terms of the projection operators

$$\hat{u}^{\uparrow}(\hat{s}) = \frac{1}{2} (I + \hat{s} \cdot \overrightarrow{\sigma}), \tag{2.11}$$

$$\hat{u}^{\downarrow}(\hat{s}) = \frac{1}{2} (I - \hat{s} \cdot \overrightarrow{\sigma}), \tag{2.12}$$

where I is the unit matrix, by making use of the equality

$$e^{(i/\hbar^2)\overrightarrow{\Delta\mu}\cdot\vec{s}t} c_{ps'} e^{-(i/\hbar^2)\overrightarrow{\Delta\mu}\cdot\vec{s}t} = \sum_{s''} \left[e^{-(i/\hbar)(\Delta\mu/2)t} \hat{u}^{\uparrow}(\hat{s}) \right.$$

$$\left. + e^{(i/\hbar)(\Delta\mu/2)t} \hat{u}^{\downarrow}(\hat{s}) \right]_{s's''} c_{ps''}. \tag{2.13}$$

The leads and the island are supposed to be in thermal equilibrium, so that $\langle c_{ks'}^\dagger c_{k's''} \rangle_\circ = f(\epsilon_{ks'}) \delta_{kk'} \delta_{s's''}$, with Fermi-Dirac distribution $f(\epsilon) \equiv (1 + e^{\beta\epsilon})^{-1}$, where β is the inverse temperature. Using the expression for the matrix elements

$$\left[U(\theta_\alpha) u^{s''}(\hat{s}) U(\theta_\alpha)^\dagger \right]_{s's'} = \frac{1}{2} \left(1 + s's''\hat{s} \cdot \overrightarrow{m}_\alpha \right),$$
$$\text{with } s', s'' \in \{\uparrow, \downarrow\} = \{+, -\}, \tag{2.14}$$

the rate of change of the number of electrons on the island reads

$$\left\langle \frac{dn_N}{dt} \right\rangle_{n_N=m} = \sum_{\alpha s''} \frac{1}{2e^2} \left(G_\alpha + s'' P_\alpha G_\alpha \hat{s} \cdot \overrightarrow{m}_\alpha \right) \times$$
$$\left[-F \left(-E_{m-1} + E_m - \mu_{cF\alpha} + s'' \frac{\Delta\mu}{2} \right) \right.$$
$$\left. +F \left(E_m - E_{m+1} + \mu_{cF\alpha} - s'' \frac{\Delta\mu}{2} \right) \right], \tag{2.15}$$

where $F(\epsilon) \equiv \epsilon \left(1 - e^{-\beta\epsilon} \right)^{-1}$ and $E_m \equiv e^2 (m - C_G V_G/e)^2 / 2C$. The relation between the up and down spin conductances ($G_\alpha^{\uparrow\uparrow}$ and $G_\alpha^{\downarrow\downarrow}$) and the tunneling coefficients is $G_\alpha^{ss} = \left(\pi e^2/\hbar \right) \rho_N \rho_{F\alpha s} |T_s^\alpha|^2$, where $|T_s^\alpha|^2$ is the value of $|T_{kqs}^\alpha|^2$ at the Fermi energy averaged over all the modes. $\rho_{F\alpha s}$ is the spin-dependent density of states in ferromagnet α.

In the low-bias regime considered here we can linearize Eq. (2.15) in $\Delta\mu$ and $\mu_{cF\alpha}$. The resulting expression for the rate for electron tunneling through contact α, increasing the excess number of electrons n_N from "0" to "1," is denoted by $\Gamma_\alpha^{0 \to 1}$. The analogous rate for removing one electron when n_N is "1" is $\Gamma_\alpha^{1 \to 0}$. Explicitly, we find

$$\Gamma_\alpha^{0\to1}(V,V_G,\overrightarrow{\Delta\mu}) = \frac{G_\alpha}{e^2}F(E_0-E_1) + \frac{G_\alpha}{e^2}F'(E_0-E_1) \times$$
$$\left(-\mu_{cF\alpha} + \frac{\Delta\mu}{2}P_\alpha\hat{s}\cdot\overrightarrow{m}_\alpha\right), \qquad (2.16)$$

$$\Gamma_\alpha^{1\to0}(V,V_G,\overrightarrow{\Delta\mu}) = \frac{G_\alpha}{e^2}F(E_1-E_0) - \frac{G_\alpha}{e^2}F'(E_1-E_0) \times$$
$$\left(-\mu_{cF\alpha} + \frac{\Delta\mu}{2}P_\alpha\hat{s}\cdot\overrightarrow{m}_\alpha\right). \qquad (2.17)$$

Now that we have determined the tunneling rates we can write down the master equation for electron transport in the orthodox model. We consider a regime in which $eV \ll k_BT \ll e^2/2C$, and restrict ourselves to a gate voltage range for which the excess number of electrons n_N alternates between "0" and "1" ($0 < C_GV_G < e$), knowing that the results will periodically repeat with this period. The center of the Coulomb oscillation for transitions between $n_N = $ "0" and "1" electrons is at $C_GV_G = e/2$.

The steady state on the island is characterized by a constant spin accumulation (to be determined below) and the probabilities p_0 and p_1 that there are "0" or "1" excess electrons. We have $p_0 + p_1 = 1$. The rate equation for the probabilities is

$$dp_n/dt = -p_n\left(\Gamma^{n\to n+1} + \Gamma^{n\to n-1}\right) + p_{n+1}\Gamma^{n+1\to n} + p_{n-1}\Gamma^{n-1\to n}. \quad (2.18)$$

From the condition of detailed balance, $p_0\Gamma^{0\to1} = p_1\Gamma^{1\to0}$, we find

$$p_0(V,V_G,\overrightarrow{\Delta\mu}) = f(E_0-E_1) + \frac{\beta f(E_0-E_1)f(E_1-E_0)}{G_1+G_2} \times$$
$$\sum_\alpha\left(G_\alpha\mu_{cF\alpha} - P_\alpha G_\alpha\frac{\Delta\mu}{2}\hat{s}\cdot\overrightarrow{m}_\alpha\right). \qquad (2.19)$$

The expression for the conductance of the SV-SET as a function of the spin accumulation can now be calculated and reads

$$G(V,V_G,\overrightarrow{\Delta\mu}) = -ep_0\Gamma_1^{0\to1} + ep_1\Gamma_1^{1\to0} \qquad (2.20)$$
$$= \frac{G_1G_2}{G_1+G_2}\frac{\beta(E_0-E_1)}{2\sinh\beta(E_0-E_1)}\left[1 - \frac{\Delta\mu}{2eV}\hat{s}\cdot(P_1\overrightarrow{m}_1 - P_2\overrightarrow{m}_2)\right].$$

2.4.2 Spin accumulation

The steady-state spin accumulation is found by setting the total rate of change of $\vec{s}$ to zero. There are several contributions to the dynamics of the spin accumulation:

$$\left\langle \frac{d\vec{s}}{dt} \right\rangle = p_0 \left\langle \frac{d\vec{s}}{dt} \right\rangle_{n_N=0} + p_1 \left\langle \frac{d\vec{s}}{dt} \right\rangle_{n_N=1}$$

$$+ \sum_\alpha \left\langle \frac{d\vec{s}}{dt} \right\rangle_{\text{ex}\alpha} + \left\langle \frac{d\vec{s}}{dt} \right\rangle_{\text{magn}} + \left\langle \frac{d\vec{s}}{dt} \right\rangle_{\text{sf}}. \qquad (2.21)$$

The first two terms are due to the tunneling processes, the remaining ones to exchange, external magnetic fields, and spin flip. We start from

$$\frac{d\vec{s}}{dt} = \frac{i}{\hbar} \left[H_T, \vec{s} \right], \qquad (2.22)$$

with an expectation value that to second order in H_T reads

$$\left\langle \frac{d\vec{s}(t)}{dt} \right\rangle = \frac{i}{\hbar} \int_{-\infty}^{t} dt' \left\langle \left[\frac{d\vec{s}(t)}{dt}, H_T(t') \right] \right\rangle. \qquad (2.23)$$

The spin current (rate of change of the spin angular momentum) due to tunneling when m excess electrons are on the island reads [cf. Eq. (2.15)]

$$
\left\langle \frac{d\vec{s}}{dt} \right\rangle_{n_N=m} = \frac{\hbar}{4e^2} \sum_{\alpha s''} \left(G_\alpha s'' \hat{s} + P_\alpha G_\alpha \overrightarrow{m}_\alpha \right) \times
$$

$$
\left[-F \left(-E_{m-1} + E_m - \mu_{cF\alpha} + s'' \frac{\Delta\mu}{2} \right) \right.
$$

$$
\left. + F \left(-E_{m+1} + E_m + \mu_{cF\alpha} - s'' \frac{\Delta\mu}{2} \right) \right] \qquad (2.24)
$$

$$
+ \frac{\hbar}{4\pi e^2} \sum_{\alpha s''} P_\alpha G_\alpha s'' \left(\overrightarrow{m}_\alpha \times \hat{s} \right) \times
$$

$$
\left(\int d\epsilon_1 \int' d\epsilon_2 \frac{f(\epsilon_1)(1-f(\epsilon_2))}{\left(\epsilon_2 - \epsilon_1 + E_{m-1} - E_m + \mu_{cF\alpha} - s'' \frac{\Delta\mu}{2} \right)} \right.
$$

$$
\left. - \int d\epsilon_1 \int' d\epsilon_2 \frac{f(\epsilon_2)(1-f(\epsilon_1))}{\left(\epsilon_2 - \epsilon_1 + E_m - E_{m+1} + \mu_{cF\alpha} - s'' \frac{\Delta\mu}{2} \right)} \right),
$$

where the prime denotes a principal value integral. Here we used the relation:

$$
\left[U(\theta_\alpha) u^{s''}(\hat{s}) \sigma^i U(\theta_\alpha)^\dagger \right]_{s's'} = \frac{1}{2} s'' \hat{s} + \frac{1}{2} s' \overrightarrow{m}_\alpha + \frac{1}{2} i s' s'' \left(\overrightarrow{m}_\alpha \times \hat{s} \right), \quad (2.25)
$$

$$
\text{with } s', s'' \in \{\uparrow, \downarrow\} = \{+, -\}.
$$

To first order in the small induced energy shifts the exchange Hamiltonian $H_{\text{ex}\alpha}$ modifies the unpaired spins as

$$
\left. \frac{d\vec{s}}{dt} \right|_{\text{ex}\alpha} = \frac{i}{\hbar} \left[H_{\text{ex}\alpha}, \vec{s}(t) \right], \qquad (2.26)
$$

which results in a precession:

$$
\left\langle \frac{d\vec{s}}{dt} \right\rangle = \frac{1}{\hbar M} \sum_m \left(\Delta\epsilon_{\alpha m\uparrow} - \Delta\epsilon_{\alpha m\downarrow} \right) \langle \vec{s} \rangle \times \vec{m}_\alpha, \qquad (2.27)
$$

where M is the number of transport channels in the normal metal and the energy shifts $\Delta\epsilon$ are found in Eq. (2.42).

The conductance parameters of an F|N contact are[27]

$$G_\alpha^{ss'} \equiv \frac{e^2}{h} \sum_{nm} \left(\delta_{nm} - r_{s\alpha}^{nm} \left(r_{s'\alpha}^{nm}\right)^*\right), (s, s' \in \uparrow, \downarrow). \qquad (2.28)$$

Here n and m denote the transport channels in the normal metal and $r_{\uparrow\alpha}^{nm}$ and $r_{\downarrow\alpha}^{nm}$ are the corresponding spin-dependent reflection coefficients. The contact conductances for spin-up and spin-down electrons are $G_\alpha^{\uparrow\uparrow}$ and $G_\alpha^{\downarrow\downarrow}$ and the mixing conductance $G_\alpha^{\uparrow\downarrow}$ governs the transverse spin currents that are absorbed and reflected by the ferromagnet α. The current polarized normal to the magnetization but in the plane of $\vec{s}$ and $\vec{m}_\alpha$ is proportional to $\operatorname{Re} G_\alpha^{\uparrow\downarrow}$ and describes the spin transfer to the magnet, thereby dissipating the spin accumulation. In the case of tunnel junctions $\operatorname{Re} G_\alpha^{\uparrow\downarrow} \to G_\alpha/2$. The out-of-the $\vec{s}, \vec{m}_\alpha$ plane spin current is caused by reflection processes that make spins precess around $\vec{m}_\alpha$ and is proportional to $\operatorname{Im} G^{\uparrow\downarrow}$. This mixing conductance has been evaluated from first principles for various contact materials and is small for intermetallic interfaces because positive and negative contributions in the space spanned by the transport channels average out.[41] However, there is no general reason that $\operatorname{Im} G^{\uparrow\downarrow}$ should be smaller than G or $\operatorname{Re} G^{\uparrow\downarrow}$. It is known to be quite large for the Fe|InAs interface[45] and found to be very significant for the magnetization dynamics of MgO magnetic tunnel junctions.[29] For a simple model barrier discussed in Appendix 2.9, we find the value $\operatorname{Im} G^{\uparrow\downarrow}/G = -0.26$. Using the relation between the reflection phases and the energy shifts as derived in Eq. (2.42), we can rewrite the contribution given in Eq. (2.27) in terms of the imaginary part of the mixing conductance as (cf. Ref. [22])

$$\left\langle \frac{d\vec{s}}{dt} \right\rangle_{\text{ex}\alpha} = \frac{\operatorname{Im} G_\alpha^{\uparrow\downarrow}}{\rho_N e^2} \vec{m}_\alpha \times \langle\vec{s}\rangle. \qquad (2.29)$$

The spin accumulation can also be affected by a magnetic field $\vec{B}$, which can either be externally applied, a stray field from the ferromagnets, or an

internal anisotropy field. The spin accumulation induced by this magnetic field can safely be neglected, but the induced precession of the spin accumulation is relevant, and is given by

$$\left\langle \frac{d\vec{s}}{dt} \right\rangle_{\text{magn}} = \frac{g\mu_B}{\hbar} \vec{B} \times \langle \vec{s} \rangle.$$ (2.30)

Finally, spin-flip relaxation in the normal metal is taken into account by spin-accumulation decay with a spin-flip relaxation time τ_{sf},

$$\left\langle \frac{d\vec{s}}{dt} \right\rangle_{\text{sf}} = -\frac{\langle \vec{s} \rangle}{\tau_{\text{sf}}}.$$ (2.31)

Combining the terms in Eq. (2.21), the spin accumulation should fulfill the stationary state condition:

$$\left\langle \frac{d\vec{s}}{dt}(V, V_G) \right\rangle = \frac{\hbar}{2e^2} \frac{\beta (E_0 - E_1)}{2 \sinh \beta (E_0 - E_1)} \left[\frac{G_1 G_2}{G_1 + G_2} eV (P_1 \vec{m}_1 - P_2 \vec{m}_2) \right.$$
$$\left. - (G_1 + G_2) \frac{\Delta\mu}{2} \left(\hat{s} + \left(\hat{s} \cdot \vec{b} \right) \vec{b} \right) \right]$$
$$+ \frac{g\mu_B}{\hbar} \vec{B}_{\text{eff}} \times \langle \vec{s} \rangle - \frac{\langle \vec{s} \rangle}{\tau_{\text{sf}}} = 0,$$ (2.32)

where

$$\vec{b} \equiv \frac{P_1 G_1}{G_1 + G_2} \vec{m}_1 + \frac{P_2 G_2}{G_1 + G_2} \vec{m}_2.$$ (2.33)

The total effective magnetic field $\vec{B}_{\text{eff}}$ consists of the external magnetic field and contributions from the exchange effects X1 and X2, and reads

$$\vec{B}_{\text{eff}}(V_G) = \vec{B} + \vec{B}_{X1} + \vec{B}_{X2}(V_G),$$ (2.34)

$$\text{with } \vec{B}_{X1} = \frac{\hbar}{\rho_N g \mu_B e^2} \sum_\alpha \text{Im} \, G_\alpha^{\uparrow\downarrow} \vec{m}_\alpha, \tag{2.35}$$

$$\vec{B}_{X2}(V_G) = -\frac{\hbar}{2\rho_N g \mu_B e^2} (G_1 + G_2) \vec{b} \tag{2.36}$$

$$\left[\frac{1}{\pi} f(E_0 - E_1) \int d\epsilon f'(\epsilon) \, \eta \left(\epsilon + E_0 - E_{-1}, \frac{e^2}{C} \right) \right.$$

$$\left. + \frac{1}{\pi} f(E_1 - E_0) \int d\epsilon f'(\epsilon) \, \eta \left(\epsilon + E_1 - E_0, \frac{e^2}{C} \right) \right].$$

Here we introduced[15]

$$\eta(\varepsilon, U) \equiv \int' d\varpi \left(\frac{1 - f(\varpi)}{\varpi - \varepsilon} + \frac{f(\varpi)}{\varpi - \varepsilon - U} \right) \tag{2.37}$$

$$= -\text{Re} \left[\Psi \left(\frac{1}{2} + \frac{i\beta\varepsilon}{2\pi} \right) - \Psi \left(\frac{1}{2} + \frac{i\beta(\varepsilon + U)}{2\pi} \right) \right],$$

where $\Psi(z)$ is the Digamma function. In appendix 2.10 we discuss the derivation of the expression for $\vec{B}_{X2}$ in more detail and comment on the differences compared to the case of a single-level quantum dot.

2.5   Results and discussion

Figure 2.2 shows the magnitude of the total effective magnetic field $\vec{B}_{\text{eff}}$ as a function of gate voltage (solid line) for a symmetric spin valve with parallel magnetizations (it vanishes for the antiparallel configuration) and a polarization $P_1 = 0.7$. The X1 term is a constant that does not depend on gate voltage (dotted line). $\vec{B}_{X2}$ vanishes when $C_G V_G$ equals 0, $e/2$ and e. At these points, contributions from incoming and outgoing electrons cancel each other (see Appendix 2.10). The curve repeats as a function of gate voltage with period e/C_G. The spin accumulation on the island found from Eq. (2.32) tends to suppress the current through the system. Spin-flip and exchange effects that dissipate or dephase the spin accumulation therefore increase the conductance. As a reference we list here the conductance $G(\theta)$
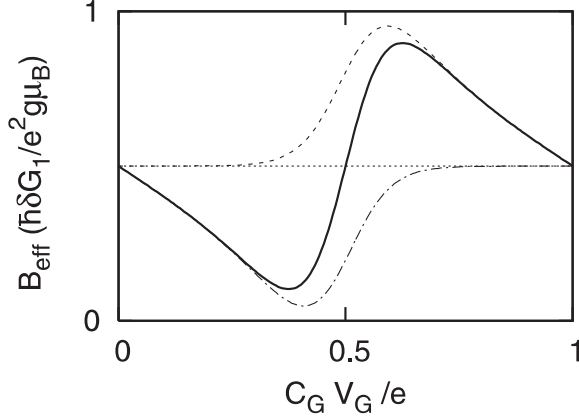
Fig. 2.2: The effective magnetic-field strength $\left|\vec{B}_{\text{eff}}\right|$ as a function of gate voltage (solid line) for a spin valve in the parallel configuration. The parameters are $G_1 = G_2$, $P_1 = P_2 = 0.7$, $\operatorname{Im} G_1^{\uparrow\downarrow} = \operatorname{Im} G_2^{\uparrow\downarrow} = G_1/4$, and $e^2/(2C) = 10k_BT$. The imaginary part of the mixing conductance gives a constant offset (dotted). The dot-dashed and dashed curves show the effective field for zero and one excess electron on the island.

for a spin valve *without interaction*, with equal conductance parameters for the left and the right tunneling barrier $G_1 = G_2$, $P_1 = P_2$:

$$G(\theta) = \frac{G_1}{2}\left(1 - \frac{P_1^2 G_1\left(G_1 + 2G_{sf}\right)\sin^2\theta/2}{[G_1 + 2G_{sf}]^2 + \left[2\cos(\theta/2)\operatorname{Im}G_1^{\uparrow\downarrow}\right]^2}\right). \qquad (2.38)$$

The final result for the symmetric spin-valve *with interaction* can be obtained simply from this expression by the substitutions

$$G_1 \to \frac{\beta\left(E_0 - E_1\right)}{2e\sinh\beta\left(E_0 - E_1\right)}G_1, \qquad (2.39)$$

$$\operatorname{Im}G_1^{\uparrow\downarrow} \to \frac{e^2}{\hbar}\frac{\rho_N g\mu_B B_{\text{eff}}}{2\cos(\theta/2)}. \qquad (2.40)$$

For nonmagnetic contacts ($P_1 = 0$) this result reduces to the known expression for normal-metal single-electron transistors.[46]
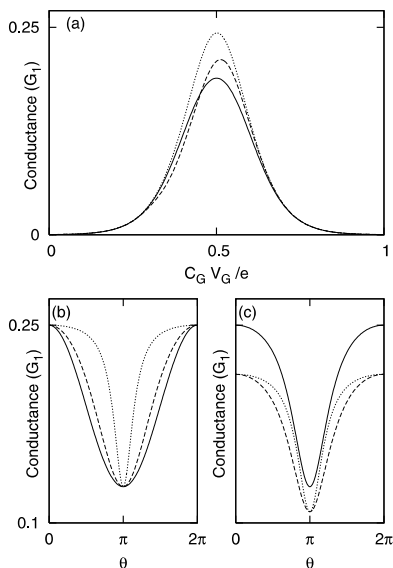

Fig. 2.3: (a) Coulomb oscillations at fixed angle $\theta = \pi/2$ for a symmetric SV-SET with ratio $\operatorname{Im} G_1^{\uparrow\downarrow}/G_1 = 0$ (solid), 0.25 (dashed), and 1 (dotted) in units of G_1. The polarization P is 0.7 and $G_{sf} = 0$. (b) Conductance as a function of the angle for the same parameters as in (a), with $C_G V_G$ fixed to 0.5. (c) Conductance as a function of θ with $\operatorname{Im} G_1^{\uparrow\downarrow}/G_1 = 0.25$. Results are shown for $C_G V_G$ equal to 0.45 (dashed), 0.5 (solid), and 0.55 (dotted).

As shown in Fig. 2.3(a), changing the relative strengths of X1 and X2, or, since the X2 contribution is proportional to the polarization of the leads, $\operatorname{Im} G_\alpha^{\uparrow\downarrow}/P_\alpha G_\alpha$, qualitatively modifies the current profile of the Coulomb oscillations. The constant offset given by B_{X1} skews the exchange field around $C_G V_G = e/2$, causing asymmetric conductance curves. When the offset starts to dominate the symmetry gets restored. The X2 contribution vanishes when the Coulomb blockade is lifted ($C_G V_G = e/2$), so the angular

dependence of the conductance for different values of $\mathrm{Im}\,G_1^{\uparrow\downarrow}/G_1$ in Fig. 2.3(b) reflects only the X1 effect. The curve is a simple cosine for $\mathrm{Im}\,G_1^{\uparrow\downarrow} = 0$, but is sharpened for larger $\mathrm{Im}\,G_1^{\uparrow\downarrow}$ because of the dephasing of the spin accumulation occurring for noncollinear angles. In Fig. 2.3(c) $\mathrm{Im}\,G_1^{\uparrow\downarrow}/G_1$ is fixed to 0.25 and curves are plotted for different values of the gate voltage. It can be seen that the angular dependence differs because the X2 depends on V_G in an asymmetric way around $C_G V_G = e/2$.

As can be seen in Fig. 2.4, the shape of the Coulomb oscillation can develop minima when the polarization is high and the magnetizations are nearly antiparallel. At the values of gate voltage where the X1 and X2 exchange effects cancel, the spin accumulation is not dephased and the conductance is suppressed.
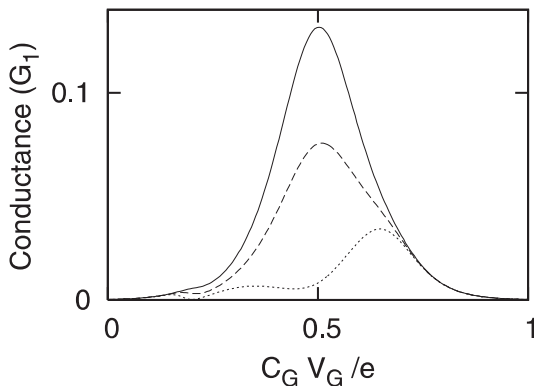

Fig. 2.4: Conductance as a function of gate voltage for a symmetric SV-SET with $\theta = 0.9\pi$, $\mathrm{Im}\,G_1^{\uparrow\downarrow}/G_1 = 0.15$, and $G_{sf} = 0$. Curves are shown for $P_1 = 0.7$ (solid), $P_1 = 0.85$ (dashed), $P_1 = 1$ (dotted).

Figure 2.5 shows results for the conductance and spin accumulation as a function of applied magnetic field in the x (solid line), y (dashed), and z (dotted) directions. The spin valve is again symmetric with $P_1 = 0.7$ and $\mathrm{Im}\,G_1^{\uparrow\downarrow} = G_1/4$. The angle θ is fixed to $\pi/2$ and $C_G V_G = e/2$. The conductance then depends only on the x component of the spin accumulation [see Eq. (2.20)]. Without applied magnetic field, the spin accumulation has

components in the x and y directions, while $\vec{B}_{\text{eff}}$ is in the y direction. The results can be understood in terms of the dephasing of the spin accumulation by the magnetic-field induced precession that, for sufficiently large and noncollinear magnetic fields, quenches the spin accumulation. This "Hanle" effect is responsible for the conductance minimum at negative applied magnetic field in the y direction. In Fig. 2.5(c) only two curves are visible because the curves for magnetic fields in the x and y directions overlap.

2.6 Summary

We studied the transport properties of single-electron spin valve transistors as a function of the magnetization configurations in the orthodox model of the Coulomb blockade. Two types of exchange effects between the spin accumulation on the island and the lead magnetizations play a role: a non-local interface exchange effect (X1) and exchange due to virtual tunneling processes (X2). For metallic dots these two effects are found to be of comparable magnitude. We predict that a line-shape analysis of the Coulomb oscillation peaks should help to experimentally disentangle the two contributions. Additional information can be obtained by the Hanle effect.

2.7 Acknowledgements

2.8 Energy shifts

Let us consider a normal-metal island in contact to a ferromagnet by a tunnel barrier (see Fig. 2.6) without Coulomb interaction. We wish to calculate the spin-dependent shifts of the energy levels due to the presence
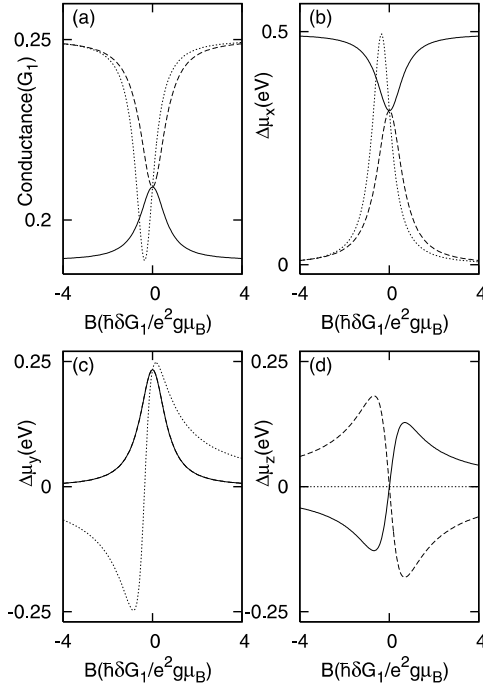
Fig. 2.5: (a) Conductance as a function of a magnetic field applied along the x (solid), y (dashed) or z (dotted) direction in units of G_1. The SV-SET has symmetric junction parameters, with polarizations $P_1 = 0.7$, $\mathrm{Im}\, G_1^{\uparrow\downarrow} = G_1/4$ and $G_{sf} = 0$. The magnetizations are fixed to $\overrightarrow{m}_{1/2} = (\pm 1, 0, 1)/\sqrt{2}$, yielding an angle $\theta = \pi/2$ and $C_G V_G = e/2$. (b)-(d) The x, y, and z components of the spin accumulation for the same parameters. The curves in (c) for magnetic fields in the x and y directions overlap.

of the F|N contact. In Ref. [30] an analogous calculation was done for a ballistic one-dimensional quantum wire. Here we consider an island in the quasiclassical regime, i.e. the de Broglie wavelength is much smaller than the size of the island.

The Bohr-Sommerfeld quantization rule [47]

$$\frac{1}{\hbar} \oint p^m(x)\, dx + \phi_0^m + \phi_s^m = 2\pi \left(n + \frac{1}{2}\right) \qquad (2.41)$$

can be used to find the energy shifts, where $p^m(x)$ is the classical momentum for an electron in mode m, and n is an integer. The integral is over a whole period of the classical motion in the quasiclassical region. The total phase shift due to the reflections at the turning points is $\phi_0^m + \phi_s^m$, where ϕ_0^m is the spin-independent phase shift picked up during the reflections from the boundaries for an isolated island without contact to the ferromagnet. The small spin-dependent phase shift $\phi_s^m \ll 1$ arises from the weak coupling to the ferromagnet. The phase shifts have to be computed quantum mechanically via the spin-dependent reflection coefficients r_s^{mm} for mode m at an interface that is assumed to be specular (see also Appendix 2.9).
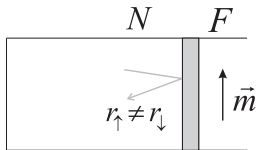

Fig. 2.6: A normal-metal island with tunnel contact to a ferromagnetic lead.

From Eq. (2.41), we see that increasing the quantum number n by one corresponds to introducing an extra phase period that increases the kinetic energy by M/ρ_N, where ρ_N is the density of states of the island and M is the number of modes. The energy shift for an electron in mode m is therefore, to linear order in ϕ_s^m,

$$\Delta\epsilon_{ms} = -\frac{M}{\rho_N} \frac{\phi_s^m}{2\pi}. \qquad (2.42)$$

The effect of the interface on the island states can be taken into account by introducing an effective Hamiltonian as in Eq. (2.6). In the case of a spin-independent tunneling barrier to a ferromagnet, the spin splitting of the energy levels is small, of the same order as the transmission probability (see Appendix 2.9).

2.9   Rectangular barriers

Here we evaluate the spin-mixing conductance $G^{\uparrow\downarrow}$ for a model barrier, giving more details of the results of Ref. [22]. We consider a smooth rectangular barrier between a normal metal and a Stoner-model ferromagnet. The solution of the Schrödinger equation for spin s in the normal metal, $\psi_s^m(x, y, z)$ can be used to determine the reflection coefficients r_s^{mm} for each mode m. It reads

$$\psi_s^m(x, y, z) = \frac{\chi^m(x, y, z)}{\sqrt{k_N^m}} \left(e^{ik_N^m x} + r_s^{mm} e^{-ik_N^m x} \right), \qquad (2.43)$$

where $\chi^m(y, z)$ is the transverse wave function and k_N^m is the longitudinal wave number for mode m in the normal metal. In terms of the wave numbers in the normal metal k_N^m, barrier k_B^m, and ferromagnet k_{Fs}^m for a given energy, the reflection coefficient for mode m at the barrier reads

$$r_s^{mm} = \rho(k_N^m, k_B^m) + e^{2iak_B^m} \tau(k_N^m, k_B^m)\rho(k_B^m, k_{Fs}^m)\tau(k_B^m, k_N^m), \qquad (2.44)$$

where a is the barrier thickness and

$$\tau(k_1, k_2) \equiv \frac{2\sqrt{k_1 k_2}}{k_1 + k_2}, \qquad (2.45)$$

$$\rho(k_1, k_2) \equiv \frac{k_1 - k_2}{k_1 + k_2}. \qquad (2.46)$$

For a tunneling barrier, k_B^m is imaginary and the spin-dependent correction to the reflection coefficient is exponentially small in the barrier thickness.

For a numerical estimate we use a Fermi energy in the normal metal of 2.6 eV, a barrier height of 3 eV and barrier thickness of $a = 1\,\mathrm{nm}$. The Fermi momenta in the ferromagnet are taken to be $k_{F\uparrow} = 1.09 \mathring{A}^{-1}$ and $k_{F\downarrow} = 0.42 \mathring{A}^{-1}$ (characteristic for Fe, see Ref. [39]). For the spin-mixing conductance $G^{\uparrow\downarrow}$, Eq. (2.28), we find that $\operatorname{Im} G^{\uparrow\downarrow}/G = -0.26$ for this choice of parameters. The effective field due the interface exchange effect is therefore not negligible compared to the conductance parameters. More realistic electronic structure calculations[45] should be carried out to obtain better estimates.

2.10 X2 exchange in classical dots

Here we present more details concerning the derivation of Eq. (2.36) for the effective exchange field X2 in classical SV-SET's, that complement the derivation in Refs. [15] for single-level quantum dots. Since the model is periodic in the gate voltage with period e/C_G, we restrict our discussion to the range $0 < C_G V_G < e$. From Eq. (2.21), the contributions from virtual tunneling processes to the rate of change of $\vec{s}$ then read

$$\left\langle \frac{d\vec{s}}{dt} \right\rangle_{X2} = p_0 \left\langle \frac{d\vec{s}}{dt} \right\rangle_{X2,n_N=0} + p_1 \left\langle \frac{d\vec{s}}{dt} \right\rangle_{X2,n_N=1} . \tag{2.47}$$

Using the spin currents from Eq. (2.24), we obtain, e.g.

$$\left\langle \frac{d\vec{s}}{dt} \right\rangle_{X2,n_N=0} = \frac{\hbar}{4\pi e^2} \sum_{\alpha s''} P_\alpha G_\alpha s'' \left(\vec{m}_\alpha \times \hat{s} \right) \times \tag{2.48}$$

$$\left(\int d\epsilon_1 \int' d\epsilon_2 \frac{f(\epsilon_1)(1 - f(\epsilon_2))}{\left(\epsilon_2 - \epsilon_1 + E_{-1} - E_0 + \mu_{cF\alpha} - s'' \frac{\Delta\mu}{2} \right)} \right.$$

$$\left. - \int d\epsilon_1 \int' d\epsilon_2 \frac{f(\epsilon_2)(1 - f(\epsilon_1))}{\left(\epsilon_2 - \epsilon_1 + E_0 - E_1 + \mu_{cF\alpha} - s'' \frac{\Delta\mu}{2} \right)} \right).$$

The first term in brackets describes virtual processes in which an electron tunnels out of the island, and the second term corresponds to incoming electrons. The expressions for the energy differences are given by

$$E_{-1} - E_0 = (C_G V_G + e/2)\, e/C, \tag{2.49}$$
$$E_0 - E_1 = (C_G V_G - e/2)\, e/C. \tag{2.50}$$

Because of the periodicity in the gate voltage

$$\left\langle \frac{d\vec{s}}{dt} \right\rangle_{X2,n_N=1} = \left\langle \frac{d\vec{s}}{dt} \right\rangle_{X2,n_N=0} \quad \text{with } V_G \to V_G - e/C_G. \tag{2.51}$$

We can now rewrite Eq. (2.48) in terms of the function $\eta\left(\epsilon, U\right)$, defined in Eq. (2.37). The probabilities p_0 and p_1 are taken from Eq. (2.19). After linearization in V and $\Delta\mu$, we arrive at the expression Eq. (2.36).

We note the differences with the results for single-level quantum dots;[15] our expression includes an additional integral over the island states. For a single-level quantum dot, X2 is active only when exactly one electron resides on the dot, since there is no unpaired spin in an empty or doubly occupied dot. In contrast, a net spin accumulation can reside on our classical dot for all numbers of electrons. The effective magnetic field is a sum weighted with the probabilities for "0" and "1" electrons on the dot, which leads to a partial cancellation of the contributions for different n_N, as is shown in Fig. 2.2.

BIBLIOGRAPHY

[1] M. M. Deshmukh and D. C. Ralph, Phys. Rev. Lett. **89**, 266803 (2002).

[2] A. N. Pasupathy, R. C. Bialczak, J. Martinek, J. E. Grose, L. A. K. Donev, P. L. McEuen, and D. C. Ralph, Science **306**, 86 (2004).

[3] J. Philip, D. Wang, M. Muenzenberg, P. LeClair, B. Diouf, J. S. Moodera, and J. G. Lu, J. Magn. Magn. Mater., **272-276**, 1949 (2004).

[4] L. Zhang, C. Wang, Y. Wei, X. Liu, and D. Davidović, Phys. Rev. B **72**, 155445 (2005).

[5] S. Sahoo, T. Kontos, J. Furer, C. Hoffmann, M. Gräber, A. Cottet, and C. Schönenberger, Nat. Phys. **1**, 99 (2005).

[6] A. Bernand-Mantel, P. Seneor, N. Lidgi, M. Muñoz, V. Cros, S. Fusil, K. Bouzehouane, C. Deranlot, A. Vaures, F. Petroff, and A. Fert, Appl. Phys. Lett. **89**, 062502 (2006).

[7] K. Ono, H. Shimada, and Y. Ootuka, J. Phys. Soc. Jpn. **66**, 1261 (1997).

[8] L. F. Schelp, A. Fert, F. Fettar, P. Holody, S. F. Lee, J. L. Maurice, F. Petroff, and A. Vaurès, Phys. Rev. B **56**, R5747 (1997).

[9] K. Yakushiji, F. Ernult, H. Imamura, K. Yamane, S. Mitani, K. Takanashi, S. Takahashi, S. Maekawa, and H. Fujimori, Nat. Mater. **4**, 57 (2005).

[10] J. Barnaś and A. Fert, Phys. Rev. Lett. **80**, 1058 (1998).

[11] K. Majumdar and S. Hershfield, Phys. Rev. B **57**, 11521 (1998).

[12] A. N. Korotkov and V. I. Safarov, Phys. Rev. B **59**, 89 (1999).

[13] A. Brataas, Yu. V. Nazarov, J. Inoue, and G. E. W. Bauer, Eur. Phys. J. B **9**, 421 (1999).

[14] A. Brataas and X. H. Wang, Phys. Rev. B **64**, 104434 (2001).

[15] J. König and J. Martinek, Phys. Rev. Lett. **90**, 166602 (2003); M. Braun, J. König, and J. Martinek, Phys. Rev. B **70**, 195345 (2004); J. König, J. Martinek, J. Barnaś, and G. Schön, in *CFN Lectures on Functional Nanostructures*, Edited by K. Busch, A. Powell, C. Röthig, G. Schön, and J. Weissmüller, Lecture Notes in Physics **658** (Springer, Berlin, 2005), pp. 145-164; M. Braun, J. König, and J. Martinek, Superlattices Microstruct. **27**, 333 (2005).

[16] L. Y. Gorelik, S. I. Kulinich, R. I. Shekhter, M. Jonson, and V. M. Vinokur, Phys. Rev. Lett. **95**, 116806 (2005).

[17] W. Rudziński, J. Barnaś, R. Świrkowicz, and M. Wilczyński, Phys. Rev. B **71**, 205307 (2005).

[18] J. N. Pedersen, J. Q.Thomassen, and K. Flensberg, Phys. Rev. B **72**, 045341 (2005).

[19] J. Fransson, Europhys. Lett. **70**, 796 (2005).

[20] S. Braig and P. W. Brouwer, Phys. Rev. B **71**, 195324 (2005).

[21] H.-F. Mu, G. Su, and Q.-R. Zheng, Phys. Rev. B **73**, 054414 (2006).

[22] W. Wetzels, G. E. W. Bauer, and M. Grifoni, Phys. Rev. B **72**, 020407(R) (2005).

[23] L. Balents and R. Egger, Phys. Rev. B **64**, 035310 (2001).

[24] C. Bena and L. Balents, Phys. Rev. B **65**, 115108 (2002).

[25] O. Parcollet and X. Waintal, Phys. Rev. B **73**, 144420 (2006).

[26] *Single Charge Tunneling*, edited by H. Grabert and M. H. Devoret, (Plenum Press, New York, 1992).

[27] A. Brataas, Yu. V. Nazarov, and G. E. W. Bauer, Phys. Rev. Lett. **84**, 2481 (2000); A. Brataas, Y. V. Nazarov, and G. E. W. Bauer, Eur. Phys. J. B **22**, 99 (2001); A. Brataas, G. E. W. Bauer, and P. J. Kelly, Phys. Rep. **427**, 157 (2006).

[28] M. D. Stiles and A. Zangwill, Phys. Rev. B **66**, 014407 (2002).

[29] A. A. Tulapurkar, Y. Suzuki, A. Fukushima, H. Kubota, H. Maehara, K. Tsunekawa, D. D. Djayaprawira, N. Watanabe, and S. Yuasa, Nature (London) **438**, 339 (2005).

[30] A. Cottet, T. Kontos, W. Belzig, C. Schönenberger, and C. Bruder, Europhys. Lett. **74**, 320 (2006).

[31] P. Zhang, Q-K. Xue, Y. P. Wang and X. C. Xie, Phys. Rev. Lett. **89**, 286803 (2002).

[32] J. Martinek, Y. Utsumi, H. Imamura, J. Barnaś, S. Maekawa, J. König, and G. Schön, Phys. Rev. Lett. **91**, 127203 (2003).

[33] R. López and D. Sánchez, Phys. Rev. Lett. **90**, 116602 (2003).

[34] M. D. Stiles, Nanomagnetism: Ultrathin Films, Multilayers and Nanostructures (Contemporary Concepts of Condensed Matter Science, Vol. 1), edited by D. Mills and J. A. C. Bland, (Elsevier, New York, 2006), pp 51-77.

[35] S. Yuasa, T. Nagahama, and Y. Suzuki, Science **297**, 234 (2002).

[36] H. T. Man, I. J. W. Wever, and A. F. Morpurgo, Phys. Rev. B **73**, 241401(R) (2006).

[37] X. Waintal, E. B. Myers, P. W. Brouwer, and D. C. Ralph, Phys. Rev. B **62**, 12317 (2000).

[38] A. Brataas, G. E. W. Bauer, and P. J. Kelly, Phys. Rep. **427**, 157 (2006).

[39] J. C. Slonczewski, Phys. Rev. B. **39**, 6995 (1989).

[40] D. Huertas-Hernando, Yu. V. Nazarov, and W. Belzig, Phys. Rev. Lett. **88**, 047003 (2002).

[41] K. Xia, P. J. Kelly, G. E. W. Bauer, A. Brataas, and I. Turek, Phys. Rev. B **65**, 220401(R) (2002).

[42] K. A. Matveev, Zh. Eksp. Teor. Fiz. **99**, 1598 (1991)[Sov. Phys. JETP **72** 892 (1991)].

[43] L. I. Glazman and K. A. Matveev, Zh. Eksp. Teor. Fiz. **98**, 1834 (1990)[Sov. Phys. JETP **71** 1031 (1990)].

[44] G. D. Mahan, *Many Particle Physics,* (Plenum, New York, 1981).

[45] G. E. W. Bauer, A. Brataas, Y. Tserkovnyak, B. I. Halperin, M. Zwierzycki, and P. J. Kelly, Phys. Rev. Lett. **92**, 126601 (2004).

[46] I. O. Kulik and R. I. Shekhter, Zh. Eksp. Teor. Fiz. **68**, 623 (1975)[Sov. Phys. JETP **41**, 308 (1975)].

[47] L. D. Landau and E. M. Lifschitz, Quantum Mechanics (Non-relativistic Theory), 3rd ed. (Pergamon, Oxford, 1977).

3. EFFICIENT MAGNETIZATION REVERSAL WITH NOISY CURRENTS

Wouter Wetzels, Gerrit E. W. Bauer, and Oleg N. Jouravlev

We propose to accelerate reversal of the ferromagnetic order parameter in spin valves by electronic noise. By solving the stochastic equations of motion we show that the current-induced magnetization switching time is drastically reduced by a modest level of externally generated current (voltage) noise. This also leads to a significantly lower power consumption for the switching process.[1]

3.1 Introduction

The dynamics of the ferromagnetic order parameter persists to pose a challenging problem of fundamental and applied nature [1]. With increasing bit density of mass data storage devices and emergence of the magnetic random access memory (MRAM) concept, the speed and energy dissipation of the magnetization switching process have become important issues. In the present MRAM generation, magnetic bits are written by spatially extended Ørsted magnetic fields, which sets limits to bit size and power consumption. An attractive alternative method is the current-induced magnetization switching predicted by theoreticians [2, 3] and confirmed experimentally in nano-pillar devices [4, 5, 6]. In these spin valves, which consist basically of an electrically connected ferromagnetic|normal|ferromagnetic metals sandwich, the electric current is polarized in a "fixed" layer of high magnetic coercivity and exerts a "spin-transfer torque" on the second magnetically soft ferromagnet as sketched in Fig. 1. Recently, time-resolved measurements of the current-induced magnetization dynamics have been reported [7]. Advanced theoretical models for the spin and charge transport in magnetic devices [10, 8, 9] lead to a reasonable description of the magnetization dynamics within the macro-spin model, in which the magnetization is assumed to move rigidly under external magnetic field and spin-transfer torques [11, 12]. We should note that in larger devices evidence has been found for spin waves and more complicated excitations that require full micromagnetic simulations [13].

The main obstacle that prevents wide application of current-induced switching is the high critical current needed to reverse the magnetization. There are proposals on how to reduce the critical current by sample design [12] and optimizing the switching process by a precessional switching strategy [14]. Since the spin-transfer torque vanishes for the collinear stable point of a spin valve, the switching time depends strongly on processes that induce a canting between the magnetizations such that the spin-transfer torque starts to kick in. This happens for example by increasing temperature, and is the basic idea of the pre-charging strategy by Devolder *et al.* [15]. More advanced strategies used in conventional magnetization switch-

ing require pulse-shaped microwaves [16] and rely on precise knowledge of the magnetization dynamics with proper feedback.

Electrical and magnetization noise usually degrades device and system performance and often efforts have to be undertaken to reduce it as much as possible. In nonlinear systems intentionally added noise may e.g. enhance the quality of signal transmission by the phenomenon of stochastic resonance. Noise generators find useful application, for example to test the response of a system to noise, to generate random signals for use in in encryption or to minimize the effect of quantization errors by a method called dithering. In this Letter, we propose a simple method to improve the energy-efficiency of current-induced magnetization switching by adding noise to the electric circuit connected to the device. We demonstrate that this leads to a reversal process with increased switching speed and less energy dissipation.
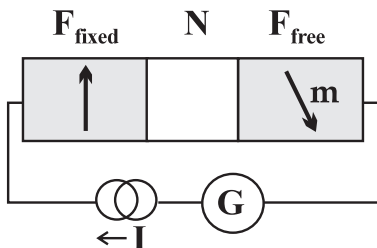

Fig. 3.1: Schematic picture of the spin valve under consideration. The applied potential on the left/right side is $\pm V/2$. The charge current I flows clockwise and G is a noise generator.

3.2   Magnetization dynamics

The magnetization dynamics in the macro-spin model for a small magnetic grain is described by the Landau-Lifshitz-Gilbert (LLG) equation [17]

$$\dot{\boldsymbol{m}} = -\gamma \mathbf{m} \times \boldsymbol{H}_{\text{eff}} + \alpha \mathbf{m} \times \dot{\mathbf{m}} \tag{3.1}$$

63

where γ is the gyromagnetic ratio and α the Gilbert damping constant. The magnetization direction $\mathbf{m} = (\cos\varphi\sin\theta, \sin\varphi\sin\theta, \cos\theta)$ is parameterized by the angles θ and φ, and we consider switching between $\theta = 0$ (magnetization pointing up) and $\theta = \pi$ (down). When a current bias is applied to the device in Fig. 3.1, the LLG equation for the free layer F_{free} needs to be modified to include the spin-transfer torque $\dot{\boldsymbol{m}}_{\text{torque}} = -(\gamma/\mathcal{M}_S)\mathbf{m} \times \mathbf{I}_{\text{free}} \times \mathbf{m}$, where $\mathcal{M}_S$ is the total magnetic moment of the ferromagnet. The electric charge and spin currents driven through the system fluctuate due to thermal and shot noise [18]. Here we wish to investigate the effect of intentionally applied current fluctuations with spectral density and bandwidth controlled by an external noise generator. The fluctuating (spin) current through the interfaces of F_{free} creates a fluctuating spin torque that can be taken into account by adding a fluctuating torque to the LLG equation, $\dot{\boldsymbol{m}}_{\text{fluct}} \equiv \mathbf{m} \times (\mathbf{h} \times \mathbf{m})$, where we introduced an effective random field $\mathbf{h} = h_\theta\widehat{\theta} + h_\phi\widehat{\phi} + h_r\widehat{r}$ in spherical coordinates, with $\langle h_i(t) \rangle = 0$ and $\langle h_i(t) h_j(t') \rangle = \mu_{ij}\delta_{ij}(t - t')$ for $i, j \in \{\theta, \phi, r\}$. Such a model befits an electromagnetic environment with a large number of degrees of freedom that generates Gaussian noise with correlation times much shorter than the magnetization response time. At room temperature, shot noise does not have to be taken into account [18]. The LLG equation in the presence of random magnetic fields leads to a stochastic equation for the three components of the unit vector $\boldsymbol{m}$, which can be reduced to the Fokker-Planck equation [17]. This allows us to access the magnetization reversal time as a function of applied switching current and current noise.

The switchable ferromagnet is assumed to be a prolate spheroid with easy axis along z, i.e. $\mathbf{H}_{\text{eff}} = H_A\cos\theta\widehat{z}$ and an eventual uniaxial crystal anisotropy with the same symmetry. For thermal stability of the equilibrium magnetization the ratio of the height of the effective energy barrier and the thermal energy should be high, i.e. $H_A\mathcal{M}_S \gg k_B T$. For a magnet with a combination of easy-plane and uniaxial anisotropy, the switching times behave very similar after taking into account that the weaker anisotropy governs the energy of the saddle point [11].

We use the formalism developed in [8] to find the charge and spin currents through the spin valve. The ferromagnet-normal metal contacts are

assumed to have identical spin-dependent conductances $g^{\uparrow\uparrow}$ and $g^{\downarrow\downarrow}$ (in units of the conductance quantum e^2/h) with $p = \left(g^{\uparrow\uparrow} - g^{\downarrow\downarrow}\right)/\left(g^{\uparrow\uparrow} + g^{\downarrow\downarrow}\right)$. We approximate the mixing conductance $g^{\uparrow\downarrow}$, the interface-specific parameter for the spin-transfer torque, by $\left(g^{\uparrow\uparrow} + g^{\downarrow\downarrow}\right)/2$, which is sufficiently accurate for our purposes. The spin accumulation in the normal metal in quasi-equilibrium can be found by using current conservation and spin conservation in the normal metal. Spin-flip in the normal metal is disregarded, while that in the ferromagnet is absorbed in the spin-dependent conductances. Under an applied voltage bias V, we then find a charge current

$$\frac{I}{eV} = \frac{e}{2h}\left(g^{\uparrow\uparrow} + g^{\downarrow\downarrow}\right)\left(1 - p^2 \sin^2 \frac{\theta}{2}\right), \tag{3.2}$$

and a spin current leaving the free ferromagnetic layer for the normal metal node

$$\frac{\mathbf{I}_{\text{free}}}{eV} = \frac{g^{\uparrow\uparrow} - g^{\downarrow\downarrow}}{16\pi}\left(-2\mathbf{m}\cos^2\frac{\theta}{2} + \widehat{\theta}\sin\theta\right). \tag{3.3}$$

By inserting this expression into $\dot{\mathbf{m}}_{\text{torque}}$, we find for the spin torque contribution to the dynamics

$$\dot{\mathbf{m}}_{\text{torque}} = \gamma J_S \sin\theta\,\widehat{\theta}, \tag{3.4}$$

$$J_S = \left(g^{\uparrow\uparrow} - g^{\downarrow\downarrow}\right) eV/(16\pi\mathcal{M}_S). \tag{3.5}$$

Since this torque vanishes at $\theta = 0, \pi$, the absence of (temperature-induced) fluctuations would imply an infinite switching time. Combining all contributions discussed above, and disregarding an angle-dependence of the Gilbert damping due to spin pumping [19], the LLG equation reduces to

$$\dot{\theta} = -\gamma\alpha H_A \cos\theta\sin\theta - \gamma J_S \sin\theta + h_\theta , \tag{3.6}$$

$$\dot{\varphi} = \gamma H_A \cos\theta + \alpha\gamma J_S \sin\theta + h_\varphi/\sin\theta . \tag{3.7}$$

In the following we focus on the effect of current fluctuations $\Delta I(t) = I(t) - \langle I \rangle$ with spectrum

$$S(\omega) = \int dt e^{i\omega t}\langle \Delta I(t)\,\Delta I(0)\rangle, \tag{3.8}$$

that are generated externally on top of the thermal noise. The noise spectral density is taken to be a constant S_w over a bandwidth $\Delta\omega$ that depends on the typical time scales of the system: the system is not sensitive to fluctuations slower than the timescale of the magnetization dynamics (the inverse Larmor frequency) or faster than the electron transfer time defined by voltage. Let us define the fluctuations of spin currents (where $\sigma = \uparrow, \downarrow$ for a chosen quantization axis), $\Delta I^\sigma(t) = I^\sigma(t) - \langle I^\sigma \rangle$ and the corresponding noise power

$$S^{\sigma\sigma'} = \frac{1}{2}\left\langle \Delta I^\sigma(t)\,\Delta I^{\sigma'}(t') + \Delta I^{\sigma'}(t')\,\Delta I^\sigma(t) \right\rangle. \qquad (3.9)$$

Since $I(t) = I^\uparrow(t) + I^\downarrow(t)$, the charge noise power can be written as $S^{\mathrm{ch}} = \sum_{\sigma,\sigma'=\uparrow,\downarrow} S^{\sigma\sigma'}$. The spin current polarized perpendicular to $\mathbf{m}$ transfers angular momentum to the ferromagnet almost instantaneously at the interface. Taking the spin quantization axis in the direction of $\widehat{\theta}$, i.e. perpendicular to the magnetization of F_{free}, there is therefore no correlation between the (transverse) spin currents $I_r^\sigma(t)$ on both sides ($r = L, R$) of F_{free}. The component of the field $\mathbf{h}$ relevant for our discussion is h_θ, transverse to the magnetization, and can be expressed as $h_\theta(t) = \sum_{r=L,R} (\gamma\hbar/2e\mathcal{M}_S)\left(I_r^\uparrow(t) - I_r^\downarrow(t)\right)$.

3.3   Results and discussion

We describe the switching process in the Néel-Brown model of thermally assisted magnetization reversal [17]. We consider a statistical ensemble of particles on the unit sphere that represents the probability density for the magnetization direction. Under the influence of the (random) forces these particles diffuse over the sphere. A Fokker-Planck equation describes the evolution of the probability density $P(\theta, \varphi, r)$ to find the magnetization vector in a certain direction [17, 11].

$$\frac{\partial P}{\partial t} = -\frac{\partial}{\partial \theta}A_\theta P + \frac{1}{2}\frac{\partial^2}{\partial\theta^2}B_{\theta\theta}P - \frac{\partial}{\partial\varphi}A_\varphi P + \frac{1}{2}\frac{\partial^2}{\partial\varphi^2}B_{\varphi\varphi}P, \qquad (3.10)$$

with $A_\theta = -\gamma\alpha H_A \cos\theta \sin\theta - \gamma J_S \sin\theta + \frac{1}{2}\mu_{\theta\theta}\cot\theta$, $B_{\theta\theta} = \mu_{\theta\theta}$, $A_\varphi = \gamma H_A \cos\theta + \alpha\gamma J_S \sin\theta$ and $B_{\varphi\varphi} = \mu_{\varphi\varphi}/\sin^2\theta$. The diffusion constant $\mu_{\theta\theta}$ is affected by the noise power S_w. We consider the limit of small polarization p in which $\mu_{\theta\theta}$ becomes independent of θ. The value of $\mu_{\varphi\varphi}$ is then equal to $\mu_{\theta\theta}$, but is not relevant for the calculation of the switching time. The new diffusion parameter can then be written in terms of S_w:

$$\mu_{\theta\theta} = \mu_{\text{thermal}} + \frac{1}{2}\left(\frac{\gamma\hbar}{e\mathcal{M}_S}\right)^2 S_w, \tag{3.11}$$

where

$$\mu_{\text{thermal}} = \frac{2\gamma\alpha k_B T}{\mathcal{M}_S} \tag{3.12}$$

is the Néel-Brown diffusion constant.

We introduce the surface probability current $\mathbf{j}(\theta,\varphi)$ defined as $\partial W/\partial t = -\nabla\cdot\mathbf{j}$ in terms of the surface probability density $W(\theta,\varphi) = P(\theta,\varphi)/\sin\theta$. In the steady state

$$\mathbf{j}\cdot\hat{\theta} = A_\theta W - \frac{1}{2\sin\theta}\frac{\partial}{\partial\theta}B_{\theta\theta}W\sin\theta \equiv 0. \tag{3.13}$$

Since W does not depend on φ,

$$W(\theta) \propto w(\theta) = \exp\frac{-\gamma\alpha H_A \sin^2\theta + 2\gamma J_S \cos\theta}{\mu_{\theta\theta}}. \tag{3.14}$$

In Fig. 3.2 the probability density is shown for some combinations of current and noise power. It can be seen that applying a current results in an asymmetric distribution because the spin torque drives the magnetization to the second well, whereas an increased noise power broadens the distribution in the wells.

For high barriers, Kramer's method can be applied to find the switching time of the magnet. In that limit equilibrium is attained separately in the regions $0 \leq \theta \leq \theta_1$ and $\theta_2 \leq \theta \leq \pi$ (potential well 1 and 2). The effective potentials at θ_1 and θ_2 should be separated from the potential minimum by several thermal energies $k_B T$ to ensure that the probability to find the
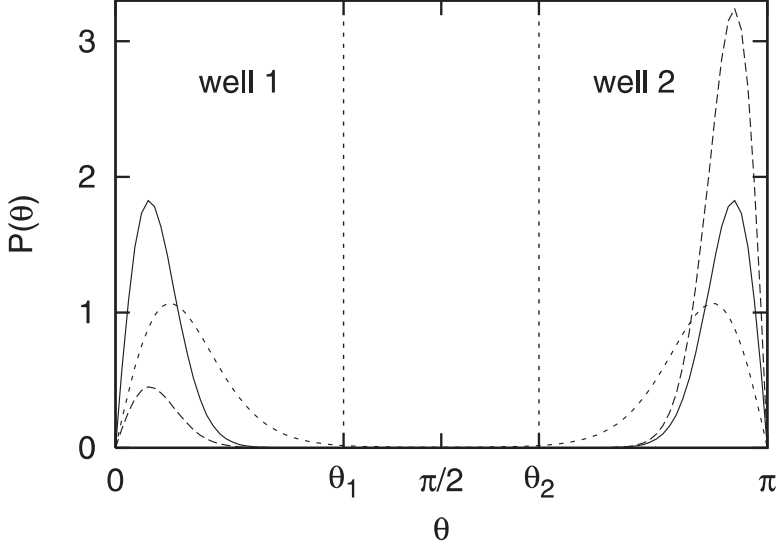
Fig. 3.2: The probability density for the magnetization direction in the steady state as a function of the angle θ. The density in the absence of a current is shown for a noise spectral density of $S_w = 3.0 \cdot 10^{-20} C^2 s^{-1}$ (solid) and $S_w = 1.0 \cdot 10^{-19} C^2 s^{-1}$ (dotted). The asymmetry in the dashed curve is caused by a current of 0.1 mA with noise spectral density $S_w = 3.0 \cdot 10^{-20} C^2 s^{-1}$.

magnetization in the middle region is low. The probability current I_m in this middle region defined as $\mathbf{j} \cdot \hat{\theta} = I_m / (2\pi \sin \theta)$, is then small and does not disturb the equilibrium distribution in the two wells significantly. In the region $\theta_1 \leq \theta \leq \theta_2$ (see Fig. 3.2) then

$$\dot{n}_1 = -\dot{n}_2 = -\frac{n_1}{\tau_1} + \frac{n_2}{\tau_2} = -I_m, \tag{3.15}$$

where n_ς is the probability to be in well $\varsigma = 1, 2$. The escape time from well 1,

$$\tau_1 = \frac{2}{\mu_{\theta\theta}} \int\limits_{0}^{\theta_1} d\theta w(\theta) \sin \theta \int\limits_{\theta_1}^{\theta_2} d\xi \left[w(\xi) \sin \xi \right]^{-1} \tag{3.16}$$

68

is a good estimate for the switching time. When $2\gamma\alpha H_A/\mu_D, |\alpha H_A/J_S| \gg 1$, we can calculate the integrals using Taylor expansions up to second order in θ and approximating $\sin\theta$ by θ (Ref. [17]):

$$\tau_1 = \sqrt{\frac{\pi\mu_{\theta\theta}}{\gamma\alpha H_A}} \frac{1}{\gamma\alpha H_A + \gamma J_S} \exp\frac{\gamma\alpha H_A \left(1 - J_S/\alpha H_A\right)^2}{\mu_{\theta\theta}}. \qquad (3.17)$$

We see that the spin-transfer torque reduces the effective barrier height [11], while the fluctuations increase the effective temperature, exponentially reducing the escape time. Because of the uniaxial symmetry $\tau_2 \to \tau_1$ with $J_S \to -J_S$. When a clearly preferred switching direction is required, $\mu_{\theta\theta}$ should be kept smaller than γJ_S. But when current and noise can be switched off immediately after a change in the magnetoresistance signifies that switching has occured, this is no longer a constraint. By combining Eq. (3.17), (3.12) and (3.11) we can establish an analytical relation between the applied noise power, current and switching time. We use Eq. (3.16) to evaluate the switching time as a function of current and noise spectral density (see Fig. 3.3). The model is here at room temperature with parameters typical for real spin valves. The ferromagnet F_{free} is specified by an anisotropy field $H_A = 50$ mT and total magnetic moment $\mathcal{M}_S = 10^{-17}\text{Am}^2$. The interface resistances are taken to be 1 Ω, the polarization of the contacts $p = 0.2$, and the damping constant $\alpha = 0.02$. A typical noise generator power is 15 dB higher than the thermal noise power of a 50 Ω resistor at 295 K. This gives a value of $S_w = 1.0 \cdot 10^{-20}$ J/Ω. Higher noise powers, corresponding to a thermal noise at thousands of Kelvins, can be readily generated.

From Fig. 3.3 we see that by keeping the current fixed and increasing the noise, the switching time can be reduced by orders of magnitude. The contours in the inset to the figure show how the current can be reduced by increasing the noise when the switching time is kept fixed. The power dissipated by the system is proportional to $\left\langle I\left(t\right)^2 \right\rangle$, which increases with external noise by $S_\omega\Delta\omega/\pi$. Since the typical bandwidth $\Delta\omega$ is of the order of 1 GHz, the main contribution to the power consumption comes from

the average switching current. We observe that the power can be reduced by an order of magnitude when a clearly preferred switching direction is necessary and can be reduced even further otherwise.

The calculations presented here are restricted to the high-barrier approximation, which sets limits to the currents and effective temperatures. Still, the mechanism of noise-assisted magnetization switching should be useful in other regimes as well. The experimental realization of this mechanism might face some difficulties such as enabling the high-frequency external fluctuations to reach the system. For instance, in the case of a large environmental capacitance between the leads, the impedance mismatch to the device might require additional measures. Another application of this system would be the measurement of the noise level: by calibration of the device, an unambiguous relation between current, switching time and noise power can be established. We also note that the same mechanism can be used as well to accelerate magnetic-field induced switching. An advantage is then that individual bits can be addressed by an unpolarized noisy current, which makes the need for localization of the magnetic field less stringent.

3.4   Conclusions

In conclusion, we propose an energy-efficient scheme for current-induced magnetization switching that is assisted by noise. Our approach is based on solving stochastic equations depending on the spectral density of an external noise source. The solution of the corresponding Fokker-Planck equation gives the dependence of the switching time on current and noise level. The current necessary to switch the magnetization can be reduced by applying externally generated current fluctuations. Without importantly complicating the device architecture the efficiency of spin-transfer torque devices can be improved by exponentially reduced switching times and an order-of-magnitude smaller power consumption. This could make the difference for the attractiveness of the current-induced switching mechanism for real-life applications.
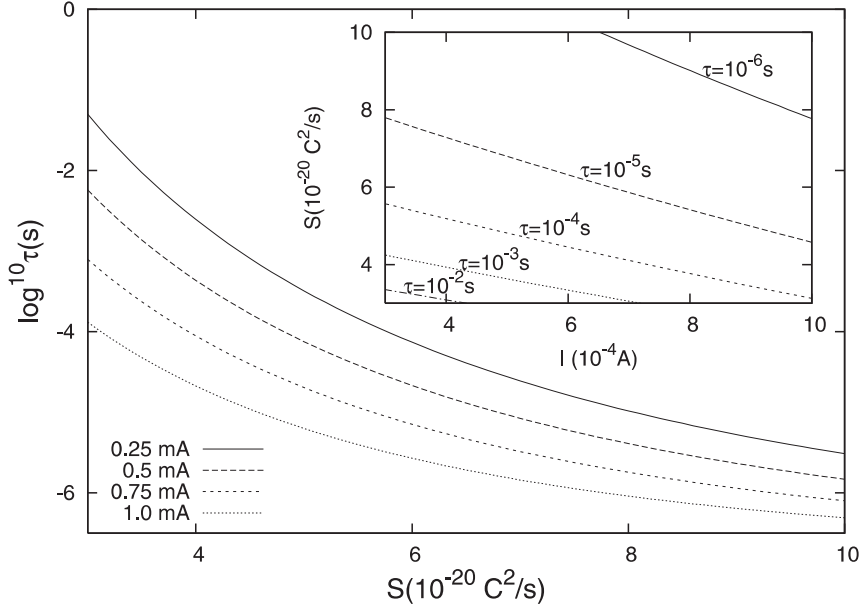
Fig. 3.3: Switching time as a function of noise spectral density for several values of the current. Inset: Equal-switching-time contours as a function of current and applied noise spectral density.

BIBLIOGRAPHY

[1] B. Hillebrands and K. Ounadjela (Eds.), Spin Dynamics in Confined Magnetic Structures, (Springer, Berlin, 2003); S. Maekawa and T. Shinjo (Eds.), Applications of Magnetic Nanostructures, (Taylor and Francis, New York, 2002).

[2] J. C. Slonczewski, J. Magn. Magn. Mater. **159** L1-L7 (1996).

[3] L. Berger, Phys. Rev. B **54**, 9353 (1996).

[4] F. J. Albert, J. A. Katine, R. A. Buhrman, and D. C. Ralph, Appl. Phys. Lett. **77**, 3809 (2000).

[5] J. A. Katine, F. J. Albert, R. A. Buhrman, E. B. Myers, and D. C. Ralph, Phys. Rev. Lett. **84**, 3149 (2000).

[6] J. Grollier, V. Cros, A. Hamzic, J. M. George, H. Jaffrès, A. Fert, G. Faini, J. Ben Youssef, and H. Legall, Appl. Phys. Lett. **78**, 3663 (2001).

[7] I. N. Krivorotov, N. C. Emley, J. C. Sankey, S. I. Kiselev, D. C. Ralph, and R. A. Buhrman, Science **307**, 228 (2005).

[8] A. Brataas, Y. V. Nazarov, and G.E.W. Bauer, Phys. Rev. Lett. **84**, 2481 (2000).

[9] M. D. Stiles, and A. Zangwill, Phys. Rev. B **66**, 014407 (2002).

[10] X. Waintal, E. B. Myers, P. W. Brouwer, and D. C. Ralph, Phys. Rev. B **62**, 12317 (2000).

[11] D. M. Apalkov, and P. B. Visscher, Phys. Rev. B **72**, 180405(R) (2005); D. M. Apalkov, and P. B. Visscher, J. Magn. Magn. Mater. **286**, 370 (2005).

[12] J. Manschot, A. Brataas, and G. E. W. Bauer, Appl. Phys. Lett. **85**, 3250 (2004).

[13] K.-J. Lee, A. Deac, O. Redon, J.-P. Nozières, and B. Dieny, Nature Materials **3**, 877 (2004).

[14] A.D. Kent, B. Özyilmaz, and E. del Barco, Appl. Phys. Lett. **84**, 3897 (2004).

[15] T. Devolder, C. Chappert, P. Crozat, A. Tulapurkar, Y. Suzuki, J. Miltat, and K. Yagami, Appl. Phys. Lett. **86**, 062505 (2005).

[16] Z. Z. Sun, and X. R. Wang, cond-mat/0511135.

[17] W. F. Brown, Phys. Rev. **130**, 1677 (1963).

[18] J. Foros, A. Brataas, Y. Tserkovnyak, and G.E.W. Bauer, Phys. Rev. Lett. **95**, 016601 (2005).

[19] Y. Tserkovnyak, A. Brataas, and G.E.W. Bauer, Phys. Rev. Lett. **88**, 117601 (2002).

4. CHARGE AND SPIN TRANSPORT IN SPIN VALVES WITH ANISOTROPIC SPIN RELAXATION

Henri Saarikoski, Wouter Wetzels, and Gerrit E. W. Bauer

We investigate effects of spin-orbit splitting on electronic transport in a spin valve consisting of a large quantum dot defined on a two-dimensional electron gas with two ferromagnetic contacts. In the presence of both structure inversion asymmetry (SIA) and bulk inversion asymmetry (BIA) a giant anisotropy in the spin-relaxation times has been predicted. We show how such an anisotropy affects the electronic transport properties such as the angular magnetoresistance and the spin-transfer torque. Counterintuitively, anisotropic spin-relaxation processes sometimes enhance the spin accumulation.[1]

4.1 Introduction

Conventional microelectronics makes use of the electron charge in order to store, manipulate and transfer information. The potential usefulness of the spin, the intrinsic angular momentum of the electron, for electronic devices has been recognized by a large community after the discovery of the giant magnetoresistance (GMR) in 1988.[1, 2, 3] The integration of the functionalities of metal-based magnetoelectronics with semiconductor-based microelectronics is an important challenge in this field. [4]

A central device concept in magnetoelectronics is a spin valve consisting of a normal conductor (N) island that is contacted by ferromagnets (F) with variable magnetization directions. An applied bias injects a spin accumulation into the island that affects charge and spin transport as a function of the relative orientation of the two magnetizations.

We consider here a spin-valve structure in which the island is a large semiconductor quantum dot, *i.e.* a patch of two-dimensional (2D) electron gas, weakly coupled to the ferromagnetic contacts. In order to observe spin-related signals the injection of spins from the ferromagnet into the quantum dot must be efficient and the injected spin accumulation must not relax faster than the dwell time of an electron on the island.

Spin injection from ferromagnets into metals has first been achieved by Johnson and Silsbee in 1988 (Ref. [5]), but early attempts to fabricate devices based on injection of spins from metallic ferromagnets into semiconductors have not been successful.

The reason for these difficulties turned out to be inefficient spin injection in the presence of a large difference between the conductances of the metallic ferromagnet and the semiconductor, *i.e.* the conductance mismatch problem. [6]

These technical difficulties, however, appear to be surmountable.[7] Effective spin injection into a semiconductor can *e.g.* be achieved using a magnetic semiconductor.[8] Schottky or tunneling barriers to a metallic ferromagnet can overcome the conductance mismatch problem,[9, 10, 11] as has been confirmed by using optical techniques.[12, 13, 14, 15, 16] Recently, all-electric measurements of spin injection from ferromagnets into semicon-

ductors have been reported. Chen *et al.* used a magnetic *p-n* junction diode to measure the spin accumulation injected from a ferromagnet into a bulk *n*-GaAs via a Schottky contact.[17] Spin accumulation in a GaAs thin film has been injected and detected by Fe contacts in a non-local 4-point configuration.[18]

Spin-relaxation mechanisms lead to decay of the spin accumulation and restore the equilibrium on the island. The main origin for spin-flip scattering in *n*-doped quantum well structures [4] is the Dyakonov–Perel mechanism[19] due to spin-orbit interaction, which is efficient when the spatial inversion symmetry is broken causing the spin-orbit coupling to split the spin-degenerate levels.[20] The relaxation arises because spins are subject to a fluctuating effective magnetic field due to frequent scattering. The inversion symmetry may be broken by a bulk inversion asymmetry (BIA) of the zinc-blende semiconductor material such as GaAs[21] or structure inversion asymmetry (SIA) in the confinement potentials of heterostructures[22] that can be modulated externally by gate electrodes.[34, 35] The SIA and BIA induced spin-orbit coupling terms linear in the wave vector often dominate the transport properties of electrons in III–V semiconductors and are known as Bychkov–Rashba and Dresselhaus terms, respectively. Their relative importance can be extracted *e.g.* from spin-resolved photocurrent measurements.[23] The growth direction of the quantum well affects the strength of the spin-orbit coupling terms. This gives rise to differences in spin-relaxation times as observed for GaAs quantum wells using optical measurements.[24] In general, the spin-relaxation processes in semiconductor quantum wells are anisotropic, *i.e.* the spin-relaxation rate depends on the direction of the spin accumulation. When the coupling constants in the Bychkov–Rashba and Dresselhaus terms in [001] grown quantum wells are equal, the interference of the spin-orbit interactions give rise to suppression of the Dyakonov–Perel spin-relaxation mechanism for the [110] crystallographic direction. This leads to a giant anisotropy in the spin lifetimes of up to several orders of magnitude.[26, 27, 25] The phenomenon can be rationalized in terms of a $SU(2)$ spin rotation symmetry that protects a spin helix state.[28] Similar behavior is expected for the [110] Dresselhaus model.[28]

Datta and Das proposed a spin-transistor based on the coherent rotation of spins by the SIA spin-orbit interaction that is tuned by a gate field.[29] An alternative transistor concept that relies on a gate-controlled suppression of the spin-relaxation by tuning of the SIA vs. BIA spin-orbit interaction is believed to work for wider channels and to be more robust against impurity scattering than the original Datta–Das proposal.[30, 31] A review of the effect of spin-orbit interactions on transport can be found in Ref. [32].

In the present work we use magnetoelectronic circuit theory [33] to calculate the transport properties of spin valves in the presence of anisotropic spin-relaxation processes. Circuit theory has been found to be applicable in both metal and semiconductor-based magnetoelectronics. It was used to describe the spin transfer through a Schottky barrier between a ferromagnetic metal and a semiconductor.[38] In this work we find that anisotropic spin-relaxation processes leave clear marks on the transport properties such as the angular magnetoresistance and the spin-transfer torque. We obtain, *e.g.*, the counterintuitive result that anisotropic spin relaxation may enhance rather than destroy the current-driven spin accumulation on the island. In Section 4.2 we introduce our model system and the theories of spin transport and relaxation. In Section 4.3 we identify the electrical signatures of anisotropic spin relaxation. The enhancement of spin accumulation due to anisotropy is discussed in Section 4.4. We present conclusions in Section 4.5.

4.2   Model for spin and charge transport

The spin valve in this work consists of a large quantum dot island between two ferromagnets. The quantum dot is assumed to be in contact with the ferromagnets by tunneling barriers, with contact resistances much larger than the resistance of the island. We derive the transport equations for a general case, and as an example discuss a quantum dot made in a [001] grown quantum well in GaAs/AlGaAs. The Dyakonov–Perel mechanism becomes then the leading source of spin relaxation and emergence of a giant anisotropy in spin relaxation has been predicted in such systems.[26, 27] A gate electrode on top of the quantum dot can be used

to tune the relative strengths of the SIA and BIA spin-orbit interactions which effectively changes the degree of anisotropy in the system. The model device is sketched in Fig. 4.1.

We model the spin and charge transport in the spin valve using the magnetoelectronic circuit theory,[33] which describes spin-dependent transport in an electronic circuit with ferromagnetic elements. The contacts between metallic or ferromagnetic nodes are parametrized as 2×2 conductance tensors in spin space. Their diagonal elements are the conventional spin-dependent conductances $G^\uparrow$ and $G^\downarrow$, whereas the non-diagonal ones are occupied by the complex mixing conductance $G^{\uparrow\downarrow}$ (and its conjugate). The mixing conductance is the material conductance parameter that governs spin currents transverse to the magnetization and becomes relevant when magnetization vectors are not collinear. The electric currents driven through the system are small and current-induced spin polarizations [36] may be disregarded. The island should be diffuse or chaotic, such that its electron distribution function is isotropic in momentum space. The quantum dot is supposed to be large enough so that Coulomb charging effects can be disregarded, although the calculations can be readily extended to include the Coulomb blockade, at least in the orthodox model.[37]

We focus here on a symmetric spin-valve device, *i.e.* the conductances of the majority and minority spin channels $G^\uparrow$ and $G^\downarrow$ and the polarization, defined as $P = (G^\uparrow - G^\downarrow)/(G^\uparrow + G^\downarrow)$, are the same for both the source and the drain contacts to the dot. In the tunneling regime, the real part of the mixing conductance $\operatorname{Re} G^{\uparrow\downarrow} \to G/2$, where $G = G^\uparrow + G^\downarrow$ is the total contact conductance.

The imaginary part of the mixing conductance is believed to be significant for ferromagnet-semiconductor interfaces.[38]

The charge current $I_{\mathrm{c},i}$ into the quantum dot through contact $i = 1, 2$ is[33]

$$I_{\mathrm{c},i}/G = V_c - V_i + P\mathbf{V}_s \cdot \mathbf{m}_i, \tag{4.1}$$

where V_i is the potential of reservoir i, V_c and $\mathbf{V}_s$ are the charge and spin potentials in the quantum dot, and $\mathbf{m}_1$ and $\mathbf{m}_2$ are the magnetizations of
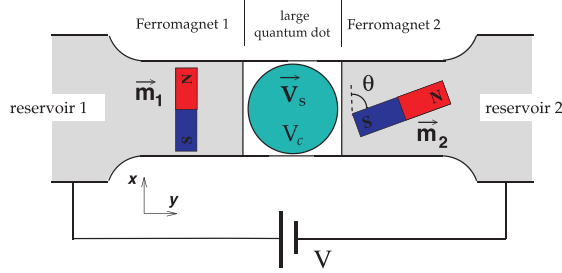
Fig. 4.1: Schematic picture of the spin-valve structure. A voltage bias $V = V_1 - V_2$ drives charge and spin currents through a layered ferromagnet-quantum dot-ferromagnet system. The magnetizations $\mathbf{m}_1$ and $\mathbf{m}_2$ point in arbitrary directions in the 2D plane of the large quantum dot. The ferromagnets inject a spin accumulation $\mathbf{V}_s$ into the dot. The coordinate system is chosen so that x-axis is parallel to $\mathbf{m}_1$ and z is perpendicular to the plane of the quantum dot.

the left and right ferromagnet, respectively. Equations for the spin currents through the interfaces into the island read (in units of A) [33]

$$
\begin{aligned}
\mathbf{I}_{\mathrm{s,i}} =& \mathbf{m}_i \left[\mathbf{V}_s \cdot \mathbf{m}_i + P(V_c - V_i) \right] G \\
& + 2 \operatorname{Re} G^{\uparrow\downarrow} \mathbf{m}_i \times (\mathbf{V}_s \times \mathbf{m}_i) + 2 \operatorname{Im} G^{\uparrow\downarrow} \mathbf{V}_s \times \mathbf{m}_i.
\end{aligned} \tag{4.2}
$$

A transverse spin current cannot penetrate a ferromagnet but they are instead absorbed at the interface and transfer the angular momentum to the ferromagnet. This gives rise to the spin-transfer torques[39]

$$
\tau_i = \frac{\hbar}{2e} \mathbf{m}_i \times (\mathbf{m}_i \times \mathbf{I}_{s,i}) \tag{4.3}
$$

on the magnetization $\mathbf{m}_i$. If the spin-transfer torque is large it may cause a switching of the magnetization direction.

The charge and spin conservation in the steady state implies that

$$
\sum_{i=1,2} I_{\mathrm{c},i} = 0, \tag{4.4}
$$

79

$$\frac{d\mathbf{V}_s}{dt} = \left.\frac{\partial \mathbf{V}_s}{\partial t}\right|_{\text{precess}} + \left.\frac{\partial \mathbf{V}_s}{\partial t}\right|_{\text{relax}} + \sum_{i=1,2} \mathbf{I}_{\text{s},i}/2e^2\mathcal{D} = 0, \qquad (4.5)$$

where $\mathcal{D}$ is the density of states at the Fermi energy of the quantum dot, which is assumed to be constant and continuous on the scale of the applied voltage and the thermal energy. The Bloch equation[40, 4] Eq. (4.5) describes changes in the spin accumulation due to spin precession and spin-relaxation processes and the spin currents. In the standard approach, spin relaxation is parametrized in terms of an isotropic, phenomenological spin-flip relaxation time. However, when the spin is coupled to orbital and structural anisotropies, spin relaxation can be anisotropic. Anisotropic spin-relaxation processes can be taken care of by replacing the spin-flip relaxation-rate constant by a tensor $\boldsymbol{\Gamma}$, that, given a spin-orbit coupling Hamiltonian and disorder, can be calculated with perturbation theory. In the presence of anisotropic spin-relaxation processes and external magnetic field $\mathbf{B}$ the terms in the Bloch equation (4.5) read

$$\left.\frac{\partial \mathbf{V}_s}{\partial t}\right|_{\text{precess}} = \gamma_g(\mathbf{V}_s \times \mathbf{B}), \quad \left.\frac{\partial \mathbf{V}_s}{\partial t}\right|_{\text{relax}} = -\boldsymbol{\Gamma}\cdot\mathbf{V}_s, \qquad (4.6)$$

where γ_g is the electron gyromagnetic ratio. Comparison of Eqs. (4.2)–(4.5) with Eq. (4.6) show that the imaginary part of the mixing conductance $\text{Im}\,G^{\uparrow\downarrow}$ acts like a magnetic field and gives rise to a precession around the direction determined by the magnetization vectors $\mathbf{m}_i$.

The quantum dot and the magnetizations are supposed to be in the xy-plane. The spin accumulation can have a component perpendicular to the quantum dot (z-direction) by the imaginary part of the mixing conductance. The spin-relaxation tensor $\boldsymbol{\Gamma}$ is diagonal in a coordinate system defined by $U = (\mathbf{u}_l, \mathbf{u}_s, \mathbf{u}_z)$, where (column) vector $\mathbf{u}_l$ denotes the direction corresponding to the longest spin lifetime $\tau_{\text{sf},l}$ in the plane of the quantum dot, $\mathbf{u}_s$ denotes the direction where the in-plane spin lifetime $\tau_{\text{sf},s}$ is shortest and $\mathbf{u}_z$ denotes the direction perpendicular to the system with spin lifetime

$\tau_{\text{sf},z}$. In the xyz-coordinate system the $\mathbf{\Gamma}$ tensor then reads

$$\mathbf{\Gamma} = U\mathbf{\Delta}U^T = U \begin{pmatrix} 1/\tau_{\text{sf},l} & 0 & 0 \\ 0 & 1/\tau_{\text{sf},s} & 0 \\ 0 & 0 & 1/\tau_{\text{sf},z} \end{pmatrix} U^T. \qquad (4.7)$$

We introduce a spin-flip conductance, which is effectively a measure of the spin-relaxation rate, as

$$G_{\text{sf},i} = \frac{e^2}{2} \frac{\mathcal{D}}{\tau_{\text{sf},i}}. \qquad (4.8)$$

for $i \in s, l, z$. The spin-valve effect depends non-monotonously on the contact resistance. When the resistance is too small, the magnetoresistance is suppressed by the conductance mismatch. When it is too large, all spins relax because the dwell time is longer than the spin-flip times[10], *i.e.* when $G \ll G_{\text{sf,i}}$. Defining the dwell time as $G = e^2\mathcal{D}/(2\tau_{\text{dwell}})$, we require that $\tau_{\text{dwell}} \ll \tau_{\text{sf},i}$, *i.e.* the spin lifetime must be long enough so that at least one component of the spin persists before the electrons tunnel out of the dot.

We discuss now the special case of a large quantum dot defined on a gated 2D electron gas in GaAs. We assume a [001] growth direction and use an effective mass $m^* = 0.067m_e$ and an electron density $N = 4 \times 10^{11}/\text{cm}^2$. In the [001] quantum wells $\mathbf{u}_l = \frac{1}{\sqrt{2}}(1, 1, 0)$ and $\mathbf{u}_s = \frac{1}{\sqrt{2}}(-1, 1, 0)$ when the electric field points in the [001] direction.[41, 27] Analytic expressions for the spin-relaxation rates in quantum wells dominated by the Dyakonov–Perel spin-relaxation mechanism are given by Averkiev *et al.*[41] They used a Hamiltonian with linear spin-orbit coupling terms

$$H = \frac{\hbar^2 k^2}{2m^*} + \frac{\alpha}{\hbar}(\sigma_x k_y - \sigma_y k_x) + \frac{\beta}{\hbar}(\sigma_x k_x - \sigma_y k_y), \qquad (4.9)$$

where α and β are SIA and BIA spin-orbit coupling constants and m^* is the effective electron mass. A variational calculation for a triangular model potential and the perturbation theory was then used to extract the spin-relaxation rates. In the case of short-range scattering and degenerate

electron gas they found

$$\frac{1}{\tau_\pm} = \frac{2\tau_{\rm tr}}{\hbar^2}\left[k_F^2(\pm\alpha-\beta)\left(\pm\alpha-\beta+\frac{\gamma}{2}k_F^2\right)+\frac{\gamma^2 k_F^6}{8}\right], \qquad (4.10)$$

$$\frac{1}{\tau_z} = \frac{4\tau_{\rm tr}}{\hbar^2}\left[k_F^2(\alpha^2+\beta^2)-\frac{\gamma\beta k_F^4}{2}+\frac{\gamma^2 k_F^6}{8}\right], \qquad (4.11)$$

where $+,-$ and z denote [110], [$\bar{1}$10] and [001] directions, respectively, and $\tau_{\rm tr}$ denotes the transport relaxation (scattering) time. The material parameter $\gamma = \beta/\langle k_z^2\rangle = 27\,eV\,{\rm \mathring{A}}^3$ for GaAs. The calculations leading to (4.10) and (4.11) are valid only when the mean free path $l = v_{\rm F}\tau_{\rm tr}$, where $v_{\rm F}$ is the Fermi velocity, is much smaller than the size of the quantum dot.

The Bychkov–Rashba term is expected to be linearly dependent on the gate-electrode induced electric field $\mathbf{E} = E\mathbf{z}$ so that $\alpha = \alpha_0 eE$, where $\alpha_0 = 5.33\,{\rm \mathring{A}}^2$ for GaAs/AlGaAs. The E dependence of the expectation value for the perpendicular component of the wave vector $\langle k_z^2\rangle = 0.78(2m^*eE/\hbar^2)^{2/3}$ in triangular asymmetric quantum wells.[42] Eq. (4.10) shows a significant reduction for the spin-relaxation rate for the [110] direction when $\alpha \simeq \beta$, whereas the spin-relaxation rate for [$\bar{1}$10] is not reduced. The spin-relaxation process is thereby strongly insotropic in this regime. A more accurate numerical analysis of the anisotropy based on a self-consistent calculations in a multiband envelope-function approximation has been carried out by Kainz $et\ al.$ and gives qualitatively similar results.[27] When $\alpha \simeq \beta$, the most stable spin direction [110] can have a lifetime that is several orders of magnitude longer than in the [$\bar{1}$10] and [001] directions, $i.e.$ $\tau_{{\rm sf},l} \gg \tau_{{\rm sf},s}$ and $\tau_{{\rm sf},l} \gg \tau_{{\rm sf},z}$.

As shown in Eqs. (4.10) and (4.11) the spin-relaxation rate of the Dyakonov–Perel mechanism is proportional to the transport relaxation time. Spin-relaxation times are therefore expected to increase with temperature and disorder in the sample. The enhancement of spin-relaxation times with temperature has been recently demonstrated experimentally.[43] For $\tau_{\rm tr} = 0.1$ ps, Averkiev $et\ al.$ predicted that the spin-relaxation times in GaAs typically range from picoseconds to nanoseconds.[41]

4.3 Signatures of anisotropy

Eqs. (4.1)–(4.5) can be solved analytically, but general expressions are lengthy. We therefore study transport in the limiting case of strong anisotropy

$$G_{\mathrm{sf},s} \gg G \gg G_{\mathrm{sf},l}. \tag{4.12}$$

By fixing the direction of the magnetization of the left ferromagnet along the x-axis the problem contains only two variables, the angle θ between the magnetizations and angle ϕ between the x-axis and $\mathbf{u}_l$, i.e. the eigenvector of the spin-relaxation rate matrix (4.7) corresponding to the most stable spin-accumulation direction. We present here the results for the spin-valve angular conductance, spin-transfer torque, and spin accumulation on the island and identify signatures of the anisotropy which could be probed in all-electric measurements. In experiments the dependence of the currents on the angle between the magnetizations and the orientation of the anisotropy axes could be probed, *e.g.*, by depositing strips of ferromagnets at different angles on the same sample wafer. Alternatively, the magnetization of a magnetically soft ferromagnet can be rotated using a magnetic field.

Fig. 4.2 shows the current of the device versus the angle θ with anisotropic and isotropic spin-relaxation processes in the central island.

The results are compared to the current $I_{\mathrm{Ohmic}} = GV/2$ through two non-magnetic interfaces with conductance G in series. For isotropic spin-relaxation the curve is symmetric with a single minimum at the center (Fig. 4.2(a)). The θ dependence is gradually suppressed when the spin-relaxation rate increases and in the limit of very fast spin relaxation the transport is governed solely by interface conductances. In the presence of anisotropic spin-relaxation processes the magnetoconductance depends strongly on the relative orientations of the magnetization axes with respect to the anisotropy axis. When one of the magnetizations is oriented perpendicular to the axis of the fastest relaxing spin component $\mathbf{u}_s$ (i.e. $\phi = \pi/2$) the magnetoresistance shows two minima in the limit of strong anisotropy (Fig. 4.2(b)). When the spin is injected along a stable magnetization direction ($\phi = 0$) the shape of the magnetoresistance curve only weakly depends on the spin-relaxation rate in the perpendicular direction (Fig. 4.2(c)). For
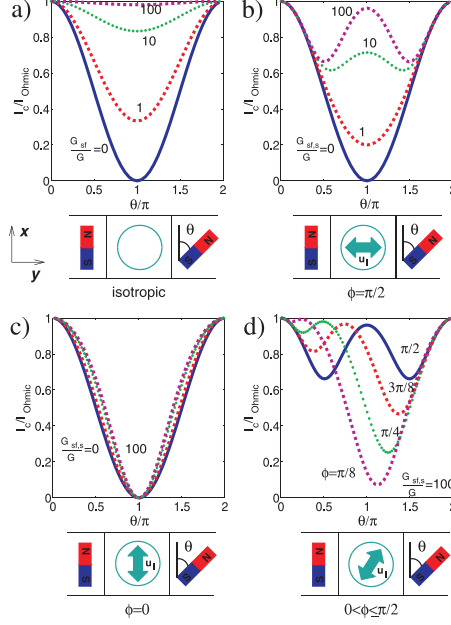
Fig. 4.2: The charge current through the device relative to $I_{\text{Ohmic}} = GV/2$. a) In the case of isotropic spin relaxation the magnetoresistance shows a single minimum. b) When the spin is injected parallel to the axis of the most short-lived spin orientation ($\phi = \pi/2$) the rapid relaxation of spin accumulation near $\theta = \pi$ causes a shift of current towards I_{Ohmic}. c) When $\phi = 0$ the spin accumulation persists and there is little change in the charge current. d) In the case of strong anisotropy and $0 < \phi < \pi/2$ the magnetoresistance generally shows two minima with unequal heights. In (b–d) $G_{\text{sf},l} = 0$, $P = 1$ and the curves are plotted for different relative spin-flip conductances $G_{\text{sf},s}/G$.

$0 < \phi < \pi/2$ the magnetoresistance generally contains two minima of unequal heights (Fig. 4.2(d)). Thus, the formation of a double minimum is a characteristic signature of the anisotropy in the system. It should be noted that such a double minimum is also possible in a system with isotropic spin relaxation, but only when the contact polarizations of the spin valve are

significantly different.[44]

Since the spin relaxation affects the spin currents, anisotropic spin relaxation is expected to change the spin-transfer torque on the magnetization as a function of the relative orientation of the magnetizations and the anisotropy axes. The torque on the right ferromagnet τ_2 in the case of strong anisotropy (4.12) is shown in Fig. 4.3. Eqs. (4.2) and (4.3) show
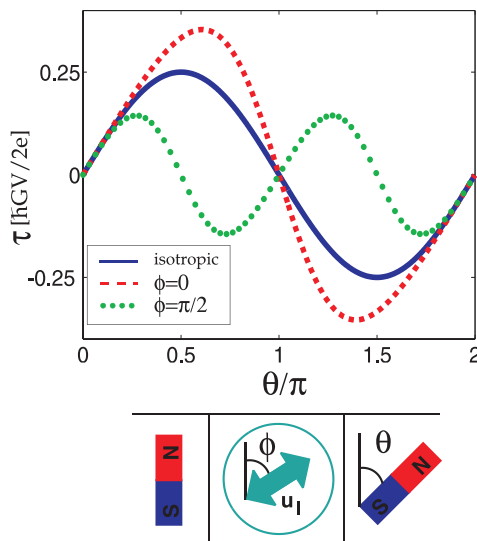

Fig. 4.3: The spin torque on ferromagnet 2 as a function of the angle θ between left and right magnetization in the absence of spin relaxation processes (solid line) and in the the presence of giant spin-relaxation anisotropy with $G_{\mathrm{sf,s}} = \infty$, $G_{\mathrm{sf,l}} = 0$ (dashed and dash-dotted lines). In the latter case the left ferromagnet injects spin parallel to $\mathbf{u}_l$ ($\phi = 0$, dashed line) or $\mathbf{u}_s$ ($\phi = \pi/2$, dash-dotted line), respectively. The polarization is here $P = 1$ and $\mathrm{Im}\, G^{\uparrow\downarrow} = 0$.

that the spin torque on the ferromagnet i is proportional to $|\mathbf{m}_i \times \mathbf{V}_s|$. When the left ferromagnet injects spin parallel to the axis of the longest spin lifetime the spin-transfer torque increases compared to the case of no spin relaxation. On the other hand, when the left ferromagnet injects spin
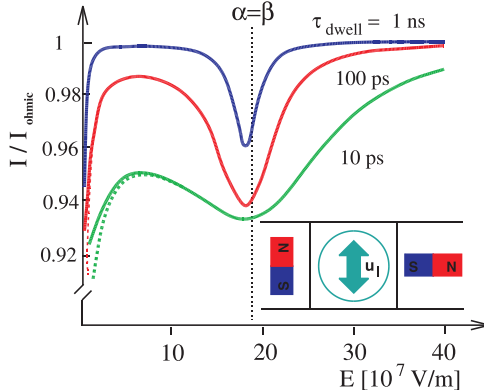
Fig. 4.4: Calculated current through a device as a function of gate voltage in-
duced electric field E for three different dwell times τ_{dwell} and using
spin-relaxation rates as given by Eqs. (4.10) and (4.11). The magneti-
zations of the left and right ferromagnetic contacts are in the [110] and
[$\bar{1}$10] directions, respectively. The polarization is set to $P = 50\%$ and
$\mathrm{Re}\,G^{\uparrow\downarrow} = G/2$. The solid lines correspond to $\mathrm{Im}\,G^{\uparrow\downarrow} = -G/2$ and the
dashed lines correspond to $\mathrm{Im}\,G^{\uparrow\downarrow} = 0$.

perpendicular to this direction the spin torque decreases as a consequence
of the loss of spin accumulation. Moreover, in this configuration the spin
torque is found to change sign at $\theta = \pi/2$. This effect is due to decay of
the perpendicular component of the spin accumulation. At $\theta = \pi/2$ the
magnetization $\mathbf{m}_2$ is therefore parallel to $\mathbf{V_s}$ and $\tau_2 = 0$.

Another way to detect anisotropy electrically is by modulating the spin-
relaxation rates via the spin-orbit interaction. We discuss this within the
model system introduced in Sec. 4.2 and use the spin-relaxation times
Eqs. (4.10) and (4.11) to calculate charge current as a function of gate-
voltage induced electric field E (Fig. 4.4). The magnetizations of the left
and right ferromagnets are set in the $\mathbf{u}_l$ and $\mathbf{u}_s$ directions, respectively, to
maximize the effect of the spin-orbit interaction. We have used $\mathrm{Re}\,G^{\uparrow\downarrow} =$
$G/2$ and $\mathrm{Im}\,G^{\uparrow\downarrow} = -G/2$ for the ferromagnet-semiconductor interface as
suggested by *ab initio* studies of Fe–InAs interfaces.[38] Since the spin-

relaxation time perpendicular to the plane of the quantum dot τ_z is of the same order of magnitude as $\tau_{\mathrm{sf},s}$ a finite imaginary part of the mixing conductance is detrimental to the spin accumulation. The results as shown in Fig. 4.4 are not particularly sensitive to the values of these parameters, however. By setting $\mathrm{Im}\, G^{\uparrow\downarrow} = 0$ the result differs significantly only in low gate fields $E < 200$ kV / cm as shown by the dashed lines in Fig. 4.4. Due to rapid spin relaxation in the $[\bar{1}10]$ and $[001]$ directions the spin accumulation is along the $[110]$ direction to a good approximation for $E > 200$ kV / cm. At the dip in the current the contributions from the SIA and BIA spin-orbit couplings are approximately equal ($\alpha \simeq \beta$), and the anisotropy is largest.

We focus now on the analytical expressions which can be obtained in the limit of weak polarization ($P \ll 1$) and $\mathrm{Im}\, G^{\uparrow\downarrow} = 0$. As a consequence the z-component of the spin accumulation vanishes. The spin accumulation to lowest order in P reads

$$\mathbf{V}_s = \frac{VP}{2} \left(\frac{\sin(\phi + \frac{\theta}{2}) \sin(\frac{\theta}{2})}{1 + 2G_{\mathrm{sf},l}/G} \mathbf{u}_l - \frac{\cos(\phi + \frac{\theta}{2}) \sin(\frac{\theta}{2})}{1 + 2G_{\mathrm{sf},s}/G} \mathbf{u}_s \right) + \mathcal{O}(P^3). \quad (4.13)$$

Eqs. (4.1) and (4.4) give the charge current through the system

$$I_c = \frac{G}{2} \left(V - P\mathbf{V}_s \cdot (\mathbf{m}_1 - \mathbf{m}_2) \right). \quad (4.14)$$

This can be combined with (4.13) to obtain the charge current to the second order in P. The $GV/2$ term in (4.14) is given by Ohm's law for two non-magnetic interfaces and the second term gives the lowest order correction. These results help to develop an intuitive picture of the effects of anisotropic spin-relaxation processes on transport. To linear order in P the components of the spin accumulation along $\mathbf{u}_l$ and $\mathbf{u}_s$ depend only on the spin-relaxation rates along these directions but do not depend on the spin-relaxation rates along perpendicular directions.

This lowest-order result explains the physics when the polarization is small. When the polarization is larger, the current and spin accumulation have a more complicated interdependence.

4.4 Enhancement of spin accumulation due to anisotropy

Fast spin-relaxation is supposed to be detrimental for the spin accumulation in the central node of a spin valve. In anisotropic systems, however, this is not necessarily the case. Anisotropic spin-relaxation processes can also enhance the spin accumulation when there is at least one direction with a long spin lifetime. We demonstrate this in a spin-valve configuration in which the injected spin accumulation is dominantly along the stable direction. Spin relaxation in the perpendicular direction then may enhance the spin accumulation.

In the absence of spin-relaxation processes the angle dependence of the x-component of the spin accumulation is

$$V_{s,x}(\theta, P) = \frac{VP}{2}\sin^2(\theta/2) \tag{4.15}$$

as shown by dashed lines in Fig. 4.5. Assume now that a fast spin-relaxation process is switched on in the y-direction only and the x-component of the spin accumulation does not decay, $i.e.$ $\mathbf{u}_s = (0, 1, 0)$, $\tau_{\mathrm{sf},s} = 0$ and $\mathbf{u}_l = (1, 0, 0)$, $\tau_{\mathrm{sf},l} = \infty$. The decay of the spin accumulation in the y-direction induces a larger current through the system for the same bias voltage. This implies a larger spin current and, as a consequence, an enhanced spin accumulation in the x-direction. Since to linear order in the contact polarization circuit theory predicts no enhancement of the spin accumulation (Eq. 4.13), we have to work out the solution for arbitrary P. In the above limit of $G_{\mathrm{sf},s} = \infty$ and $G_{\mathrm{sf},l} = 0$, the solution to the set of equations (4.1)–(4.5) is

$$V_{s,x}(\theta, P) = \frac{2VP(\cos\theta - 1)}{P^2(\cos\theta + \cos 2\theta + 3) - 8}, \tag{4.16}$$

as shown by solid lines in Fig. 4.5. The results prove that spin accumulation in the x-direction may be enhanced due to spin relaxation in the y-direction. The y component of the spin accumulation decays but the total modulus of the spin accumulation vector may increase as a result of the spin relaxation. The enhancement of the spin accumulation is substantial in the limit of high
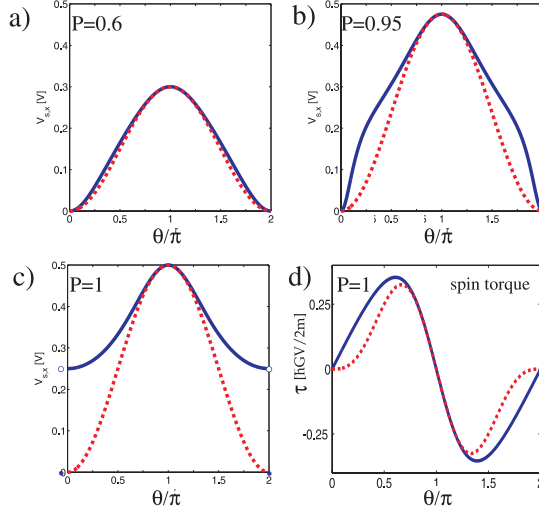
Fig. 4.5: a–c) The component of spin accumulation in the direction of the injecting magnetization $V_{s,x}$ is enhanced in the presence of fast spin relaxation in the perpendicular direction ($\phi = 0$, $G_{\mathrm{sf,s}} = \infty$). The solid line presents the results from the circuit theory (4.16) and the dashed line shows the spin accumulation in the linear-order approximation (4.13). The spin accumulation is not assumed to decay in the direction of the injecting magnetization ($G_{\mathrm{sf,l}} = 0$). The enhancement of the spin accumulation strongly depends on the magnetization polarization P. d) Enhancement of the spin accumulation is also reflected by the spin-transfer torque on the right ferromagnet as shown here for $P = 1$.

polarization $P > 0.9$. At lower polarizations, the increased spin current and reduced y-component of the spin compete and the phenomenon disappears in the low P limit in Eq. (4.13). In the limiting case of 100% polarization the spin enhancement is discontinuous at $\theta = 0$ (Fig. 4.5c). There is no spin accumulation at $\theta = 0$, in line with the results from collinear circuit theory, but infinitely close to this point the spin accumulation jumps to $1/2$ of the maximum value at $\theta = \pi$. The enhancement of the spin accumulation has an impact on the spin-transfer torque on the ferromagnets

as well. Fig. 4.5(d) shows an increase in the spin torque on ferromagnet 2 at $P = 1$ compared to the spin torque calculated from the linear-order approximation (4.13).

4.5   Conclusions

Magnetoelectronic circuit theory has been used to calculate the spin and charge transport through a spin valve with a diffuse or chaotic quantum dot in the presence of anisotropic spin-relaxation processes. Analytical expressions for charge current, spin accumulation and spin-transfer torques in the tunneling regime illustrate the sensitivity of the charge current on the relative orientation of the anisotropy axes and the magnetizations of the ferromagnets. Signatures of anisotropy have been identified in the magnetoresistance. The anisotropy can be probed either by rotating the magnetization directions of the ferromagnets or alternatively by using a gate electrode to change the spin-relaxation rates. Counterintuitively, anisotropic spin-relaxation processes may enhance the spin accumulation. This effect is attributed to an increased charge current due to removal of one component of the spin, which increases the spin-injection rate in the perpendicular direction. The enhancement was found to be remarkably large in the limit of high polarization.

BIBLIOGRAPHY

[1] P. Grünberg, Phys. Today, May 2001, 31.

[2] G. Binasch, P. Grünberg, F. Saurenbach, and W. Zinn, Phys. Rev. B **39**, 4828 (1989).

[3] M. N. Baibich, J. M. Broto, A. Fert, F. N. Vandau, F. Petroff, P. Etienne, G. Creuzet, A. Friedrich, and J. Chazelas, Phys. Rev. Lett. **61**, 2472 (1988).

[4] I. Žutić, J. Fabian, and S. Das Sarma, Rev. Mod. Phys. **76**, 323 (2004).

[5] M. Johnson, and R. H. Silsbee, Phys. Rev. B **37**, 5326 (1988).

[6] G. Schmidt, D. Ferrand, L. W. Molenkamp, A. T. Filip, and B. J. van Wees, Phys. Rev. B **62**, R4790 (2000).

[7] For a review see: G. Schmidt, J. Phys. D: Appl. Phys **38**, R107 (2005).

[8] R. Fiederling, M. Keim, G. Reuscher, W. Ossau, G. Schmidt, A. Waag, and L. W. Molenkamp, Nature **402**, 787 (1999).

[9] E. I. Rashba, Phys. Rev. B **62**, R16267 (2000).

[10] A. Fert, and H. Jaffrès, Phys. Rev. B **64**, 184420 (2001).

[11] H. Jaffrès, and A. Fert, J. Appl. Phys. **91**, 8111 (2002).

[12] H. J. Zhu, M. Ramsteiner, H. Kostial, M. Wassermeier, H.-P. Schönherr, and K. H. Ploog, Phys. Rev. Lett **87**, 016601 (2001).

[13] V. F. Motsnyi, J. De Boeck, J. Das, W. Van Roy, G. Borghs, E. Goovaerts, and V. I. Safarov, Appl. Phys. Lett. **81**, 265 (2002).

[14] A. T. Hanbicki, B. T. Jonker, G. Itskos, G. Kioseoglou, and A. Petrou, Appl. Phys. Lett. **80**, 1240 (2002).

[15] O. M. J. van 't Erve, G. Kioseoglou, A. T. Hanbicki, C. H. Li, B. T. Jonker, R. Mallory, M. Yasar, and A. Petrou, Appl. Phys. Lett. **84**, 4334 (2004).

[16] C. Adelmann, J. L. Hilton, B. D. Schultz, S. McKernan, C. J. Palmstrøm, X. Lou, H.-S. Chiang, and P. A. Crowell, Appl. Phys. Lett. **89**, 112511 (2006).

[17] P. Chen, J. Moser, P. Kotissek, J. Sadowski, M. Zenger, D. Weiss, and W. Wegscheider, cond-mat/0608453.

[18] P. A. Crowell, private communication.

[19] M. I. Dyakonov and V. I. Perel, Fiz. Tverd. Tela **13**, 3581 (1971) (Engl. translation Sov. Phys. - Solid State **13**, 3023 (1971)).

[20] Roland Winkler, *Spin-orbit coupling effects in two-dimensional electron and hole systems*, Springer Tracts in Modern Physics **191**, Springer-Verlag (2003).

[21] G. Dresselhaus, Phys. Rev. **100**, 580 (1955).

[22] Y. A. Bychkov, E. I. Rashba, J. Phys. C: Solid State Phys. **17**, 6039 (1984); Y. A. Bychkov, E. I. Rashba, JETP Lett. **39**(2), 78 (1984).

[23] S. D. Ganichev, V. V. Bel'kov, L. E. Golub, E. L. Ivchenko, Petra Schneider, S. Giglberger, J. Eroms, J De Boeck, G. Borghs, W. Wegscheider, D. Weiss, and W. Prettl, Phys. Rev. Lett. **92**, 256601 (2004).

[24] Y. Ohno, R. Terauchi, T. Adachi, F. Matsukura, and H. Ohno, Phys. Rev. Lett. **83**, 4196 (1999).

[25] C. P. Weber, J. Orenstein, B. Andrei Bernevig, Shou-Cheng Zhang, Jason Stephens, and D. D. Awschalom, cond-mat/0610054.

[26] N. S. Averkiev and L. E. Golub, Phys. Rev. B **60**, 15582 (1999).

[27] J. Kainz, U. Rössler, and R. Winkler, Phys. Rev. B **68**, 075322 (2003).

[28] B. Andrei Bernevig, J. Orenstein, and Shou-Cheng Zhang, cond-mat/0606196.

[29] S. Datta and B. Das, Appl. Phys. Lett. **56**, 665 (1990).

[30] J. Schliemann, J. Carlos Egues, and D. Loss, Phys. Rev. Lett. **90**, 146801 (2003).

[31] X. Cartoixa, D. Z.-Y. Ting, Y.-C. Chang, Appl. Phys. Lett. **83**, 1462 (2003).

[32] R. H. Silsbee, J. Phys.: Condens. Matter **16**, R179 (2004).

[33] A. Brataas, Y. V. Nazarov, and G. E. W. Bauer, Phys. Rev. Lett. **84**, 2481 (2000); Eur. Phys. J. B **22**, 99 (2001); A. Brataas, G. E. W. Bauer, and P. J. Kelly, Phys. Rep. **427**, 157 (2006).

[34] J. Nitta, T. Akazaki, H. Takayanagi, and T. Enoki, Phys. Rev. Lett. **78**, 1335 (1997).

[35] J. S. Sandhu, A. P. Heberle, J. J. Baumberg, and J. R. A. Cleaver, Phys. Rev. Lett. **86**, 2150 (2001).

[36] Y. K. Kato, R. C. Myers, A. C. Gossard, and D. D. Awschalom, Phys. Rev. Lett. **93**, 176601 (2004).

[37] W. Wetzels, G. E. W. Bauer, and M. Grifoni, Phys. Rev. B **72**, 020407 (2005); cond-mat/0608217 (Phys. Rev. B, in press).

[38] G. E. W. Bauer, A. Brataas, Y. Tserkovnyak, B. I. Halperin, M. Zwierzycki, P. J. Kelly, Phys. Rev. Lett. **92**, 126601 (2004).

[39] J. C. Slonczewski, J. Magn. Magn. Mater. **159** L1 (1995).

[40] F. Bloch, Phys. Rev. **70**, 460 (1946).

[41] N. S. Averkiev, L. E. Golub, and M. Willander, J. Phys. Condens. Matter **14**, R271 (2002).

[42] N. S. Averkiev, L. E. Golub, and M. Willander, Semiconductors **36**, 91 (2002).

[43] W. J. H. Leyland, G. H. John, R. T. Harley, M. M. Glazov, E. L. Ivchenko, D. A. Ritchie, A. J. Shields, and M. Henini, cond-mat/0610587.

[44] J. Manschot, A. Brataas, and G. E. W. Bauer, Phys. Rev. B **69**, 092407 (2004).

5. ELECTRON TRANSPORT THROUGH A SINGLE-ELECTRON SPIN-VALVE TRANSISTOR WITH A LUTTINGER-LIQUID ISLAND

5.1 Introduction

Electronic transport in one-dimensional systems has received a lot of attention because it offers the possibility to study non-Fermi liquid physics. The low-energy properties of interacting one-dimensional electron systems are described by Luttinger-liquid theory. In this chapter we consider a single-electron spin-valve transistor with a Luttinger-liquid island. The one-dimensional island is attached to two noninteracting ferromagnetic leads, which have magnetization directions that can be either parallel or antiparallel. The Luttinger-liquid correlations in the island affect the tunneling rates, and thereby the transport through the system as a whole. Transport through Luttinger-liquid quantum dots attached to normal-metal contacts was studied in Ref. [1, 2, 3, 4, 5]. Results were also found for Luttinger liquids contacted to ferromagnetic contacts outside of the Coulomb blockade regime [6, 7, 8].

Several energy scales play a role in this system. For a one-dimensional wire with a length L, the single-particle level spacing is given by $\varepsilon_0 = \pi \hbar v_F / L$. There is also a charging energy E_c. The energy scale for the excitations of charge plasmons in the Luttinger liquid is $\varepsilon_\rho = \varepsilon_0 / g$, where g is the Luttinger parameter. Repulsive interactions are characterized by $g < 1$, whereas $g = 1$ for noninteracting electrons. Here we restrict the discussion to the regime $E_c \gg k_B T \gg \varepsilon_\rho, \varepsilon_0$. For this hierarchy of energy scales, the charging energy is dominant and the single-electron transistor is in the Coulomb blockade regime. Since the thermal energy is much larger than the single-particle level spacing and the plasmon excitation energies, we can consider the bosonic excitations in the island to be thermalized. This regime is relevant for Luttinger liquids with a Luttinger parameter $g \ll 1$ [9]. It is not relevant for carbon nanotubes, since the Luttinger parameter for nanotubes is typically in the range of 0.2 to 0.3, with $g \approx (1 + 2E_c/\varepsilon_0)^{-1/2}$ [10]. For a discussion of the Luttinger-liquid energy scales for carbon nanotubes, see Ref. [11]. The regime discussed here gives additional insight into the effect of Luttinger-liquid correlations compared to studies taking into account the details of the low-energy spectrum. Luttinger liquids in the limit $\varepsilon_0 \ll k_B T \ll \varepsilon_\rho$, so-called spin incoherent Luttinger liquids, are

reviewed in Ref. [12].

In this chapter we present results for the transport in the linear response regime ($eV \ll k_B T$) to leading order in the transmission matrix elements. The thermal length scale $\hbar v_F/(k_B T)$ is shorter than the length of the wire, which means that incoherent sequential tunneling processes govern the transport. We include spin flip in the Luttinger liquid by introducing a phenomenological spin-flip time $\tau_{\rm sf}$. The X1 and X2 exchange effects do not play a role here because the magnetizations are collinear and the transport is only determined to leading order in perturbation theory (see Sec. 2.3). In Refs. [6, 7] it was concluded that magnetoresistance effects for this system in the limit $k_B T \gg E_c$ are strongly suppressed for noncollinear configurations, since the spin accumulation can be relaxed efficiently by the X1 and X2 exchange effects.

5.2   Model system

The Hamiltonian for this system is

$$H = H_{LL} + \sum_{l=S,D} \left(H_l + H_{Tl} \right), \qquad (5.1)$$

where H_{LL} describes the Luttinger-liquid island. In a bosonized representation it is given by (Cf. Ref. [13]):

$$
\begin{aligned}
H_{LL} =& \frac{1}{2} E_C \left(n_c - C_G V_G/e \right)^2 + \frac{1}{4}\varepsilon_0 \left(n_c - 1 \right)^2 + \frac{1}{4}\varepsilon_0 n_s^2 \\
&+ \sum_{m_c=1}^{\infty} m_c \varepsilon_\rho a_{m_c}^\dagger a_{m_c} + \sum_{m_s=1}^{\infty} m_s \varepsilon_0 a_{m_s}^\dagger a_{m_s}.
\end{aligned}
\qquad (5.2)
$$

The terms in the first line can be considered as the fermionic part of the Hamiltonian that accounts for the energy due to the Coulomb interaction and the Pauli principle. The operator n_c counts the excess number of electron charges on the island, and n_s counts the excess number of spins. The second line describes the charge and spin density waves, which are

bosonic excitations with a charge and spin character. $a^\dagger_{m_c}$ and $a^\dagger_{m_s}$ are creation operators for these charge and spin excitations.

The noninteracting leads are described by the Hamiltonians H_l (for $l \in \{S, D\} = \{\text{source, drain}\}$), which are given by $H_l = \sum_{k\sigma} \varepsilon_{lk\sigma} c^\dagger_{lk\sigma} c_{lk\sigma}$. The operator $c^\dagger_{lk\sigma}$ creates a quasi-particle with orbital index k and spin $\sigma \in \{\uparrow, \downarrow\}$ in lead l. A tunneling Hamiltonian H_T accounts for the coupling between the leads and the island. We assume that the tunneling occurs at the end points of the Luttinger liquid, positioned at $x_S = 0$ and $x_D = L$.

$$H_T = \sum_{l=S,D} \sum_{\sigma=\uparrow,\downarrow} T_{l\sigma} \psi^\dagger_\sigma (x_l) c_{\sigma l} (x_l) + h.c. \tag{5.3}$$

To calculate the transport characteristics we use a density matrix formalism as used in Ref. [4, 5]. An exposition of density-matrix theory is given by Blum [14]. The density matrix for the whole system, including the leads and the island, is $\rho^I(t)$. We use the interaction picture with the tunneling Hamiltonian H_T as perturbation. The equation of motion for the density matrix is:

$$i\hbar \frac{\partial \rho^I(t)}{\partial t} = \left[H^I_T(t), \rho^I(t) \right]. \tag{5.4}$$

The large leads are only weakly coupled to the island and are treated as reservoirs in thermal equilibrium. The density matrix can now be factorized as $\rho^I(t) = \rho^I_{LL}(t) \rho_{\text{leads}}$ [14]. The reduced density matrix $\rho^I_{LL}(t)$ can then be obtained by tracing out the lead degrees of freedom, $\rho^I_{LL}(t) = \text{Tr}_{\text{leads}} \rho^I(t)$. The density matrix $\rho_{\text{leads}} = \rho_S \rho_D$ is time-independent. The expression for the individual density matrix of lead l is $\rho_l = e^{-\beta(H_l - \mu_l N_l)}/Z_l$, where Z_l is the partition function and N_l is the number of electrons in lead l.

Using the solution for the equation of motion

$$\rho^I(t) = \rho^I(t_0) - \frac{i}{\hbar} \int\limits_{t_0}^{t} dt' \left[H^I_T(t'), \rho^I(t') \right], \tag{5.5}$$

we find

$$i\hbar \frac{\partial \rho_{LL}^{I}(t)}{\partial t} = \mathrm{Tr}_{\mathrm{leads}} \left[H_{T}^{I}(t), \rho^{I}(t_{0}) \right]$$

$$- \frac{i}{\hbar} \mathrm{Tr}_{\mathrm{leads}} \left[H_{T}^{I}(t), \int_{t_{0}}^{t} dt' \left[H_{T}^{I}(t'), \rho^{I}(t) \right] \right]. \qquad (5.6)$$

The first term on the right hand side vanishes because $\langle c_{\sigma l} \rangle = 0$. In the second term, $\rho^{I}(t')$ was replaced by $\rho^{I}(t)$. This is the Markov approximation [14], which is valid when the density matrix does not change significantly during the correlation time of the leads, i.e. the time after which the correlations in the leads vanish. We set $t_{0} \to -\infty$ and have

$$\frac{\partial \rho_{LL}^{I}(t)}{\partial t} = -\frac{1}{\hbar^{2}} \mathrm{Tr}_{\mathrm{leads}} \int_{0}^{\infty} dt'' \left\{ H_{T}^{I}(t) H_{T}^{I}(t - t'') \rho^{I}(t) \right.$$

$$\left. - H_{T}^{I}(t) \rho^{I}(t) H_{T}^{I}(t - t'') + h.c. \right\}. \qquad (5.7)$$

We now assume that the bosonic degrees of freedom are thermalized as well. The reduced density matrix can be factorized into a fermionic (f) and a bosonic (b) part as $\rho_{LL}^{I}(t) = \rho_{LLf}^{I}(t) \rho_{LLb}$, and the bosonic degrees of freedom are traced out. The lead operators can be moved by using the anticommutation relations, and we also make use of the cyclic property of the trace. The result for the dynamics of the fermionic part of the reduced

density matrix is

$$
\frac{\partial \rho^I_{LLf}(0)}{\partial t} = -\frac{1}{\hbar^2} \sum_{\sigma l} \frac{|T_{\sigma l}|^2}{2L} \int\limits_0^\infty dt'' \{
$$

$$
+ \left\langle c_{\sigma l}(0) c^\dagger_{\sigma l}(-t'') \right\rangle_{th} \left\langle \psi^\dagger_\sigma(x_l, 0)\psi_\sigma(x_l, -t'') \right\rangle_b \eta^\dagger_\sigma(0)\eta_\sigma(-t'')\rho^I_{LLf}(0)
$$

$$
+ \left\langle c^\dagger_{\sigma l}(0) c_{\sigma l}(-t'') \right\rangle_{th} \left\langle \psi_\sigma(x_l, 0)\psi^\dagger_\sigma(x_l, -t'') \right\rangle_b \eta_\sigma(0)\eta^\dagger_\sigma(-t'')\rho^I_{LLf}(0)
$$

$$
- \left\langle c^\dagger_{\sigma l}(-t'') c_{\sigma l}(0) \right\rangle_{th} \left\langle \psi_\sigma(x_l, -t'')\psi^\dagger_\sigma(x_l, 0) \right\rangle_b \eta^\dagger_\sigma(0)\rho^I_{LLf}(0)\eta_\sigma(-t'')
$$

$$
- \left\langle c_{\sigma l}(-t'') c^\dagger_{\sigma l}(0) \right\rangle_{th} \left\langle \psi^\dagger_\sigma(x_l, -t'')\psi_\sigma(x_l, 0) \right\rangle_b \eta_\sigma(0)\rho^I_{LLf}(0)\eta^\dagger_\sigma(-t'')
$$

$$
+ \, h.c.\} \, . \tag{5.8}
$$

This expression can be evaluated at $t = 0$ since we are not considering any transient effects. The Klein factors η_σ are operators that reduce the excess number of charges n_c by one and take n_s to $(n_s - \sigma)$ [15]. The time dependence of the Klein factors is determined by the equation $i\hbar\dot{\eta}_\sigma = [\eta_\sigma, H_{LL}]$, which has a solution

$$
\eta_\sigma(t) = e^{-\frac{i}{\hbar}\left[E_c(n_c+\frac{1}{2} - C_G V_G/e) + \frac{1}{2}\varepsilon_0(n_c - \sigma n_s)\right]t}\eta_\sigma(0) \, . \tag{5.9}
$$

We introduce a basis of eigenstates $|\kappa\rangle$ of the fermionic system, that are characterized by the excess number of charges $\kappa \in \mathcal{N}$. It is not necessary to use the number of spins on the island as an additional quantum number because the fluctuations of the number of spins are negligible compared to the average value [16] (see also Ch. 2). We use a static quasi-equilibrium value for the spin accumulation. In this basis, the elements of the density matrix are $\rho^I_{LLf\kappa\lambda}(t) = \langle\kappa|\rho^I_{LLf}(t)|\lambda\rangle$. We now define rates Γ for the change of the density matrix elements as:

$$
\frac{\partial \rho^I_{LLf}(0)_{\kappa\lambda}}{\partial t} \equiv \sum_{\kappa'\lambda' l\sigma} \Gamma^{\kappa'\lambda' \to \kappa\lambda}_{l\sigma}\rho^I_{LLf}(0)_{\kappa'\lambda'} - \sum_{\kappa'\lambda' l\sigma} \Gamma^{\kappa\lambda \to \kappa'\lambda'}_{l\sigma}\rho^I_{LLf}(0)_{\kappa\lambda} \, . \tag{5.10}
$$

In the Coulomb blockade regime and for small bias voltage it suffices to consider transitions between the states with $n_c = 0$ and $n_c = 1$ (see Ch. 2). We can evaluate the rate

$$\Gamma_{l\sigma}^{00\to11} = \frac{1}{\hbar^2} \frac{|T_{l\sigma}|^2}{2L} \int\limits_0^\infty dt'' \left\{ e^{-\frac{i}{\hbar}\left[E_c\left(\frac{1}{2}-C_GV_G/e\right)+\frac{1}{2}\varepsilon_0\sigma n_s\right]t''} \times \right.$$

$$\left. \left\langle \psi_\sigma(x_l,0)\psi_\sigma^\dagger(x_l,-t'')\right\rangle_{\mathrm{b}} \left\langle c_{\sigma l}^\dagger(x_l,0)c_{\sigma l}(x_l,-t'')\right\rangle_{\mathrm{th}} + h.c. \right\} \qquad (5.11)$$

$$= \frac{\pi\rho_{l\sigma}|T_{l\sigma}|^2}{L\hbar} \int\limits_{-\infty}^\infty d\varepsilon f(\varepsilon)\rho_{LL\sigma}\left(\varepsilon - E_c(1/2 - C_GV_G/e) - \frac{1}{2}\varepsilon_0\sigma n_s + \mu_l\right)$$

The expression for the correlation function in the leads is

$$\left\langle c_{l\sigma}^\dagger\left(x_l,t''\right)c_{l'\sigma'}\left(x_{l'},0\right)\right\rangle_{\mathrm{th}} = \delta_{\sigma\sigma'}\delta_{ll'}\int\limits_{-\infty}^\infty d\varepsilon \rho_{l\sigma} e^{\frac{i}{\hbar}\varepsilon t''}f\left(\varepsilon - \mu_l\right), \qquad (5.12)$$

where $f(\varepsilon)$ is the Fermi-Dirac distribution and $\rho_{l\sigma}$ is the spin-dependent density of states in lead l. The tunneling density of states for the Luttinger liquid is

$$\rho_{LL\sigma}\left(\varepsilon,x\right) = \frac{1}{2\pi\hbar}\int_{-\infty}^\infty dt \left\langle \psi_\sigma(x,0)\psi_\sigma^\dagger(x,t)\right\rangle e^{\frac{i}{\hbar}\varepsilon t}, \qquad (5.13)$$

which for the end contacts is given by the expression [17, 18, 19]

$$\rho_{LL\sigma}\left(\varepsilon,x_l\right) = Ae^{\varepsilon/2k_BT}(k_BT/D)^{\frac{1}{2}(1/g-1)}\left|\Gamma\left(\frac{1}{4}(1+1/g) + i\varepsilon/2\pi k_BT\right)\right|^2, \qquad (5.14)$$

where A is an arbitrary constant and D is a large cut-off energy. The quasi-equilibrium state can now be found from the detailed balance condition $\partial\rho_{LLf00}^I/\partial t = 0$, the condition that $\rho_{LLf00}^I + \rho_{LLf11}^I = 1$ and the conservation of spin in the island

$$\frac{\partial n_s}{\partial t} = \sum_{l\sigma}\sigma\Gamma_{l\sigma}^{00\to11}\rho_{LLf00}^I - \sum_{l\sigma}\sigma\Gamma_{l\sigma}^{11\to00}\rho_{LLf11}^I - \frac{n_s}{\tau_{\mathrm{sf}}} = 0, \qquad (5.15)$$

101

in which spin-flip is taken into account. The expression for the current from the source to the drain contact is

$$I = e \sum_{\sigma} \Gamma_{S\sigma}^{00 \to 11} \rho_{LLf00}^{I} - e \sum_{\sigma} \Gamma_{S\sigma}^{11 \to 00} \rho_{LLf11}^{I}. \qquad (5.16)$$

5.3   Results

We now present linear-response results for the conductance as a function of gate voltage for a symmetric spin-valve system. The conductance in the parallel configuration is given by

$$G_P(V_G) = (\gamma_\uparrow + \gamma_\downarrow)\,(k_B T/D)^{\frac{1}{2}(1/g-1)}\,\frac{H'(-\Delta)H(\Delta) + H'(\Delta)H(-\Delta)}{H(\Delta) + H(-\Delta)}, \qquad (5.17)$$

where $\Delta = E_c(1/2 - C_G V_G/e)$. For compactness of notation we have introduced $\gamma_s = \pi A \rho_s \left| T_s \right|^2 /(2L\hbar)$ for $(s = \uparrow, \downarrow)$. The function $H(\varepsilon)$ is defined as

$$H(\varepsilon) = \int_{-\infty}^{\infty} d\varepsilon' f(\varepsilon' + \varepsilon)\, e^{\varepsilon'/2k_B T} \left| \Gamma\left(\frac{1}{4}(1 + 1/g) + i\varepsilon'/2\pi k_B T\right) \right|^2. \qquad (5.18)$$

The Luttinger-liquid correlations cause a power-law suppression of the tunneling density of states in the island. From Eq. 5.17 we see that for strong interaction $(g \ll 1)$ the conductance is strongly suppressed when $k_B T \ll D$. The conductance maximum of the Coulomb oscillations exhibits power-law behavior as a function of temperature with an exponent $\frac{1}{2}(1/g - 1)$. The conductance in the anti-parallel configuration is given by

$$G_{AP}(V_G) = G_P(V_G) \left(1 - \frac{P^2}{1 + 2G_{\mathrm{sf}}/G_P(V_G)}\right), \qquad (5.19)$$

where we have defined a polarization $P = (\gamma_\uparrow - \gamma_\downarrow)/(\gamma_\uparrow + \gamma_\downarrow)$ and a spin-flip conductance parameter $G_{\mathrm{sf}} \equiv e^2/(2\varepsilon_0\tau_{\mathrm{sf}})$. In the antiparallel configuration, a spin accumulation can reduce the conductance. Spin-flip processes relax this spin accumulation efficiently when τ_{sf} is short compared to the dwell time, which is defined as $\tau_{\mathrm{dwell}}(V_G) \equiv e^2/(\varepsilon_0 G_P(V_G))$.

The shape of the Coulomb oscillations is affected by the Luttinger-interaction effects as well. In Fig. 5.1 we plot the conductance versus gate voltage for a Luttinger-liquid island characterized by a Luttinger parameter $g = 0.05$ for parallel as well as antiparallel lead-magnetization directions. For comparison, the shape of a Coulomb oscillation for a symmetric spin-valve with a Fermi-liquid island, which is given by the expression $G_P(V_G) = G_{P\mathrm{max}}2\beta\Delta/\sinh(2\beta\Delta)$, is shown in the same figure (cf. Sec. 2.5). In the case of a Luttinger-liquid island, the peak has a broader shape because correlations suppress tunneling most effectively at the conductance maximum.

Coulomb blockade effects cause a reduction of the tunneling currents, and thereby diminish the spin accumulation. To observe magnetoresistance effects, the spin-flip time τ_{sf} will have to be much larger for an interacting Luttinger-liquid island than for a noninteracting island. The curves for the parallel and antiparallel configurations converge with increasing detuning from the current maximum because spin flip prevents build-up of a spin accumulation.

In conclusion, we have discussed electronic transport through a single-electron spin-valve transistor with a Luttinger-liquid island for a regime in which the charging energy is the dominant energy scale. The bosonic degrees of freedom of the Luttinger liquid are thermalized. Transport results were obtained by means of a density-matrix method to leading order in perturbation theory. We find that the Luttinger-liquid correlations and the Coulomb blockade both suppress the tunneling in the anti-parallel configuration and therefore suppress the spin accumulation and resistance contrast compared to a parallel configuration. A comparison of the shape of the Coulomb oscillations for Luttinger-liquid and Fermi-liquid islands shows that the peak shape is broadened by the Luttinger correlations.
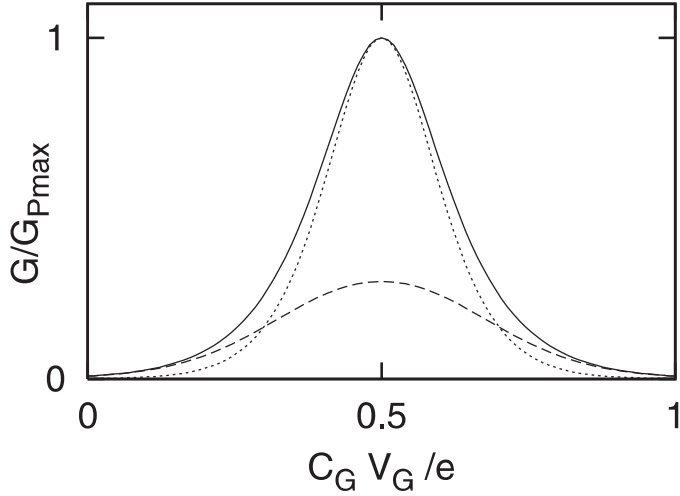
Fig. 5.1: Conductance as a function of gate voltage for a symmetric SV-SET with a Luttinger-liquid island, normalized with respect to the conductance at $C_G V_G = e/2$. Curves are shown for $g = 0.05$ for parallel (solid line) and antiparallel (dashed line) magnetization configurations. The charging energy $E_c = 10 k_B T$, the polarization $P = 1$, and the spin-flip conductance $G_{\mathrm{sf}} = G_{P\max}/5$. The shape of a Coulomb oscillation for a single-electron spin-valve transistor with a Fermi-liquid island in the parallel configuration is shown for comparison (dotted line).

BIBLIOGRAPHY

[1] A. Braggio, M. Sassetti, and B. Kramer, Phys. Rev. Lett. **87**, 146802 (2001).

[2] F. Cavaliere, A. Braggio, M. Sassetti, and B. Kramer, Phys. Rev. B **70**, 125323 (2004).

[3] F. Cavaliere, A. Braggio, J. T. Stockburger, M. Sassetti, and B. Kramer, Phys. Rev. Lett. **93**, 036803 (2004).

[4] L. Mayrhofer and M. Grifoni, Phys. Rev. B **74**, 121403(R) (2006).

[5] L. Mayrhofer and M. Grifoni, cond-mat/0612286 (2006).

[6] L. Balents and R. Egger, Phys. Rev. Lett. **85**, 3464 (2000).

[7] L. Balents and R. Egger, Phys. Rev. B **64**, 035310 (2001).

[8] C. Bena and L. Balents, Phys. Rev. B **70**, 245318 (2004).

[9] L. Balents, Moriond Les Arcs Conference Proceedings, cond-mat/9906032 (1999).

[10] R. Egger, A. Bachtold, M.S. Fuhrer, M. Bockrath, D.H. Cobden, and P.L. McEuen, in *Interacting Electrons in Nanostructures*, edited by R. Haug and H. Schoeller, (Springer, Berlin, 2001).

[11] C. Kane, L. Balents, and M. P. A. Fisher, Phys. Rev. Lett. **79**, 5086 (1997).

[12] G. A. Fiete, cond-mat/0611597 (2006).

[13] F. Anfuso and S. Eggert, Phys. Rev. B **68**, 241301(R) (2003).

[14] K. Blum, *Density matrix theory and applications*, 2nd ed. (Plenum, New York, 1996).

[15] J. von Delft and H. Schoeller, Ann. Phys. (Leipzig) **7**, 225 (1998).

[16] J. Martinek, J. Barnaś, G. Schön, S. Takahashi, and S. Maekawa, J. Supercond.: Incorp. Novel Magnetism **16**, 343 (2002).

[17] U. Weiss, *Quantum dissipative systems*, 2nd ed. (World Scientific, Singapore, 1993).

[18] T. Giamarchi, *Quantum physics in one dimension*, (Clarendon Press, Oxford, 2004).

[19] M. Bockrath, D. H. Cobden, J. Lu, A. G. Rinzler, R. E. Smalley, L. Balents, and P. McEuen, Nature **397**, 598 (1999).

SUMMARY

Interaction effects in spin-valve structures

Wouter Wetzels

Most applications in electronics are based on manipulation of the electron charge. Currently, there is also a lot of research into the possibility to make use of the electron spin, for example in magnetoelectronics. This field of research studies hybrid systems consisting of ferromagnetic metals, paramagnetic metals and insulators. An important breakthrough in magnetoelectronics was the discovery of the Giant Magnetoresistance (GMR) effect, which is already applied widely, e.g. in magnetic-field sensors in read heads for hard disk drives.

In this thesis we present a theoretical description of a number of physical structures whose operation is based on the spin-valve principle. A spin valve consists of two ferromagnetic elements with a non-magnetic material in between. The electrical resistance of a spin valve can be varied by changing the angle between the magnetization directions of the two ferromagnets. In experiments an external magnetic field is usually used to do this.

We are interested in effects of the interaction between electrons on electronic transport in spin-valve structures. As the experimentally studied structures are getting smaller, interactions play an increasingly important role. Often, theoretical investigations in magnetoelectronics are restricted to systems with magnetization directions that are either parallel or antiparallel. In most parts of this thesis we study how the electronic transport properties depend on an arbitrary angle between the magnetization directions. The so-called magnetoelectronic circuit theory turns out to be an

efficient and transparent instrument. This theory can be used to determine the transport properties of electronic circuits containing ferromagnetic elements with arbitrary magnetization directions.

In the introduction we present an overview of important concepts and recent developments in magnetoelectronics. In chapter 2 we discuss the transport properties of a specific system, namely the so-called single-electron spin-valve transistor. In single-electron transistors, the charge current can be controlled by external gates up to the level of single electron charges. We discuss a single-electron transistor with ferromagnetic contacts that is the subject of increasingly successful experimental investigations. To describe the Coulomb interaction we use the "orthodox" model for Coulomb blockade, and we calculate the spin and charge current through the tunnel contacts by means of perturbation theory. In particular, we focus on two different exchange interaction mechanisms between the spin accumulation and the ferromagnetic contacts. One is caused by virtual tunneling processes, the other is an interface scattering effect that exists also in noninteracting systems. We determine the conductance of the system in the quasi-stationary state as a function of gate voltage and the angle between the magnetization directions. We also discuss the possibility to observe the Hanle effect, i.e. relaxation of the spin accumulation by an external magnetic field.

The current-induced magnetization reversal in spin valves based on the spin-transfer torque mechanism is by now well established. In chapter 3 we discuss the effect of current fluctuations that cause a fluctuating spin-transfer torque on the magnetization. We predict that the switching times can be shortened and that less energy is needed for the switching process. We find these results by solving a stochastic differential equation, the so-called Fokker-Planck equation. We use the Kramers method to derive explicit expressions for the reduced switching times.

Datta and Das proposed a scheme for a spin-field effect transistor that makes use of the spin-orbit interaction that stimulated a lot of research on spin-injection into a two-dimensional electron gas. In chapter 4 we consider a spin-valve system consisting of a small island in a two-dimensional electron gas attached to ferromagnetic contacts. The Rashba as well as the

Dresselhaus spin-orbit interaction play a role here, and others have found before that in this case a large anisotropy in the relaxation of the spin accumulation can occur. Using magnetoelectronic circuit theory, we find characteristic signatures of this anisotropy on the charge transport properties of this system as a function of the magnetic configuration as well as the spin accumulation and the spin-transfer torque.

Finally, in chapter 5 we consider single-electron transistors with a one-dimensional island that can be described as a Luttinger liquid. Also in this system, there are two ferromagnetic contacts that inject and detect spin. We use a density matrix method to determine the tunnel currents between the island and the contacts. The system is in the Coulomb blockade regime, and we consider a hierarchy of energy scales in which the Coulomb charging energy is the most important and the level splitting is negligible compared to the thermal energy. In earlier publications it has been claimed that spin-charge separation has a characteristic influence on the conductance as a function of the angle between the magnetizations. The results for the conductance show that Luttinger-liquid effects and Coulomb blockade effects are both important for the system under consideration.

SAMENVATTING

Interactie effecten in spinventiel structuren

Wouter Wetzels

De meeste toepassingen in de elektronica zijn gebaseerd op manipulatie van de lading van het elektron. Tegenwoordig is er ook veel onderzoek naar de mogelijkheid om gebruik te maken van de elektronspin, onder andere in de magnetoelektronica. Dit vakgebied bestudeert hybride systemen bestaande uit ferromagnetische metalen, paramagnetische metalen en isolatoren. Een belangrijke doorbraak in de magnetoelektronica was de ontdekking van het reuze magnetoweerstand effect (GMR effect) dat nu al op grote schaal wordt toegepast, bijvoorbeeld in magnetisch-veld sensoren in leeskoppen voor harde schijven.

In dit proefschrift geven we een theoretische beschrijving van een aantal fysische structuren waarvan de werking gebaseerd is op het principe van een spinventiel. Een spinventiel bestaat uit twee ferromagnetische elementen met daartussen een niet-magnetisch materiaal. De elektrische weerstand van een spinventiel is te variëren door de hoek tussen de magnetisatierichtingen van de twee ferromagneten te veranderen. In experimenten wordt daarvoor doorgaans een extern magnetisch veld gebruikt.

We zijn geïnteresseerd in de invloed van interactie tussen elektronen op elektronentransport in spinventiel structuren. Omdat de structuren die experimenteel bestudeerd worden steeds kleiner worden spelen interactie-effecten namelijk een steeds belangrijkere rol. Vaak beperkt theoretisch onderzoek in de magnetoelektronica zich tot systemen met magnetisatierichtingen die parallel dan wel antiparallel zijn. In het grootste gedeelte van

dit proefschrift bestuderen we hoe elektronische transporteigenschappen afhankelijk zijn van een willekeurige hoek tussen de magnetisatierichtingen. De zogenaamde magnetoelektronische netwerktheorie blijkt een efficiënt en transparant hulpmiddel. Deze theorie is geschikt om de transporteigenschappen te bepalen van elektronische circuits met daarin ferromagnetische elementen met willekeurige magnetisatierichting.

In de introductie geven we een overzicht van belangrijke concepten en van de ontwikkelingen die in de magnetoelektronica hebben plaatsgevonden. In hoofdstuk 2 bespreken we de transporteigenschappen van een specifiek systeem, namelijk de zogenaamde enkel-elektron spinventiel transistor. In enkel-elektron transistoren is de ladingsstroom met externe gates te controleren tot op het niveau van individuele elektronladingen. Wij beschouwen een enkel-elektron transistor met ferromagnetische contacten dat ook experimenteel met toenemend succes wordt bestudeerd. Om de Coulomb wisselwerking te beschrijven gebruiken we het "orthodoxe model" voor Coulomb blokkade, en berekenen we de spin- en ladingsstroom door de tunnelcontacten met storingstheorie. We gaan in het bijzonder in op twee mechanismen voor exchange wisselwerking tussen de spin accumulatie en de ferromagnetische contacten. Daarvan wordt er één bepaald door virtuele tunnel processen en het andere is een grensvlakverstrooiingseffect dat ook bestaat voor niet-wisselwerkende systemen. We bepalen de geleiding van het systeem in de quasi-evenwichtstoestand als functie van de gate-spanning en de hoek tussen de magnetisatierichtingen. Ook bespreken we de mogelijkheid tot observatie van het Hanle effect, d.w.z. relaxatie van de spin accumulatie door een extern magnetisch veld.

Stroomgeïnduceerde magnetisatie schakeling in spinventielen gebaseerd op het mechanisme van het spinoverdrachtsmoment is nu overtuigend vastgesteld. In hoofdstuk 3 bespreken we het effect van fluctuaties in de stroom die zorgen voor een fluctuerend spinoverdrachtsmoment op de magnetisatie. We voorspellen dat op deze manier de schakeltijden kunnen worden verkort en dat er minder energie nodig is voor het schakelproces. Deze resultaten vinden we door het oplossen van een stochastische differentiaalvergelijking voor de magnetisatie dynamica, de zogenaamde Fokker-Planck vergelijking. We gebruiken de methode van Kramers om uitdrukkingen voor de

schakeltijden te bepalen.

Datta en Das hebben een voorstel gedaan voor een spin veldeffect transistor die gebruik maakt van de spin-baan wisselwerking. Dit voorstel heeft tot veel onderzoek gericht op het injecteren van spins in een twee-dimensionaal elektronengas geleid. In hoofdstuk 4 beschouwen we een spin-ventiel systeem dat bestaat uit een klein eiland in een twee-dimensionaal elektronengas met ferromagnetische contacten. Zowel Rashba als Dressel-haus spin-baan interactie spelen hierbij een rol, en het is door anderen al eerder gevonden dat er in dat geval een grote anisotropie in de relaxatie van de spin accumulatie kan bestaan. Met behulp van de magnetoelek-tronische netwerktheorie vinden we de karakteristieke signatuur van deze anisotropie op de ladingstransport eigenschappen van dit systeem as functie van de magnetische configuratie, en voor de spin accumulatie en het spinoverdrachtsmoment.

Tenslotte beschouwen we in hoofdstuk 5 enkel-elektron transistoren met een één-dimensionaal eiland dat beschreven kan worden als een Luttinger vloeistof. Ook in dit systeem zijn er twee ferromagnetische contacten die spin kunnen injecteren en detecteren. We gebruiken een dichtheidsma-trix methode om de tunnelstromen tussen het eiland en de contacten te bepalen. Het systeem is in het Coulomb blokkade regime en we beschouwen een hiërarchie van energieschalen waarin de Coulomb ladingsenergie het belangrijkste is en de niveausplitsing verwaarloosbaar is ten opzichte van de thermische energie. In eerdere publicaties is al beweerd dat de spin-ladingsscheiding een karakteristieke invloed heeft op de geleiding als functie van de hoek tussen de magnetisaties. Uit de resultaten voor de geleiding blijkt dat Luttinger vloeistof effecten én Coulomb blokkade van belang zijn voor het beschouwde systeem.

CURRICULUM VITAE

June 19, 1978   Born in Tilburg, the Netherlands

1990-1996   Gymnasium van het Bernardinuscollege, Heerlen. Cum Laude

1996-2002   Master of Science, Physics, Utrecht University. Cum Laude

2002-2007   PhD research under supervision of prof. dr. ir. G. E. W. Bauer
             and prof. dr. M. Grifoni, Delft University of Technology

PUBLICATIONS

Henri Saarikoski, Wouter Wetzels, and Gerrit E. W. Bauer, *Charge and spin transport in spin valves with anisotropic spin relaxation*, Phys. Rev. B. **75**, 075313 (2007).

Wouter Wetzels, Gerrit E. W. Bauer, and Milena Grifoni, *Exchange effects on electron transport through single-electron spin-valve transistors*, Phys. Rev. B **74**, 224406 (2006).

Wouter Wetzels, Gerrit E. W. Bauer, and Oleg N. Jouravlev, *Efficient Magnetization Reversal with Noisy Currents*, Phys. Rev. Lett. **96**, 127203 (2006).

Wouter Wetzels, Gerrit E. W. Bauer, and Milena Grifoni, *Noncollinear single-electron spin-valve transistors*, Phys. Rev. B **72**, 020407(R) (2005).

Nick van Eijndhoven and Wouter Wetzels, *In-event background and signal reconstruction for two-photon invariant-mass analyses*, Nucl. Instr. and Methods A **482**, 513 (2002).

ACKNOWLEDGEMENTS

amazing how you always get us into trouble with night trains, I'm really impressed by your determination to get everything out of life, Omar, always fun to be with, full of amusing provocations, and very efficient (in making a big mess), Jeroen, who, with an unconventional and positive attitude, can be relied on to keep the theory group together in the future, Xuhui, the poker fanatic, for all the entertaining conversations and curious blog entries, Jens, for all the movies in Lumen, whose always-changing enthusiasms have brought him very far already, and Alex, always with an original perspective, who offered me the exceptional privileges of being invited to his wedding and to help him move.

Two very friendly new roommates (having little in common besides their prompt bicycle incidents after arriving) changed the atmosphere in the room completely (although this depended on the international political situation). Moosa, who doesn't choose the easy way and is always willing to explain and make me understand, and Vitaly, with whom I enjoyed to play badminton and who has made such an impressing effort in order to never have to do the dishes again. I hope Kevin will have a really good time in the group. For all the nice dinners, parties and friendship, I also want to thank Vika (learn Dutch soon!), Saverio and Monica (I really hope you will find a way to both continue your careers), Anna (for an excellent Sinterklaas celebration), Antonio and Vera.

It was really nice and interesting to get to know so many different people from all over the world during my time in the group, and I wish all the best to Jiang (you're welcome to stay over again when moving into another apartment that is still too messy to live in), Dima F. (who, one day, brought cake without wanting to tell the reason), Freek (who did his PhD the really hard way, I'm glad everything turned out alright), Gabriele, Wataru, Babak (we would have liked to see more of you), Joël, Izak, Hongduo, Marnix, Rutger, Dima B., Hayk, Inanc, Michael, Youjin, Sigi, Catherine, Rachid, Jan, Richard, Martin, Hatami and Gayathri.

The summer I spent in Regensburg was a fantastic experience. It was very nice to work and discuss with Sonja and Leo (and to cycle along the Danube together). Everyone in the group made me feel very welcome, especially Francesco (playing Italian songs on his guitar in the mountain

hut) and my roommates Maxim (who I could discuss literature with over a warm beer) and Dana, who surprised me by baking two cakes for my birthday. Many thanks to Lizy for organizing everything so well and the excellent idea to let me stay in the Horizonte language school at the time of the World Cup (this, I admit, may have harmed my scientific output a bit).

It has been great to live in Breestraat 12 all these years (despite some minor problems with our landlord), and I really enjoyed the many dinners together with Dirkjan (still around after being kicked out at least four times), Peter (who unfortunately left to Leiden voluntarily), Frank (much more of a Limburgian than I am), Jan, Marco, Jelle and all the others.

I am very glad that Garrelt and Maarten, who have been good friends since I was 10, agreed to be my paranimfs. And finally, I want to thank my family and friends for their support. The encouragements and the confidence my grandmother, my parents and sister have in me have been really important.

Eind goed, al goed.

Wouter Wetzels
Delft, 12 March, 2007